Università di Pisa


Dipartimento di Fisica "Enrico Fermi"

Tesi di Laurea Magistrale in Fisica Teorica

Lavoro svolto presso

**Centre de Physique Théorique - CNRS, Aix-Marseille Université, Marseille, France**

e

**Perimeter Institute for Theoretical Physics, Waterloo, Ontario, Canada**

# Investigating Static and Dynamic Non-Singular Black Holes

Candidato

**Tommaso De Lorenzo**

Relatore Interno
**Prof. Enore Guadagnini**
Dipartimento di Fisica "E. Fermi", Università di Pisa

Relatore Esterno
**Dott. Simone Speziale**
Aix-Marseille Université et Université de Toulon, CPT-CNRS

Anno Accademico 2013/2014

*Dice il Saggio:*
*"Il buco nero nasconde,*
*ma non ruba."*

# Table of Contents

# Introduction

*The present thesis has been prepared in two different phases. The initial work has been carried out in Marseille (France) under the supervision of* Simone Speziale*, during an internship at the* 'Centre de Physique Théorique (CPT)-CNRS, Aix-Marseille Université' *in the* 'Equipe de Gravité Quantique'*, the Quantum Gravity group leaded by* Carlo Rovelli*. The last Chapter, on the other hand, contains the work done in Waterloo (Ontario, Canada) during the* 'Undergraduate Students Summer Program' *conducted at the* "Perimeter Institute for Theoretical Physics"*, under the supervision of* Matteo Smerlak *and flowed into the paper Bianchi, De Lorenzo, and Smerlak [2014].*

Einstein's General Relativity is undoubtedly one of the more fascinating and intriguing theories of modern Theoretical Physics. Among its predictions we find the so called *Black Holes*. Roughly speaking, they are regions of SpaceTime such that, because of an enormous gravitational force, everything, included light, is attracted to and cannot escape from them. Initially considered just as a mathematical curiosity, during the 1960s they were shown to be generic predictions of General Relativity: any sufficiently massive collapsing star will form a black hole. More intriguing, we now have empirical evidences that our Milky Way, as well as other galaxies, hosts a supermassive black hole in its center.

In the deep interior of a black hole, however, a singularity arises. This ill-defined region of infinite curvature causes a breakdown of the predictability of theory itself and, due to the so called *Singularity Theorems*, its formation seems unavoidable in classical General Relativity. Nevertheless, the singularity is expected to be cured by quantum gravitational effects that become important in regions with high density of matter, as in the last stages of the life of a collapsing star. When matter reaches Planck density, it has been argued that Quantum Gravity generates pressure sufficient to counterbalance weight and the collapse stops, avoiding the formation of a singularity, exactly as in a hydrogen atom [Ashtekar and Bojowald 2006; Modesto 2004, 2006].

While a complete and satisfactory theory of Quantum Gravity giving exact results in the resolution of the singularity is not yet available, it is possible to start from the hypotheses of the Singularity Theorems and ask which one could be relaxed, as consistently as possible with physical requirements, in order to mimic background-independent effects that allow the avoidance of the singularity.

This semi-classical approach leads to the interesting area of research in which this thesis collocates, namely that of *non-singular (or regular) black holes*.

The basic idea is to build effective metrics solutions of the Einstein Equations such that the resulting SpaceTime is Schwarzschild-like in the outer region and, at the same time, singularity-free in the deep interior (see for example [Bardeen 1968; Dymnikova 1992; Hayward 2006; Hossenfelder, Modesto, and Premont-Schwarz 2010; Mazur and Mottola 2001; Nicolini 2005]).

The main goal of this work is to deeply study, thanks to classic and new tools, both static and dynamic properties of such solutions, in order to verify their physical plausibility.

The analysis is divided in three Parts, each of which contains two Chapters.

## Part I

The First Part is consecrated to a presentation of the principal features of *classic black holes*. Nevertheless, its aim is not to make a complete satisfactory review of the *classical black hole physics*, but to discuss those aspects that will be relevant in the following analysis.

Therefore, the First Chapter starts with the presentation of the *Schwarzschild's solution* to the Einstein's equations from where the study of black holes initially arose. The following more mathematical Section is dedicated to the proof of the Singularity Theorems that, as we already mentioned, lay at the basis of the motivations of this thesis.

Going beyond the purely classical properties, in Chapter 2 we introduce the machinery of *Quantum Field Theory in Curved SpaceTime* and *Bogoliubov's formalism* for particle creation. The astonishing result of *Hawking's radiation* naturally arises applying these formalisms to the Vaidya-Schwarzschild's metric: black holes radiate energy away with a Planck spectrum. Their complete evaporation implies the so called *information-loss paradox*: the evolution of a pure quantum state propagating on Vaidya-Schwarzschild metric is not unitary. Moreover, a discussion on the importance of the Hawking's result for the so called *black hole thermodynamics* introduces us to the concepts of black hole entropy and *entanglement entropy*. Since the latter plays as basis for the entire Chapter 6, we dedicate the last Section of this Part to its definition and basic features.

The Second and the Third Part represent the core of the thesis. As said before, the goal is to analyze *non-singular black holes* metrics both in their static and dynamic behavior. Therefore, we dedicate the Second Part to the study of the properties of such objects settled by the gravitational collapse of a spherical body and remaining in their static configuration. In the Third Part Hawking's radiation is turned on and the dynamic features are analyzed.

## Part II

The Second Part starts, in its first Chapter (Chapter 3), with the introduction of what is known about non-singular black holes. The first Section presents the proof of a theorem by Dymnikova [2002] asserting that, if such non-singular black holes exist, they must have a rather universal causal structure. This structure is

deeply studied in the second Section, focusing on the particular example proposed by Hayward [2006] and recently reconsidered by many authors [Bardeen 2014; Frolov 2014; Rovelli and Vidotto 2014].

Chapter 4, on the other hand, contains the first original results. We point out *two physical requirements that are not satisfied by the current metrics*, and show how to properly take them into account. Indeed, it seems physically unreasonable that a clock at the (regular) center of the star suffers no time delay with respect to a clock at infinity. Moreover, an effective metric that supposes to mimic quantum effects should capture the 1-loop quantum corrections to the Newton's potential obtained by John Donoghue using effective field theory. In the last Section a relatively easy *solution* is proposed (Modified Hayward's Metric), providing *a more realistic description of a non-singular black hole*.

## Part III

Static non-singular black holes form an event horizon. Therefore we expected Hawking's radiation and consequent evaporation to take place and the after-formation system to become *dynamic*.

In the introductory brief Chapter 5 we present some first insights in the problem considering the so called *quasi-statical approximation* to hold during the entire evaporation process. As in the original Hawking's evaporation case, the dynamics will be simply encoded allowing the mass of the black hole to decrease in time. Different scenarios are shortly discussed.

The main results, however, are presented in the last Chapter. Here the plausibility of evaporation processes is studied through the investigation of their *entanglement entropy production*, the so called *Page's curve*. This analysis is made quantitative possible thanks to a new covariant definition of entanglement entropy developed by Bianchi and Smerlak [2014a]. From this definition follows the possibility to give a precise characterization of entanglement entropy production and to analytically compute the Page's curve associated to any SpaceTime. In particular, applied to the Hayward's metric, this analysis *confirms the recover of unitarity*, but at the same time shines a light on *two non-easily solvable problems*. Namely, (*i*) the total energy radiated by the hole turns out to be much bigger than the initial ADM mass, and (*ii*) the so called purification time does not satisfies a physical lower bound we can impose on it. These inconsistencies undermine the physical validity of the dynamic Hayward's metric itself (and, because of the Dymnikova's theorem, of almost all the metrics so far proposed) as a good semi-classical approach to the resolution of the singularity and of the information loss paradox. Different ideas are needed. The new definition of entanglement entropy provides a powerful tool to analyze the physical plausibility of any semi-classical scenario of formation and consequent unitary evaporation that can be proposed, as for example the 'black hole firework' proposed by Haggard and Rovelli [2014] studied in the last Section of this work.

Up to now, however, no one of the proposal we encountered seems to satisfy all the requirements one can impose on it.

**Notation** Throughout this thesis we use metric signature $(-,+,+,+)$ and the Planck units $G = \hbar = c = 1$.

# Part I

# The Framework: Black Holes Physics

*Black holes are one of the most fascinating objects present in our Universe. They are regions of SpaceTime such that, because of an enormous gravitational force, everything is attracted to and cannot escape from them. Since "everything" includes light, the reason for the name* black *holes becomes clear. Initially considered just a as mathematical curiosity, during the 1960s they were shown to be generic predictions of General Relativity: any sufficiently massive collapsing star will form a black hole. More intriguing, we now know that our Milky Way, as well as other galaxies, hosts a supermassive black hole in its center.*

Black Holes are part of Nature.

# Summary



The main goal of this thesis is to deeply study static and dynamic properties of the so called *non-singular black holes*. To understand motivations and original results, however, we need to start form a presentation of the principal features of *classic black holes*. Nevertheless, the aim of this first part is not to make a complete satisfactory review of the *classical black hole physics*, but to discuss those aspects that will be relevant in the following analysis.

Therefore, the first Chapter starts with the presentation of the *Schwarzschild's solution* to Einstein's equations from where the study of black holes initially arose. At the basis of the motivations of this thesis is the presence of a *singularity* in such a solution which implies a breakdown of the theory. One of the main results of classical black hole physics is that *singularities are unavoidable*. The second Section is consecrated to make this statement mathematically precise, through the proof of the so called *Singularity Theorems*. While the aim of the first Section is to introduce the concept of black hole in a pictorially and intuitive way, the second presents a more mathematical approach.

Going beyond the purely classical properties, in the second Chapter we introduce the machinery of *Quantum Field Theory in Curved SpaceTime* and *Bogoliubov's formalism* for particle creation. *Hawking's radiation* naturally arises applying these formalisms to the Vaidya-Schwarzschild's metric and leading to the so called *information-loss paradox*: the evolution of a pure quantum state propagating on Vaidya-Schwarzschild metric is not unitary. In the last Sections, a discussion on the importance of the Hawking's result for the so called *black hole thermodynamics* introduces us to the concepts of black hole entropy and *entanglement entropy*. Since the latter plays as basis for the entire Chapter 6, we dedicate the last Section of this Part to its definition and basic features.

Chapter 1

# Classical Properties

## 1.1 Schwarzschild solution

In 1916, a few months after Einstein's presentation of the theory of General Relativity, Karl Schwarzschild found a solution of the Einstein Field Equation for the exterior of a *static, stationary, spherically symmetric* source of gravitational mass, for example a spherical star. The resulting SpaceTime is described by the well known line element

$$ds^2 = -\left(1 - \frac{2m}{r}\right) dt^2 + \left(1 - \frac{2m}{r}\right)^{-1} dr^2 + r^2\, d\Omega^2 \tag{1.1}$$

where $d\Omega^2 = d\theta^2 + \sin^2\theta\, d\varphi^2$ is the standard solid angle element.[1] The coordinate $r$ is defined as the function such that the euclidean expression for the aerea $A$ of a two-sphere is preserved, i.e.

$$A = 4\pi\, r^2 \tag{1.2}$$

and $dq^2 = r^2\, d\Omega^2$ is the induced metric, in spherical coordinates $(\theta, \varphi)$, on each two-sphere $S^2_\omega$. The set $(t, r, \theta, \varphi)$ is usually called *Schwarszchild coordinates set*, and $r$ the "radial coordinate", even if, in curved space, it doesn't represent the distance from the surface of the sphere to its center, itself ill-defined.

The source object, say a star, can have a spatial dimension being a sphere of radius $R$. The exterior solution (1.1) has then to be glued with a solution describing the interior, as for example the one proposed by Oppenheimer and Snyder [1939]. However, in the following, the SpaceTime of interest is the one generated by a dimensionless source fixed at the "origin" $r = 0$: the line element is then (1.1) on $\mathbb{R}_t \times ]0, +\infty[_r \times S^2_\omega$.

**Singularities** The metric becomes singular both at the origin $r = 0$ and at the so called *Schwarzschild radius* $r_H \equiv 2m$. The existence and nature of this surface, which is of fundamental relevance for the definition of the black hole

[1] For the complete derivation of the solution see [Wald 1984, pp. 118-125].

itself, is cause of historical controversy because of the singular behavior of the metric on it. Of particular help for the acceptance of such a weird object was the construction of a coordinate system which is regular on $r = r_H$. Indeed, a singularity can be of two different types: it can be an *essential singularity* or a *coordinates singularity*, also called *apparent singularity* since it can be eliminated with a change of coordinate system.[2] Coordinates invariant objects can give us strong indications on the nature of the singularities, as for example the so called *Kretschmann scalar*

$$\mathcal{K}^2 \equiv R_{abcd}R^{abcd} = \frac{48\,m^2}{r^6}\ , \tag{1.3}$$

where $R_{abcd}$ is the *Riemann tensor*; it indicates that nothing special happens at $r = r_H$, in contrast with the origin $r = 0$ where the singularity seems to be essential.[3] Only in the 60th the controversy was answered satisfactorily by the explicit construction of new coordinates systems such that the apparent singularity is eliminated. Nevertheless, this led to the concept of *extension* of a SpaceTime region, defined as finding a non-singular SpaceTime which includes the original one as a subset. In this way is possible to build a coordinates system that cannot be extended further. The resulting SpaceTime is said to be *maximally extended*. In the following, throughout the definition of various coordinates sets, we'll construct the *maximal extension* of the Schwarzschild SpaceTime. Furthermore, the intermediate sets of coordinates will play a crucial role in the following Chapters.

### 1.1.1 Eddington-Finkelstein Extension

For a generic function $F(r)$, let us define the *tortoise coordinate* $r^\star$ as

$$dr^\star \equiv \frac{dr}{F(r)}\ , \tag{1.4}$$

the *retarded null coordinate* $v$ as

$$v \equiv t + r^\star \tag{1.5}$$

and the *advanced null coordinate* $u$ as

$$u \equiv t - r^\star\ . \tag{1.6}$$

In the Schwarzschild SpaceTime, radial ($d\Omega^2 = 0$) null geodesics ($ds^2 = 0$) verify the equation

$$dt^2 = \frac{dr^2}{F(r)^2} \tag{1.7}$$

that in terms of the tortoise coordinate reads

$$d(t \pm r^\star) = 0\ , \tag{1.8}$$

[2] This is true not only in GR. Take for example spherical coordinates in 3D and an object moving along a meridian, say 0 degrees longitude, on the surface of a sphere. It will suddenly experience an instantaneous change in longitude at the pole, passing from 0 to 180 degrees. However it is intuitively clear that no real singularity is present. This discontinuity is an artifact of the coordinate system chosen, which is singular at the poles.

[3] For a mathematical definition of singularity see Section 1.2.1.

where $r^\star$ assumes the explicit expression

$$r^\star \equiv r + 2m \log \left| \frac{r}{2m} - 1 \right| \ , \tag{1.9}$$

and diverges in the limit $r \to 2m$. From Eq. (1.8), therefore, one can notice that the time required to an observer sits at $r > 2m$ to see an object crossing the surface $r = 2m$ diverges.[4] This means that the SpaceTime described by Schwarzschild coordinates has two disconnected patches: the *outer region* $r > 2m$ and the *inner region* $r < 2m$. Moreover, one can naturally parametrize an *ingoing* (resp. *outgoing*) radial null geodesic by fixing the value of the coordinate $v$ (resp. $u$), and label the SpaceTime points by giving values for $(v, r, \theta, \varphi)$ (resp. $(u, r, \theta, \varphi)$). In this way, we defined two new coordinates sets: the *advanced Eddington-Finkelstein coordinates set* $(v, r, \theta, \varphi)$ and the *retarded Eddington-Finkelstein coordinates set* $(u, r, \theta, \varphi)$ [Eddington 1924; Finkelstein 1958]. In terms of the first, the metric (1.1) reads

$$ds^2 = -\left(1 - \frac{2m}{r}\right) dv^2 + 2\, dv\, dr + r^2\, d\Omega^2 \ ; \tag{1.10}$$

no singularity appears in $r = 2m$, so that the SpaceTime is regular on $\mathbb{R}_v \times ]0, +\infty[_r \times S^2_\omega$. Usually, the term "Schwarzschild coordinates set" refers only to the connected outer patch $r > 2m$; $(t, r, \theta, \phi)$ are then defined only in $\mathbb{R}_t \times ]2m, +\infty[_r \times S^2_\omega$ and the Eddington-Finkelstein set represents an *extension* of the original one.

To investigate the physical structure of this SpaceTime, take radially propagating light rays. The geodesic equation for which

$$0 = ds^2 = -\left(1 - \frac{2m}{r}\right) dv^2 + 2\, dv\, dr \tag{1.11}$$

gives two solutions

$$dv = 0 \tag{1.12a}$$

$$\frac{dr}{dv} = \frac{1}{2}\left(1 - \frac{2m}{r}\right) \ , \tag{1.12b}$$

respectively for *in-going* and *out-going* null rays. Their behavior is plotted in Fig. 1.1(a) in the plane $t^\star$-$r$, where $t^\star$ is the *Eddington-Finkelstein time* defined as $t^\star \equiv v - r$. When $r \to \infty$ light cones are *tilted* approaching the surface $r = 2m$, pointing *inward* in the region $r < 2m$. Since any physical object moves along either timelike or null geodesics,[5] nothing can escape from the surface to reach a static external observer, but it is *condemned to fall* into the singularity at $r = 0$. That's why the interior region $r < 2m$ is called the *black hole (BH) region* and its boundary $r = 2m$ the *future event horizon*.

[4] The name *tortoise coordinate* comes form the well known Zenone's paradoxes on an imaginary footrace between Achille and a tortoise. The motivation is clear: just like Achille who can never reach the tortoise, a static observer in the outer region can never see an object crossing $r = r_H$.

[5] See Appendix A.

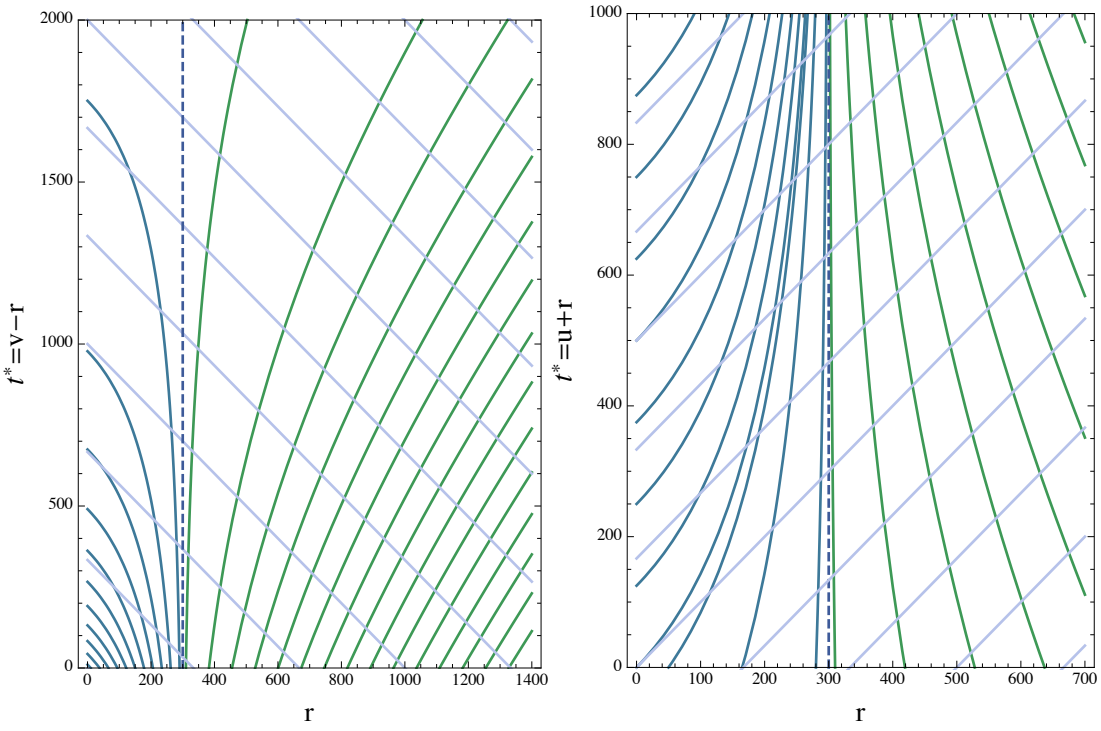


(a) Advanced — black hole.

(b) Retarded — white hole.

**Figure 1.1.** Null radial geodesics equation solutions for the advanced and retarded Eddington-Finkelstein SpaceTime. The dashed vertical line is the future (resp. past) horizon $r = 2m$. Here $m = 150$ (Planck units).

**White Holes** If we extend the Schwarzschild SpaceTime with retarded Eddington-Finkelstein coordinates, the line element (1.1) becomes

$$ds^2 = -\left(1 - \frac{2m}{r}\right) du^2 - 2\, du\, dr + r^2\, d\Omega^2 \,. \tag{1.13}$$

The same analysis reveals that the light cones are still tilted, but in a crucially different way with respect to the previous case (see Fig. 1.1(b)). Any timelike or null geodesic *must now escape* from the surface $r = 2m$ which acts as a one-way membrane, but in the opposite direction. It is called the *past event horizon* and the interior region is called *white hole region.*

Roughly speaking a white hole (WH) is a region of spacetime which cannot be entered from the outside, although matter and light must escape from it. In this sense, it is the *time-reverse* of a black hole, which can only be entered from the outside and from which nothing, including light, can escape. We have to remark that WH regions do not exist in a gravitational collapse geometry.

### 1.1.2 Kruskal-Szekeres Extension

Up to now we have seen three different coordinates systems: the patch of $(t, r, \theta, \varphi)$ only covers the exterior region $r > 2m$, $(v, r, \theta, \varphi)$ allows to cover the black hole region as well as $(u, r, \theta, \varphi)$ to cover the white hole one. This suggests the existence

of a new extension that can include both back and white hole regions. To find this new set of coordinates, one starts by writing the metric using coordinates $v$ and $u$ together:

$$ds^2 = -\left(1 - \frac{2m}{r}\right) du\, dv + r(u,v)^2 d\Omega^2 \tag{1.14}$$

where now $r$ is a function of $(u, v)$ defined by

$$e^{\frac{r}{2m}} \left(\frac{r}{2m} - 1\right) = e^{\frac{v-u}{4m}} , \tag{1.15}$$

and the Schwarzschild time can be recovered by

$$t = \frac{u+v}{2} . \tag{1.16}$$

In this double-null form, the metric presents the same drawback of the standard Schwarzschild one: both future and past horizons are located, respectively, at the limit points $u = +\infty$ and $v = -\infty$. However, performing another change of coordinates via the definition of

$$\begin{cases} V & \equiv 4m\, e^{\frac{v}{4m}} \\ U & \equiv -4m\, e^{-\frac{u}{4m}} , \end{cases} \tag{1.17}$$

called *Kruskal-Szekeres* coordinates [Kruskal 1960; Szekeres 1960], points in the future horizon turn out to be parametrized by the coordinates $(U = 0, V, \theta, \varphi)$ and those in the past horizon by $U, V = 0, \theta, \varphi)$. The metric becomes

$$ds^2 = -\frac{2m}{r}\, e^{-\frac{r}{2m}}\, dV\, dU + r^2(U,V) d\Omega^2 , \tag{1.18}$$

with $r(U, V)$ defined implicitly by

$$e^{\frac{r}{2m}} \left(\frac{r}{2m} - 1\right) = -\frac{UV}{16m^2} , \tag{1.19}$$

and coordinate $t$ by

$$\frac{t}{2m} = \log\left(-\frac{U}{V}\right) . \tag{1.20}$$

Even if, from the definition (1.17), Kruskal coordinates belong to the ranges $V \in (0, +\infty)$ and $U \in (-\infty, 0)$, the metric is not singular and can be extended to the full $\mathbb{R}_V \times \mathbb{R}_U \times S^2_\omega$. Therefore they represent the *maximal extension* of the original Schwarzschild SpaceTime.

The term "Kruskal-Szekeres extension" refers sometimes also to its *time-space variant*, constructed defining

$$\begin{aligned} T &\equiv \frac{V+U}{2} \\ X &\equiv \frac{V-U}{2} , \end{aligned} \tag{1.21}$$

which gives

$$ds^2 = \frac{2m\, e^{-\frac{r}{2m}}}{r} \left(-dT^2 + dX^2\right) + r^2(T,X)\, d\Omega^2 \tag{1.22}$$

where the definition of $r(X, T)$ follows from Eq. (1.19)

$$e^{\frac{r}{2m}} \left(\frac{r}{2m} - 1\right) = \frac{X^2 - T^2}{16m^2} . \tag{1.23}$$

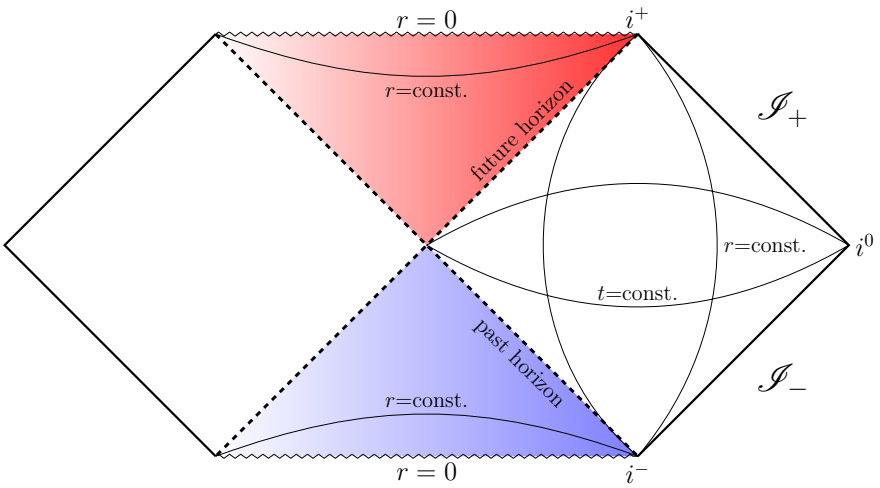


**Figure 1.2.** Penrose-Carter diagram of the Kruskal-Szekeres SpaceTime. The black hole region is red-shaded, while the blue-shaded triangle is the white hole region.

**Causal structure** As we know, the relevant features of a given SpaceTime are encoded in its *causal structure*, i.e. in the causal relationships between events (which events can influence which other events).[6] As explained in Appendix A, the easiest way to figure out that structure is to draw the Carter-Penrose diagram, namely the figurative result of a process of conformal compactification of the SpaceTime into a finite region. In the Appendix this technique is presented and the diagram in the Kruskal-Szekeres is obtained. The result is depicted in Fig. A.3. Without going into the details, it is sufficient to understand what lines and points represent in that figure. Thanks to the spherical symmetry of the system, $\theta$-$\varphi$ dimensions are suppressed, so that at each point inside the contour corresponds an event at a given $U$ and $V$, namely a 2-sphere of radial coordinate $r(U, V)$ at a given instant of time. Thanks to the compactification process, asymptotic regions are squeezed into the peculiar points $i_0$, $i_+$, $i_-$ and lines $\mathscr{I}_+$ and $\mathscr{I}_-$. Their interpretation is summarized in the following Table:

| | | Schwarzschild | Kruskal |
|---|---|---|---|
| spacelike infinity | $i^0$ | $r \to +\infty$ at fixed $t$ | $V \to +\infty$, $U \to -\infty$ |
| future timelike infinity | $i^+$ | $t \to +\infty$ at fixed $r$ | $V \to +\infty$, $U \to 0$ |
| past timelike infinity | $i^-$ | $t \to -\infty$ at fixed $r$ | $V \to 0$, $U \to -\infty$ |
| future null infinity | $\mathscr{I}_+$ | $t \to +\infty$, $r \to +\infty$ at fixed $t - r$ | $V \to +\infty$ at fixed $U$ |
| past null infinity | $\mathscr{I}_-$ | $t \to -\infty$, $r \to +\infty$ at fixed $t + r$ | $U \to -\infty$ at fixed $V$ |

Straight lines at 45 degrees are either $U$ or $V$ constant geodesics, i.e. outgoing and ingoing null ray that form 90 degrees light cones, while the horizontal lines $r = 0$ are the (spacelike) past and future singularities. The diagram presents four different regions, depending on the signs of $U$ and $V$, which are bounded by the horizons $U = 0$ and $V = 0$.

[6] See Appendix A.

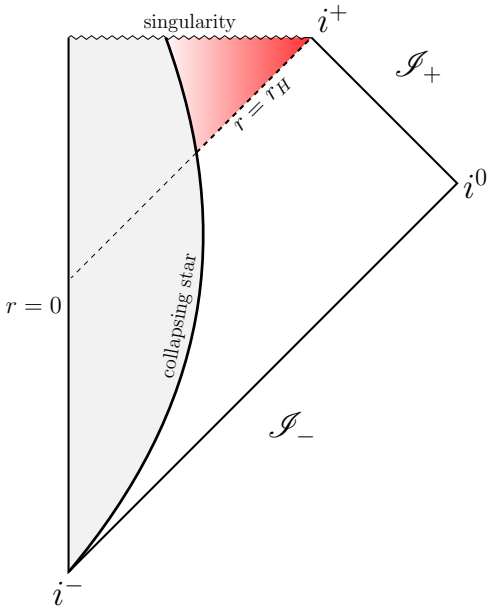


**Figure 1.3.** Penrose-Carter diagram of a collapsing star process. The black hole region is red-shaded.

| | | |
|---|---|---|
| I | $U < 0,\ V > 0$ | Usual outer region $r > 2m$ |
| II | $U > 0,\ V > 0$ | Black hole region |
| III | $U < 0,\ V < 0$ | White hole region |
| IV | $U < 0,\ V > 0$ | Another outer region causally disconnected |

From definitions (1.17) follows that the advanced (resp. retarded) Eddington-Finkelstein coordinates set only covers Regions I and II (resp. I and III), as expected.

The presence of Region II and IV is a mathematical consequence of the time reversibility of Einstein Equations. However, in the physical spherical collapse scenario the time symmetry is broken and those regions do not exist, replaced by a regular metric describing the collapsing body. The Penrose diagram for this process is given in Fig. 1.3: only Region I and II have survived.

### 1.1.3 Vaidya Solution

The dynamical scenario of the collapse of a spherical distribution of mass should be solved assuming some explicit form for the distribution of the collapsing mass, for example the before mentioned Oppenheimer-Snyder proposal. Nevertheless, the process can be described in ideal terms using a metric due to Vaidya [1951], namely

$$ds^2 = -\left(1 - \frac{2m(v)}{r}\right) dv^2 + 2\, dv\, dr + r^2\, d\Omega^2 \ . \tag{1.24}$$

The only non-null component of the associated momentum-energy tensor is

$$T_{vv} = \frac{m'(v)}{4\pi\, r^2} \tag{1.25}$$

i.e. a purely ingoing radial flux of radiation described by $m'(v)$, where prime denotes the derivative with respect to $v$.

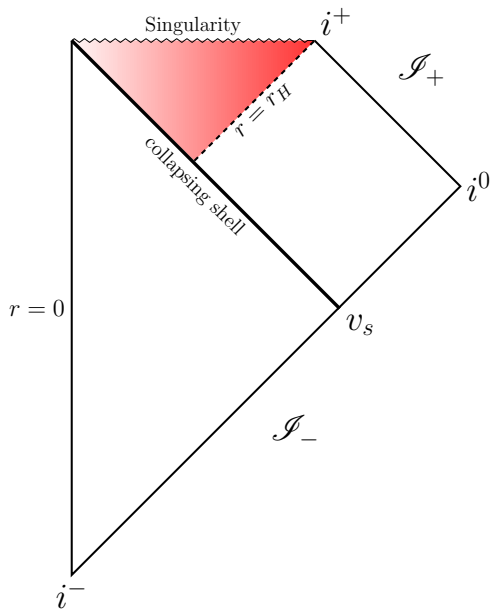


**Figure 1.4.** Penrose-Carter diagram of a collapsing star process in the thin shell Vaidya approximation. A Minkowski patch is glued with the black hole SpaceTime along a null line $v = v_s$. The black hole region is shaded.

The simplest case is to imagine an influx radiation turned on at some finite advanced time $v_s$, that is $m(v) = m\Theta(v - v_s)$: this simplified scenario will play a crucial role in the following discussion, in particular in Chapters 2 and 6. It represents a thin null shell collapsing at the speed of light carrying a non-null energy-momentum tensor resulting in a black hole of mass $m$. The Penrose diagram of this process is depicted in Fig 1.4 and is the result of the gluing of a Minkowski patch *inside the shell* with a Schwarzschild region outside of it.

**Remark** Gluing two different metrics along a general hypersurface $\Sigma$ is not always possible in a way such that the union of the metrics forms a valid solution to the Einstein Equations. Some conditions on the three-tensors on $\Sigma$ have to be imposed to ensure a smooth passage from one metric to one another. This restrictions, known as *junction conditions*, rely the *jump* of three-tensors (as *induced metric* and *intrinsic curvature*) across the hypersurface with the matter content of the resulting space time, as very clearly explained in Poisson [2004, p. 84-94].

A complete introduction to the classical properties of black holes should continue in discussing the possibility of such objects to be charged or to rotate, as well as the *Penrose and Floyd [1971] mechanism* to extract energy from them; the *Birkhoff and Langer [1923]* and the *no-hair* theorems; the so called *laws of BH thermodynamics* [Bekenstein 1973], and the crucial Singularity Theorems. However, in the entire thesis only *spherical, non-rotating and non-charged collapsing objects* are considered and only the last argument, namely the Singularity Theorems, will play a fundamental role. For these reasons, we skip the excursus on non-crucial topics that will be just touched on during the main discussion.

What we are going to do in the next Section, therefore, is to formalize the pictorial picture given before, introducing more precise mathematical definitions and tools, essential for the goal of this Section, that is *the proof* of Singularity

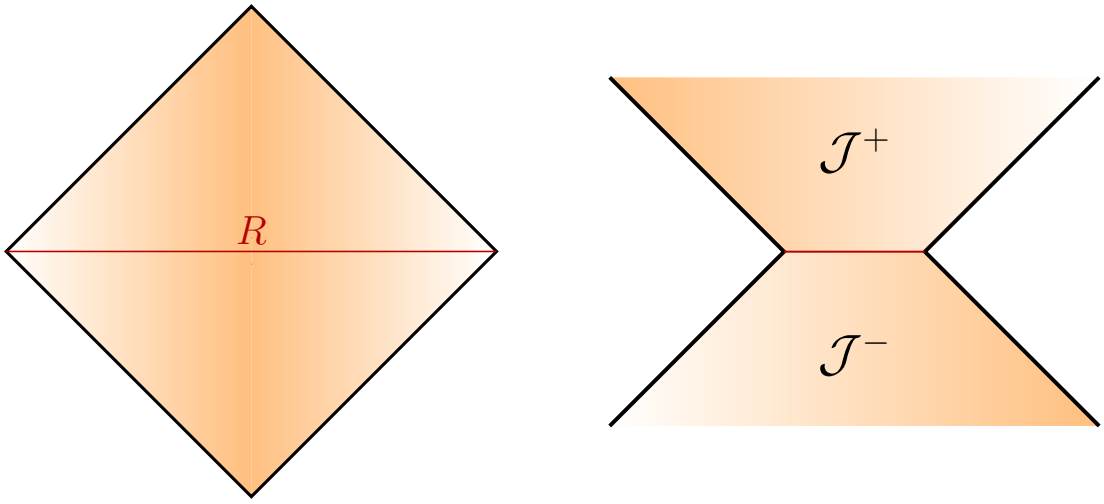


(a) (b)

**Figure 1.5.** Pictorial representation of (a) causal future $\mathcal{J}^+$ and past $\mathcal{J}^-$, and (b) future $\mathcal{D}^+$ and past $\mathcal{D}^-$ Cauchy developments of a set of points in $(1+1)$-dimensional Minkowski SpaceTime.

Theorems.

## 1.2 Singularity Theorems

The following analysis requires the basic knowledge on differential geometry that each book on General Relativity can provide, as for example Wald [1984] and Hawking and Ellis [1973] (see Isham [2002] for a more complete dissertation).

### 1.2.1 Mathematical Definitions

In the previous Section, we introduced the concept of black hole region as a "region of SpaceTime from which nothing can escape". How to translate this sentence in a precise mathematical expression? In Appendix A the notions of *causal past (resp. future)* $\mathcal{J}^-$ *(resp.* $\mathcal{J}^+$*)* and of *Cauchy developments* $\mathcal{D}^-$ *(resp.* $\mathcal{D}^+$*)* of points and sets in a SpaceTime $(\mathscr{M}, g_{ab})$ are defined. In Fig. 1.5 their intuitive representations in $(1+1)$-dimensional flat space are reproduced. Thinking in terms of these objects and looking at the Penrose's diagram in Fig. 1.3, the first idea could be to define a *black hole region as a subset* $E$ *of the whole SpaceTime* $\mathscr{M}$ *such that for any point* $x \in E$ *we have the causal future of* $x$ *to be contained in* $E$. However, with this definition the causal future of any subset would be a black hole region.

A precise characterization can be given restricting our discussion to *strongly asympotically predictable* SpaceTimes, namely to *asymptotically flat* SpaceTimes which do not contain *naked singluarities*. Asymptotically flat means that there is a region far from which the SpaceTime is flat. In the case of Schwarzschild solution this region can be any sphere at finite radius coordinate $r$ at a given time $t$: indeed $F(r) \to 1$ as $r \to \infty$ and the SpaceTime tends to be Minkowskian.

A naked singularity, on the other hand, is a singularity which is not covered ('hidden') by an event horizon. Precise definitions can be found in Frolov and Zelnikov [2011, p. 355].

Since all the systems we will work with satisfy these requirements, let us say that:

**Definition 1.1 — Black hole**
A SpaceTime $\mathscr{M}$ is said to contain a *black hole* if $\mathscr{M}$ is not a subset of the causal past $\mathcal{J}^-$ of future null infinity $\mathscr{I}_+$, namely

$$\mathscr{M} \nsubseteq \mathcal{J}^-(\mathscr{I}_+) \,. \tag{1.26}$$

The *black hole region* $\mathcal{B}$ is

$$\mathcal{B} \equiv \mathscr{M} \setminus \mathcal{J}^-(\mathscr{I}_+) \tag{1.27}$$

and its boundary

$$\mathcal{H} \equiv \dot{\mathcal{J}}^-(\mathscr{I}_+) \cap \mathscr{M} \tag{1.28}$$

is the *event horizon*.

Next step is to properly define a *singularity*. The before given intuitive notion of such objects as 'the place in a SpaceTime where the metric is pathological and the curvature blows up' is, as it was for the notion of black hole, non directly translatable in mathematical term. The reason is subtle and well illustrated in the Section "What is a singularity?" in Wald's book [Wald 1984, p. 212] and in Dieks [2008, p. 111]. Again, a satisfactory characterization can be provided in a restrict class of SpaceTime: the class of *inextensible* SpaceTime, i.e. which are not isometric to a subset of another SpaceTime. Thus the following definition is given:

**Definition 1.2 — Singularity**
A *singularity* is an event of a SpaceTime from which *at least one* geodesic cannot be extended further in the past or in the future, where the future is the direction along which the affine parameter of the geodesic increases.

Pictorially, a SpaceTime is singular if there exists an unlikely observer that ends his life in a finite proper time, disappearing when it "meets" the singularity. The need of the restriction to inextensible SpaceTime is now clear: it avoids the possibility to remove artificially a point that would be considered singular. Another important fact to remark is the presence of the emphasized expression "at least one" in the definition. The proof of the Singularity Theorems, indeed, will be based on it.

Provided a technical definition of the objects found in the first Section, we can now go further on the road to the Singularity Theorems, introducing new concepts and tools.

### 1.2.2 Global hyperbolicity

In the proof of such theorems, as well as in the discussion on non-singular black holes in the next Part of this thesis, a crucial role is played by the notion of *global*

*hyperbolicity* of a SpaceTime. To properly define it, we need some more concepts about causal structures. A set $S$ of points in a SpaceTime $(\mathscr{M}, g_{ab})$ is said to be *achronal* if there do not exist $q, r \in S$ such that $r \in \mathcal{J}^+(q)$ or, equivalently, $S$ is disjoint from $\mathcal{J}^+(S)$. Roughly speaking, a set is achronal if it does not influence itself. Take now a closed and achronal set $S$. It is said to be a *slice* of $(\mathscr{M}, g_{ab})$ if there are no $q \in \mathcal{J}^+(S)$ and $p \in \mathcal{J}^-(S)$ which can be connected by a timelike curve without intersecting $S$. Finally,

**Definition 1.3 — Globally Hyperbolic SpaceTime**
A SpaceTime $(\mathscr{M}, g_{ab})$ is said to be *globally hyperbolic* if admits a slice $\Sigma$ such that $\mathcal{D}^+(\Sigma) \cup \mathcal{D}^-(\Sigma) = \mathscr{M}$, that is the Cauchy development of $\Sigma$ covers the entire SpaceTime. In this case, the slice $\Sigma$ is said to be a *Cauchy surface* for $(\mathscr{M}, g_{ab})$.

This definition generalizes to curved SpaceTimes the intuitive behavior of causal structure we have for the flat case. Indeed, the presence of global hyperbolicity implies the possibility to choose a global timelike vector field $(\partial/\partial t)^a$ such that hypersurface of constant $t$ are Cauchy surfaces of $(\mathscr{M}, g_{ab})$: $\mathscr{M}$ has topology $\mathscr{M} \cong \mathbb{R} \times \Sigma$. The natural interpretation is that Cauchy slices correspond to *initial conditions* surface at fixed time from which the entire history of the SpaceTime can be predicted.

An asymptotically flat SpaceTime $(\mathscr{M}, g_{ab})$ possesses a property that will be crucial in the proof of the Singularity Theorems. Namely, it comes out that for each point $p \in \mathscr{M}$ *the its future causal development* $\mathcal{J}^+$ *is closed*. Another way to say this is that *the future light cone* $E^+(p)$ *of any point* $p$ *coincides with the boundary of its causal development* $\dot{\mathcal{J}}^+$. The results extend to compact submanifolds $K \subset \mathscr{M}$. A SpaceTime that satisfies this requirement is said to be *future causally simple*.

## 1.3 Raychaudhuri's Equation

**Definition 1.4 — Congruence**
Consider now an open set $O \in \mathscr{M}$. A *congruence* in $O$ is a family of curves such that through each point $p \in O$ passes precisely one curve in this family.

In this way, the tangents to a congruence will produce a vector field in $O$ and at the same time any continuos vector field generates a congruence of curves. Now, take a geodesic $\gamma$ with affine parameter $\tau$ in a congruence and call $\xi^a$ the vector field tangent to it such that $\xi^a \xi_a = -1$. Take another geodesic $\gamma'$ infinitesimally close to $\gamma$ and call $\eta^a$ the vector field orthogonal to $\xi^a$: it represents the *infinitesimal spatial displacement* from $\gamma$ to the nearby geodesic. Due to the curvature of the SpaceTime an observer who is moving along $\gamma$ would see the nearby geodesic to move away, to rotate, to be stretched and so on. See Fig. 1.6. Mathematically this means that the displacement vector is not *parallelly transported* along $\gamma$, namely

$$\frac{d\eta^a}{d\tau} = \xi^b \nabla_b \eta^a = \eta^b \nabla_b \xi^a \equiv B^a_b \eta^b \,, \tag{1.29}$$

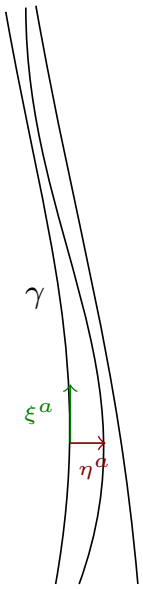


**Figure 1.6.** Pictorial representation of a congruence of geodesic. Thinking of the curves as infinitesimally nearby, the vector $\eta^a$ is the *infinitesimal displacement vector*.

where the second equivalence comes from the fact that the *Lie derivative* of $\eta$ along $\xi$ is null. The linear map $B_{ab} \equiv \nabla_b \xi_a$, therefore, represents the measures of this failure of $\eta^a$ to be parallelly transported. Moreover, in the tangent space, the vector $\xi^a$ defines a subspace orthogonal to it. The induced metric $h_{ab}$ on this hypersurface can be defined as

$$h_{ab} = g_{ab} + \xi_a \xi_b \ . \tag{1.30}$$

To depict the situation, we can think of $\xi^a$ as the time direction and the orthogonal subspace as the space at a given moment of time, with $h^a_b$ the projector operator onto it.

We can now define the irreducible components of the tensor $B_{ab}$ as

$$\begin{cases} \theta \equiv B^{ab} h_{ab} & \text{expansion ;} \\ \sigma_{ab} \equiv B_{(ab)} - \dfrac{1}{3}\theta\, h_{ab} & \text{shear ;} \\ \omega_{ab} \equiv B_{[ab]} & \text{twist ,} \end{cases} \tag{1.31}$$

in which $B_{ab}$ is decomposed

$$B_{ab} = B_{[ab]} + B_{(ab)} = \frac{1}{3}\theta\, h_{ab} + \sigma_{ab} + \omega_{ab} \ . \tag{1.32}$$

The pictorial interpretation of these quantities is depicted in Fig. 1.7. Furthermore, from the normalization of $\xi^a$ follows that $B_{ab}$ is *purely spatial*, i.e.

$$B_{ab}\xi^a = B_{ab}\xi^b = 0 \tag{1.33}$$

and from here analogous equations for shear and twist. Given these quantities, a simple computation brings to the so called *Raychaudhuri's equation*:

$$\frac{d\theta}{d\tau} = -\frac{1}{3}\theta^2 - \sigma_{ab}\sigma^{ab} + \omega_{ab}\omega^{ab} - R_{ab}\xi^a\xi^b \ , \tag{1.34}$$

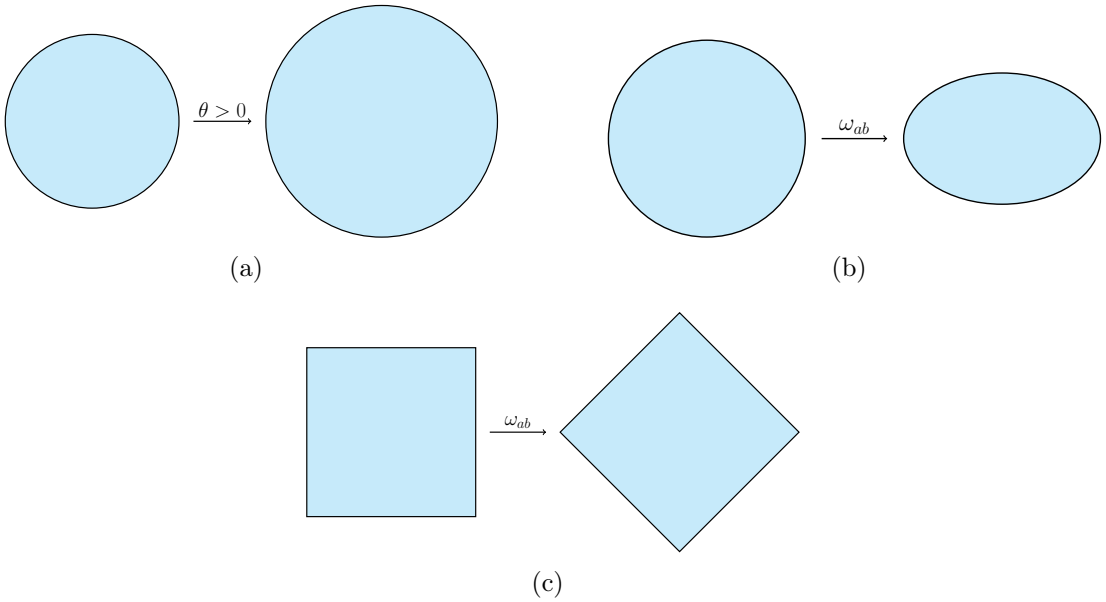


**Figure 1.7.** Pictorial meaning of (a) expansion, (b) shear and (c) twist.

where $R_{ab}$ is the Ricci tensor. In the case of hypersurfaces orthogonal congruence, i.e the tangent vectors in the congruence are everywhere orthogonal to the spatial hypersurfaces in some foliation of the spacetime, $\omega_{ab}$ vanishes (Frobenius' theorem — see Wald [1984, App. B3]) and the equation reduces to

$$\frac{d\theta}{d\tau} = -\frac{1}{3}\theta^2 - \sigma_{ab}\sigma^{ab} - R_{ab}\xi^a\xi^b \,. \tag{1.35}$$

The term $\omega_{ab}\omega^{ab}$ is positive because the induced metric has signature $(+++)$. As shown in Appendix B, the term $R_{ab}\xi^a\xi^b$ is exactly the quantity considered non-negative in the definition of the strong energy condition (SEC). Thus, if we require gravity to be attractive (this is the physical significance of the SEC) $R_{ab}\xi^a\xi^b \geq 0$, we find the important inequality

$$\frac{d\theta}{d\tau} \leq -\frac{1}{3}\theta^2 \,, \tag{1.36}$$

that integrated in $[0, \tau]$ gives

$$\theta(\tau) \leq \frac{3\,\theta(0)}{3 + \theta(0)\,\tau} \,. \tag{1.37}$$

That's it. If the expansion is initially negative, i.e. the congruence is initially converging, it will reach $-\infty$ in a finite amount of proper time $\tau \leq \frac{3}{|\theta(0)|}$. The reasoning is generalizable, with some slight modification, to null geodesic congruence (see Wald [1984, p. 221]). Let us summarize and fix the result in the following Lemma.

**Lemma 1.1**
*Let $\xi^a$ be a tangent field of a hypersurfaces orthogonal timelike* (resp. null) *geodesic congruence. Suppose $R_{ab}\xi^a\xi^b \geq 0$ as in the case the matter content of*

*the SpaceTime satisfies the SEC* (resp. either SEC or WEC). *If the expansion* $\theta$ *takes the negative value* $\theta_0$ *at some point, then* $\theta \to -\infty$ *in a finite proper time* $\Delta\tau \leq 3/|\theta_0|$ (resp. $\Delta\lambda \leq 2/|\theta_0|$).

The point where all the geodesics of the congruence converge is called *caustic*. At first sight it could seem that the presence of a caustic implies the presence of a singularity. However this is not generally true for any SpaceTime. Singularity Theorems tell us under which requirements it becomes true.

Strongly related to the concept of caustic is the notion of *conjugate points*. In curved SpaceTimes, the idea of a geodesic connecting two points as the *unique* path that *extremizes* the proper length fails. Take for example a sphere: the geodesics connecting the north and the south pole are all the infinite "meridians" and they have the same proper length. Given two points $q, p \in (\mathscr{M}, g_{ab})$, therefore, they can be connected by two geodesics. If this two geodesics $\gamma$ and $\gamma'$ are infinitesimally close, then the points $p, q$ are said to be *conjugate*.

Now, take the point $p$ and a congruence of timelike curves that pass through $p$; of course, the congruence is singular in $p$. In Wald [1984, p. 226] is shown that a point $q$ is conjugate to $p$ if and only if the congruence of timelike geodesics emanating from $p$ has $\theta \to -\infty$ at $q$. Since it is possible to show that such a congruence is hypersurface orthogonal [Hawking and Ellis 1973, Lemma 4.5.2], Lemma 1.1 implies the following result on the existence of conjugate points:

**Lemma 1.2**
*Let* $(\mathscr{M}, g_{ab})$ *be a SpaceTime satisfying* $R_{ab}\xi^a\xi^b$ *for all timelike* $\xi^a$. *Let* $\gamma$ *be a timelike geodesic and let* $p \in \gamma$. *Suppose the convergence of timelike geodesics emanating from* $p$ *attaints the negative value* $\theta_0$ *at* $r \in \gamma$. *Then within proper time* $\Delta\tau \leq 3/|\theta_0|$ *from* $r$ *along* $\gamma$ *there exists a point* $q$ *conjugate to* $p$, *assuming* $\gamma$ *extends that far.*

Moreover, the two infinitesimally close geodesics defining two conjugate points $p$ and $q$, define also a displacement vector $\eta^a$. It is clear that $\eta^a$ vanishes both at $p$ and $q$, while can be non-null in between. This idea can be used to generalize the definition of conjugate points to the concept of *conjugate points to a hypersurface*. Think the curves $\gamma$ and $\gamma'$ to be cut in their path from $p$ to $q$ by a hypersurface $\Sigma$ orthogonal to the curves. Reversely, we can now think to $\gamma$ and $\gamma'$ as geodesics of a congruence orthogonal to $\Sigma$. Therefore, we can say that the point $p$ is *conjugate to* $\Sigma$ *along the geodesic* $\gamma$, if there exists an orthogonal displacement vector $\eta^a$ to $\gamma$ that is non-zero on $\Sigma$ and vanishes at $p$.

In terms of conjugate point to hypersurfaces, Lemma 1.2 becomes

**Lemma 1.3**
*Let* $(\mathscr{M}, g_{ab})$ *be a SpaceTime such that* $R_{ab}\xi^a\xi^b \geq 0$ *for all timelike vector field* $\xi^a$, *and let* $\Sigma$ *be a spacelike 3-dimensional hypersurface with negative expansion* $\theta < 0$ *at a point* $q$. *Then every timelike geodesic* $\gamma$ *orthogonal to* $\Sigma$ *develops a conjugate point within a proper time* $\Delta\tau \leq 3/|\theta|$, *assuming that* $\gamma$ *can be extended so far.*

If we consider null geodesics, we need to be more cautious. Indeed, by definition

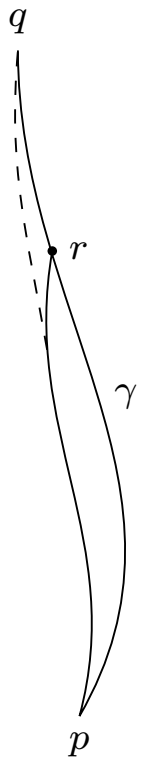


**Figure 1.8.** The geodesic $\gamma$ possess a conjugate point between $p$ and $q$. Then it is always possible to construct a nearby geodesic with larger elapsed time. $\gamma$ doesn't extremize the proper length.

$\xi^a\xi_a = 0$, a null vector is orthogonal to itself or equivalently, any orthogonal vector to $\xi^a$ is also tangent to it. Without going into details, we just need to know that the transverse hypersurface of a congruence of null geodesics is 2-dimensional instead of 3-dimensional. A $2D$ surface possesses two null orthogonal vectors that we can arbitrarily label as *outgoing* and *ingoing*. Therefore, it possesses also an outgoing and an ingoing expansion. With these remarks, the previous Lemma can be slightly modified in the null case:

**Lemma 1.4**
*Let $(\mathscr{M}, g_{ab})$ be a SpaceTime such that $R_{ab}\xi^a\xi^b \geq 0$ for all null vector field $\xi^a$, and let $S$ be a spacelike 2-dimensional hypersurface with negative outgoing (or ingoing) expansion $\theta < 0$. Then within a proper length $\Delta\lambda \leq 2/|\theta|$, there exists a point $p$ conjugate to $S$ along the null geodesic $\gamma$ passing through $p$, assuming that $\gamma$ can be extended that far.*

More importantly, the concepts of conjugate points answer the question whether there exists a geodesic which extremizes the proper length between two points. The idea is that if a geodesic $\gamma$ connecting two points $p$ and $q$ has a conjugate point $r$ in between, then it is always possible to construct a nearby timelike geodesic which has greater elapsed proper time than $\gamma$. A representation of this idea is shown in Fig. 1.8. Formally, it is encoded in the following Theorem:

**Theorem 1.5**
*Let $\Sigma$ be a 3-dimensional spacelike hypersurface and let $\gamma$ be a timelike curve connecting a point $p \in \mathscr{M}$ to a point $q \in \Sigma$. Then the necessary and sufficient*

*condition that $\gamma$ maximize the proper time between $p$ and $\Sigma$ is that $\gamma$ be a geodesic orthogonal to $\Sigma$ in $q$, with no conjugate point to $\Sigma$ between $\Sigma$ and $p$.*

that generalize to null geodesics as

**Theorem 1.6**
*Let $S$ be a 2-dimensional spacelike hypersurface and let $\gamma$ be a smooth causal curve connecting a point $p \in \mathscr{M}$ to a point $q \in S$. Then the necessary and sufficient condition that $\gamma$ cannot be smoothly deformed to a timelike curve is that $\gamma$ be a geodesic orthogonal to $S$ in $q$, with no conjugate point between $q$ and $p$.*

The last Theorem we need connects the concept of conjugate points with globally hyperbolicity of a SpaceTime:

**Theorem 1.7**
*Let $(\mathscr{M}, g_{ab})$ be a globally hyperbolic SpaceTime and $K \subset \mathscr{M}$ a $2-$dimensional compact spacelike hypersurface. Then, every point $p \in \dot{\mathcal{J}}^+(K)$ lies on a future directed null geodesic orthogonal to $K$ with no conjugate points between $p$ and $K$.*

*Proof.* Since a globally hyperbolic $\mathscr{M}$ is future causally simple, then each $p \in \dot{\mathcal{J}}^+(K)$ lies on a null curve $\gamma$ connecting $p$ and $K$. If this curve is not a null geodesic orthogonal to $K$ or has a conjugate point, then from Theorem 1.6 we can deform $\gamma$ to a timelike curve in such a way that $p \in \mathcal{J}^+(M)$, that implies $p \notin \dot{\mathcal{J}}^+(K)$. Contraddiction. □

We are finally ready to proof the Singularity Theorems.

## 1.4 The Theorems

In Section 1.2.1 we gave a mathematical definition of black hole and event horizon. The latter, however, is a teleological notion: we can locate the event horizon only after we have constructed the whole SpaceTime. "Thus, for example, an event horizon may well be developing in the room you are now sitting *in anticipation* of a gravitational collapse that may occur in this region of our galaxy a million years from now" [Ashtekar and Krishnan 2004, p. 4]. The Singularity Theorem we are going to proof, however, is based on a more local definition of "region from which nothing can escape": the definition of *trapped surface*.

**Definition 1.5 — Trapping surface**
A smooth compact 2-dimensional spacelike surface is said to be *a trapping surface* if both the ingoing and outgoing expansions of future null geodesics are negative, namely

$$\theta_{\text{in}} < 0 \qquad \theta_{\text{out}} > 0 \,. \tag{1.38}$$

With this definition we can finally state and proof the Penrose's Singularity Theorem:

**Theorem 1.8 | Penrose 1965**
*Let $(\mathscr{M}, g_{ab})$ be a SpaceTime containing a trapping surface $T$. Then the following three conditions cannot simultaneously be true:*

1. *$R_{ab}\xi^a\xi^b \geq 0$ for all null $\xi^a$, as in the case the matter content of system satisfies either SEC or WEC;*

2. *there exists a non-compact Cauchy surface $\Sigma$, i.e. the SpaceTime is globally hyperbolic;*

3. *the SpaceTime is null geodesically complete, namely every null geodesic is extendible to infinite values of the affine parameter (no singularity forms).*

*Proof.* As first step we will show that $\dot{\mathcal{J}}^+(T)$ is compact. The second step will show that this conclusion is incompatible with condition 1.

Let us define a function $\psi_{\text{in}}\big(T \times (0, A)\big) \to \mathscr{M}$ such that $\psi(p, a)$ is the point lying on the null future directed ingoing geodesic, starting from $p \in T$ at an affine distance $a$ from $p$. In the same way define $\psi_{\text{out}}$ for outgoing null geodesics and let be $\psi = \psi_{\text{in}} \cup \psi_{\text{out}}$.

Since from Condition 3 every null geodesic is extendible to infinite values of the affine parameter, Lemma 1.4 always applies for any future directed null geodesics $\gamma$ starting from a point $p \in T$ (remember that $T$ has negative expansion). Therefore $\gamma$ will develop a conjugate point within proper distance $2/|\theta(p)|$. As a consequence, by Theorem 1.7, $\dot{\mathcal{J}}^+(T) \subset \psi\big(T \times [0, 2/|\theta_0|]\big)$, where $\theta_0$ is the minimum value for the expansion on $T$. Hence, $\dot{\mathcal{J}}^+(T)$ is closed and bounded, i.e. compact.

Now, as discussed in Section 1.2.2, global hyperbolicity implies the existence of a timelike vector field $t^a$ which intersects $\Sigma$ exactly once. Moreover, since $\dot{\mathcal{J}}^+(T)$ is achronal, $t^a$ intersects it at most once. Thus, it defines a continuos one-to-one map $\alpha : \dot{\mathcal{J}}^+(T) \to \Sigma$. Since $\dot{\mathcal{J}}^+(T)$ is compact, then also its image $\alpha\big(\dot{\mathcal{J}}^+(T)\big)$. However as $\Sigma$ is not compact $\dot{\mathcal{J}}^+$ cannot contain the whole $\Sigma$ and therefore must have a boundary in $\Sigma$. Nevertheless, a result of differential topology assures that in a time-orientable SpaceTime, causal boundaries are $C^0$ sets. This implies that $\alpha\big(\dot{\mathcal{J}}^+(T)\big)$ is open as subset of $\Sigma$. This brings to a contradiction. □

The result tells us that *if a trapping surface forms, either SEC or WEC together with global hyperbolicity forces the SpaceTime to be not null geodesically complete, i.e. at least one null geodesic is not infinitely extensible. That is, by definition a singularity forms.*

The Theorem we proved is just one (and actually the first) of the huge amount of Singularity Theorems present in literature, some of them applicable to cosmological situations, some to star or galaxy collapse, and others to the collision of gravitational waves. However, in the family of that applicable to star collapse, the one we discussed is particularly interesting for our purpose because it is valid when WEC is satisfied. In most cases, indeed, $R_{ab}\xi^a\xi^b \geq 0$ is required to be satisfied for each timelike $\xi^a$ as in the case SEC holds.

The main goal of this thesis is to discuss the so called *non-singular black hole*, i.e. scenarios of collapsing stars that form trapped surface but do not fall into a singularity. The most conservative way to do that is to relax one of the

hypothesis of the Singularity Theorems. As we will see in Chapter 3, such scenarios usually discard SEC, while require WEC to be satisfied. Theorem 1.8 is therefore important because allows us to understand which other physical condition breaks when WEC doesn't.

Chapter 2

# Hawking's Radiation

- «Tommaso! It's been ages since we last met each other! How are you? What are you doing? Studying? University? PhD?»

- «Hey! Nice to see you again! I'm really good, actually. I'm in Marseille writing my master thesis and I'm going to graduate soon. What about you?»

- «Marseille ... cool! Why there? What are you working on? ... if I can understand of course ...»

- «Marseille? You know, it is a nice city ... there is the sea, sun, nice temperature! No, I'm kidding! I'm there because there is a big group working on a theory called Loop Quantum Gravity ...»

- « ... ? ...»

- « Take a sit, I'll briefly explain you. You know that twentieth century has been one of the most revolutionary centuries ever in the field of theoretical physics. You surely have heard about both *General Relativity* and *Quantum Mechanics*. Well, both of them drastically changed the way we look at the Nature and the way we explain its secrets. Space and time that can be curved, guys older than their twin brother and black holes on one hand, discrete energies, quanta, particles that are waves at the same time and Higgs boson on the other. The best news is that these two theories work extremely well with respect to the experiments.»

-«And so, what's the problem?»

-«The problem is that in Nature we observe four different forces: electromagnetic force, weak force, strong force and gravitational force. Well, since the first three are completely controlled and understood in the framework of quantum mechanics, or better Quantum Field Theory which is based on quantum mechanics, the latter is understood *via* General Relativity and the two theories seem to not communicate.»

If Tommaso's interlocutor was interested in the details, the (not completely) imaginary dialog should continue with Tommaso trying to explain that when the framework of Quantum Field Theory (QFT) is naively applied to General Relativity (GR), the resulting quantum theory is not renormalizable [Goroff and Sagnotti 1985]. Usually, the reason why the two most liked theories of modern physics seem to be incompatible, can be phrased saying that they describe

phenomena at totally different scales. General Relativity well explain systems at energy and lengths much larger than those exploited in particle physics. At the same time, we saw that a singularity forms when matter is compressed in microscopic volumes, underlining a breakdown of the theory itself. Moreover, the search of a *unified theory of interaction* has to pass through the construction of a satisfactory theory of Quantum Gravity (QG). The before mentioned Loop Quantum Gravity (LQG) is one of the attempts to *quantize gravity*[1] together with String Theory, Asymptotically Safe QG, Causal Sets Theory and many others. The main problem of all these theories is the absolute absence of experiments able to discard or confirm them. The reason sits in the enormous energies, or equivalently incredibly small distances at which eventual effects of quantum gravity could appear, invalidating the results of the usual GR and QFT. Indeed, it was originally pointed out by Planck in 1899 that the universal constants $G$, $\hbar$ and $c$ can be combined to give a new fundamental length scale, called *Planck length*:

$$l_{\text{planck}} = \sqrt{\frac{G\hbar}{c^3}} \sim 10^{-35}\, m \tag{2.1}$$

as well as a mass scale, called *Planck mass*:

$$m_{\text{planck}} = \sqrt{\frac{\hbar\, c}{G}} \sim 10^{19}\, \frac{Gev}{c^2}\ . \tag{2.2}$$

These are the scales the quantum nature of SpaceTime should manifest.

In the absence of a complete theory of Quantum Gravity is however possible to investigate the influence of gravitation field on quantum phenomena. In the early days of quantum theory many calculations were performed considering electromagnetic field as a classical background source interacting with quantized matter. In analogy, one can consider gravitational field as a classical source of curvature of the SpaceTime where canonically quantized matter fields propagate.

This approach leads to the subject of Quantum Field Theory in Curved SpaceTime on which this Chapter is based and of which the first Section resumes the principal aspects. In the second Section the formalism is applied to the SpaceTime of our interest, namely the Vaidya-Schwarszchild one, to derive the main result: a black hole emits a thermal radiation called *Hawking's radiation*. Such an emission forces the black hole to lose mass and disappear. If all the information on the matter fallen in to create the black hole is ultimately turned into the thermal Hawking's radiation, with no left over, there is a puzzle over the associated non unitary evolution and loss of information. The situation is known as the *information-loss paradox*, and was first pointed out 40 years ago by Hawking [1976]. This results is particularly important also for the so called *black hole thermodynamics*; a brief review on this will introduce the concepts of black hole entropy and *entanglement entropy*. Since the latter plays as basis for the entire Chapter 6, the last Section is entirely dedicated to its definition and basic features.

[1] Or *gravitize Quantum Mechanics* as new approaches suggest [Penrose 2014a,b].

# 2.1 QFT in Curved SpaceTimes

## 2.1.1 Scalar Field in Flat SpaceTime

Following Birrell and Davies [1984], we start with a short review of the quantization of a scalar field[2] in Minkowski SpaceTime, stressing those points which are relevant for the generalization to curved SpaceTime.

Consider a scalar field $\phi$ with action

$$\mathcal{S} = -\frac{1}{2}\int d^4x \, \left(\partial_a\phi\partial^a \, \phi + m^2 \, \phi^2\right) \, , \tag{2.3}$$

and consequent equation of motion given by the Klein-Gordon's equation

$$\partial_a\partial^a \, \phi - m^2\phi = 0 \, . \tag{2.4}$$

One set of solutions are plane-wave functions of the type

$$f_{\mathbf{k}}(t, \mathbf{x}) \sim \exp\{i\mathbf{k}\cdot\mathbf{x} - i\omega \, t\} = e^{ik_\mu x^\mu} \, , \tag{2.5}$$

where $\omega^2 = |\mathbf{k}|^2 + m^2$ is the frequency and is considered to be positive. They are said to be *positive frequency modes* with respect to the *global inertial time* $t$ of Minkowski space, being eigenfunctions of the operator $\partial/\partial t$, i.e.

$$\frac{\partial}{\partial t} f_{\mathbf{k}}(t, \mathbf{x}) = -i \, \omega \, f_{\mathbf{k}}(t, \mathbf{x}) \qquad \text{with } \omega > 0 \, . \tag{2.6}$$

Similarly, *negative frequency modes* $f^\star$ can be defined satisfying

$$\frac{\partial}{\partial t} f^\star_{\mathbf{k}}(t, \mathbf{x}) = +i \, \omega \, f^\star_{\mathbf{k}}(t, \mathbf{x}) \qquad \text{with } \omega > 0 \, . \tag{2.7}$$

Moreover they are orthogonal with respect to the scalar product defined by

$$\langle f, g\rangle = -i \int_\Sigma (f^\star\partial_a g - g\partial_a f^\star) n^a d\Sigma \tag{2.8}$$

where $f$ and $g$ are two generic solutions, $\Sigma$ a Cauchy hypersurface and $n_a$ its normal.

Once normalized as

$$f_{\mathbf{k}} = \frac{1}{(2\pi)^{3/2}} \frac{1}{\sqrt{2\omega}} e^{ik_\mu x^\mu} \tag{2.9}$$

the positive frequency modes provide a basis on the space of classical field configurations $\phi(x)$ solutions of the Klein-Gordon's equation. Therefore, any $\phi(x)$ can be expanded in terms of these modes

$$\phi(x) = \int d^3\mathbf{k} (a_{\mathbf{k}} \, f_{\mathbf{k}} + a^\star_{\mathbf{k}} \, f^\star_{\mathbf{k}}) \, . \tag{2.10}$$

[2] The result can be generalized to higher spin also.

The system is canonically quantized by replacing the classical fields and its momentum by operators acting on a Hilbert space and imposing the canonical commutation relations

$$\begin{aligned}[\hat{\phi}(t,\mathbf{x}),\hat{\phi}(t,\mathbf{x}')] &= 0\\ [\hat{\pi}(t,\mathbf{x}),\hat{\pi}(t,\mathbf{x}')] &= 0\\ [\hat{\phi}(t,\mathbf{x}),\hat{\pi}(t,\mathbf{x}')] &= i\delta^3(\mathbf{x}-\mathbf{x}')\end{aligned} \tag{2.11}$$

By Eq. (2.10), this is equivalent to promote the coefficients $a$ and $a^\star$ as operators with commutation relations given by

$$\begin{aligned}[\hat{a}_{\mathbf{k}},\hat{a}_{\mathbf{k}'}] &= 0\\ [\hat{a}^\dagger_{\mathbf{k}},\hat{a}^\dagger_{\mathbf{k}'}] &= 0\\ [\hat{a}_{\mathbf{k}},\hat{a}^\dagger_{\mathbf{k}'}] &= \delta^3(\mathbf{k}-\mathbf{k}')\ .\end{aligned} \tag{2.12}$$

The Hilbert space where they act is the so called *Fock space*, defined applying the creation operators to the *vacuum state*, namely the state $|0\rangle$ such that

$$a_{\mathbf{k}}\,|0\rangle = 0 \qquad \forall\mathbf{k}. \tag{2.13}$$

A quantum state containing an exited modes, say $f_{\mathbf{k}}$, is called a *one-particle state*

$$|1_{\mathbf{k}}\rangle = a^\dagger_{\mathbf{k}}\,|0\rangle\ . \tag{2.14}$$

and similarly

$$\left|n_{\mathbf{k}_1},n_{\mathbf{k}_2},\ldots,n_{\mathbf{k}_j}\right\rangle = (n_{\mathbf{k}_1}!n_{\mathbf{k}_2}!\ldots n_{\mathbf{k}_j}!)^{-1/2}(a^\dagger_{\mathbf{k}_1})^{n_{\mathbf{k}_1}}(a^\dagger_{\mathbf{k}_2})^{n_{\mathbf{k}_2}}\ldots(a^\dagger_{\mathbf{k}_j})^{n_{\mathbf{k}_j}}\,|0\rangle \tag{2.15}$$

is called a *many-particles state*, containing $n_{\mathbf{k}_j}$ exited modes of type $f_{\mathbf{k}_j}$. The $n!$ terms are necessary to accommodate Bose-Einstein statistics of identical scalar particles. The creation and annihilation operators act on a many-particle state respectively as

$$\begin{aligned}a^\dagger_{\mathbf{k}}\,|n_{\mathbf{k}}\rangle &= (n+1)^{1/2}\,|(n+1)_{\mathbf{k}}\rangle\\ a_{\mathbf{k}}\,|n_{\mathbf{k}}\rangle &= n^{1/2}\,|(n-1)_{\mathbf{k}}\rangle\ ,\end{aligned} \tag{2.16}$$

i.e. creating and annihilating a $f_{\mathbf{k}}$ mode, as their names suggest. Considering the operator $N_{\mathbf{k}} \equiv a^\dagger_{\mathbf{k}}a_{\mathbf{k}}$, from Eq. (2.16) we obtain

$$\left\langle n_{\mathbf{k}_1},n_{\mathbf{k}_2},\ldots,n_{\mathbf{k}_j}\right| N_{\mathbf{k}_i}\left|n_{\mathbf{k}_1},n_{\mathbf{k}_2},\ldots,n_{\mathbf{k}_j}\right\rangle = n_{\mathbf{k}_i}\ ; \tag{2.17}$$

that is, given a state, $N_{\mathbf{k}_i}$ counts the number of particles $f_{\mathbf{k}_i}$ present in the state. For this reason it is called *number operator*.

The generalization of such a formalism in a curved background can be done in a straightforward way when restricted to globally hyperbolic SpaceTimes (see Section 1.2.2).

### 2.1.2 Generalization to Curved SpaceTime

Consider therefore a globally hyperbolic SpaceTime $(\mathscr{M}, g_{ab})$ and a scalar field $\phi$ propagating on it. The action (2.3) can be generalized introducing the covariant derivative $D^a$

$$S = \int d^4x\sqrt{-g}(-\frac{1}{2}D_a\phi D^a\phi - \frac{1}{2}m^2\phi^2) \ : \tag{2.18}$$

the scalar field is said to be *minimally coupled* to the curved background. The relative equation of motion reads

$$\frac{1}{\sqrt{-g}}\partial_a(\sqrt{-g}g^{ab}\partial_b)\phi - m^2\phi^2 \equiv D_aD^a\phi - m^2\phi^2 = 0 \ . \tag{2.19}$$

The inner product on solutions space of the curved Klein-Gordon's equation is generalized by

$$\langle f, g\rangle = -i\int_\Sigma \sqrt{\gamma}\big(fD_ag^\star - g^\star D_af\big)n^a d\Sigma \tag{2.20}$$

where $\Sigma$ is a Cauchy surface with normal $n^a$ and induced metric $\gamma$. Moreover, it can be shown that the inner product definition does not depend on the choice of the Cauchy surface. See Hawking and Ellis [1973, Sec. 2.8].

As before, there exists an orthonormal basis $\{f_i\}$ with respect to this scalar product, i.e.

$$\langle f_i, f_j\rangle = \delta_{ij} \qquad \langle f_i^\star, f_j^\star\rangle = -\delta_{ij} \tag{2.21}$$

where the subscript $i$ synthetically represents the set of quantities necessary to label the modes. Any field $\phi$ can be therefore expanded as

$$\phi(x) = \sum_i (a_i\, f_i + a_i^\star\, f_i^\star) \ . \tag{2.22}$$

At this point, however, the construction of the vacuum state, Fock space, etc. cannot proceed exactly as before because it will cause an ambiguity. In Minkowski space, indeed, it was possible to properly define positive and negative frequency modes thanks to the presence of the *global time coordinate* $t$. In a curved SpaceTime the notion of *preferred time coordinate* is ambiguous. To generalize the quantization in such situations, therefore, we need to require one more restriction on the metric background. The assumption we need is *stationarity*. In the first sentence of this thesis, we presented the Schwarzschild solution as "a solution of Einstein's equations for the exterior of a *static, stationary, spherically symmetric* source of gravitational mass". However, we didn't explain what 'static' and 'stationary' mean. Let us briefly formalize it now. A SpaceTime $(\mathscr{M}, g_{ab})$ is said to be *stationary* if it admits a timelike Killing vector field $\chi^a$. $\mathscr{M}$ is *static* if it is stationary and if, in addition, there exists a spacelike hypersurface $\Sigma$ which is orthogonal to the orbit of $\chi^a$.

In the stationary case, symmetry allows us to pick up a preferred time coordinate, defined by the timelike Killing vector field $\chi^a$, and therefore to generalize the definition of *positive frequency modes* in the context of curved space. They can be defined as the modes $\{f_i\}$ such that

$$\mathcal{L}_\chi f_i = -i\omega f_i, \qquad \omega > 0 \tag{2.23}$$

whereas the ones $\{f_i^\star\}$ such that

$$\mathcal{L}_\chi f_i^\star = i\omega f_i^\star, \qquad \omega > 0 \tag{2.24}$$

define the *negative frequency modes*. Here $\mathcal{L}_\chi$ is the Lie derivative along the flow of the Killing vector field $\chi^a$.

In this framework the system can be quantized exactly as in flat space by promoting classical fields to operators, acting on a Hilbert space, which satisfy the canonical commutation relations. From Eq. (2.22), the procedure is again equivalent to promote the coefficients to creation and annihilation operators associated to the basis $\{f_i\}$. The field becomes

$$\hat{\phi}(x) = \sum_i \hat{a}_i f_i + \hat{a}_i^\dagger f_i^\star. \tag{2.25}$$

and the vacuum is still defined by

$$\hat{a}_i|0\rangle = 0 \qquad \forall i \tag{2.26}$$

with subsequent Fock space and number operators.

## 2.2 Particle Production

When the SpaceTime is not stationary, there is not a natural splitting of modes between positive and negative frequency solutions, because there is not a preferred 'time' coordinate to which definitions (2.23) and (2.24) can be applied. Different choices of positive frequency modes lead, in general, to different definitions of the vacuum state and of the Fock space, and the unambiguous concept of particles state of Minkowski space disappears.

Let us for instance consider two different bases, $\{f_i, f_i^\star\}$ and $\{g_i, g_i^\star\}$, in the space of the solutions of the Klein-Gordon's equation of motion. Any field configuration $\phi(x)$ can be expanded in both the two sets

$$\begin{aligned} \phi(x) &= \sum_i (a_i f_i + a_i^\star f_i^\star) \\ \phi(x) &= \sum_j (b_j g_j + b_j^\star g_j^\star). \end{aligned} \tag{2.27}$$

Since both sets are complete, one can also expand one sets of modes in terms of the other. So in general we have finding the so called *Bogolubov transformations*:

$$\begin{aligned} g_i &= \sum_j (\alpha_{ij} f_j + \beta_{ij} f_j^\star) \\ g_i^\star &= \sum_j (\beta_{ij}^\star f_j + \alpha_{ij}^\star f_j^\star)\ . \end{aligned} \tag{2.28}$$

where $\alpha_{ij}$, $\beta_{ij}$ are the *Bogolubov coefficients*. Taking into account the orthonormality of the of the modes, namely

$$\begin{aligned} \langle f_i, f_j \rangle &= \delta_{ij} \\ \langle f_i^\star, f_j^\star \rangle &= -\delta_{ij} \\ \langle f_i^\star, f_j \rangle &= 0\ , \end{aligned} \tag{2.29}$$

the Bogolubov coefficients are given by

$$\alpha_{ij} = \langle g_i, f_j \rangle \ , \qquad \beta_{i,j} = -\langle g_i, f_j \rangle \ , \tag{2.30}$$

and the following relation between them holds

$$\sum_k (\alpha_{ik}\beta_{jk} - \beta_{ik}\alpha_{jk}) = \delta_{ij} \ . \tag{2.31}$$

Inverting relations (2.28) finding

$$f_i = \sum_j (\alpha^\star_{ji} g_j - \beta_{ji} g^\star_j) \tag{2.32}$$

and using Eqs. (2.27) and (2.29), one find for expansion coefficients of a field $\phi$

$$\begin{aligned} a_i &= \sum_j (\alpha_{ji} b_j + \beta^\star_{ji} a^\star_j) \ ; \\ b_i &= \sum_j (\alpha^\star_{ij} a_j - \beta^\star_{ij} a^\star_j) \ . \end{aligned} \tag{2.33}$$

Therefore, as long as the coefficients $\beta_{ij}$ do not vanish, the vacuum states $|0_f\rangle$ and $|0_g\rangle$ defined by the quantizations relative to the two different sets of modes as

$$\begin{aligned} \hat{a}_i \, |0_f\rangle = 0 \\ \hat{b}_i \, |0_g\rangle = 0 \end{aligned} \qquad \forall i \tag{2.34}$$

are different. Namely

$$\begin{aligned} \hat{b}_i \, |0_f\rangle \neq 0 \ , \\ \hat{a}_i \, |0_g\rangle \neq 0 \ . \end{aligned} \tag{2.35}$$

Now, imagine that our SpaceTime has two *stationary regions* $F \subset \mathscr{M}$ and $G \subset \mathscr{M}$, and imagine the modes $\{f_i\}$ and $\{g_i\}$ to be the *positive frequency modes* with respect to the Killing vector field respectively in $F$ and in $G$. For this regions we have a natural particle interpretation. However, Eq. (2.35) tells us that a state perceived as vacuum by an observer in $F$ is not perceived as vacuum by an observer in $G$ and viceversa (if $\beta_{ij} \neq 0$). In fact, one can also compute the expectation value of for instance the $g_i$ mode in the $F$-vacuum $|0_f\rangle$ finding

$$\langle 0_f | \, N_{g_i} \, |0_f\rangle = \sum_j |\beta_{ij}|^2 \ . \tag{2.36}$$

Again, if the coefficient $\beta_{ij}$ are different from zero, the particle content of the $|0_f\rangle$ vacuum state, with respect to the Fock space defined in $G$, is non-trivial. In contrast, if all the coefficients $\beta_{ij}$ vanish, the relation (2.31) becomes

$$\sum_k \alpha_{ik} \alpha^\star_{jk} = \delta_{ij} \tag{2.37}$$

showing that the positive frequency mode basis $f_i$ and $g_i$ are related by a *unitary transformation*. The definition of the vacuum state remains unchanged and $|0_f\rangle = |0_g\rangle$.

### 2.2.1 Gravitational Collapse

This framework can be applied now to the scenario of our interest, namely the process of gravitational collapse. To simplify the discussion, we follow Fabbri and Navarro-Salas [2005] considering the simplified Vaidya's collapse process defined in Section 1.1.3. The resulting SpaceTime is clearly non-stationary and, at the same time, allows a really simple identification of the two stationary regions $F$ and $G$ as respectively the inside-the-shell minkowskian patch and the outside-the-shell schwarzschildian one. The results of the previous section, therefore, tells us immediately that the vacuum state of a scalar field prepared before the collapse and propagating through the collapsing geometry, could result as a non-vacuum one with respect to an observer on the Schwarzschild region. That is: particles can be created from a black hole SpaceTime.

To show that this is actually the case, let us make the complete computation. To simplify it we consider the propagation of a minimally coupled *massless* scalar field $\phi$. The Klein-Gordon's equation reduces to

$$\nabla^a \nabla_a \phi = 0. \tag{2.38}$$

Thanks to the spherical symmetry of the background metric, we can expand the field as

$$\phi(x) = \sum_{l,m} \frac{\phi_l(t,r)}{r} Y_{lm}(\theta,\phi) \tag{2.39}$$

where $Y_{lm}(\theta,\phi)$ are spherical harmonic functions. In this way, Eq. (2.38) is converted into a two-dimensional wave equation for $\phi_l(t,r)$, namely

$$\begin{aligned} \left(-\frac{\partial^2}{\partial t^2} + \frac{\partial^2}{\partial r^2} - \frac{l(l+1)}{r^2}\right)\phi_l(t,r) = 0 \qquad &\text{(Minkowski sector)} \\ \left(-\frac{\partial^2}{\partial t^2} + \frac{\partial^2}{\partial r_\star^2} - V_l(r)\right)\phi_l(t,r) = 0 \qquad &\text{(Schwarzschild sector)} \end{aligned} \tag{2.40}$$

where $V_l(r)$ is the gravitational effective potential

$$V_l(r) = \left(1 - \frac{2m}{r}\right)\left(\frac{l(l+1)}{r^2} + \frac{2m}{r^3}\right). \tag{2.41}$$

and $r_\star$ is the tortoise coordinate defined by eq. (1.4)

$$r^\star = r + 2m \log\left|\frac{r}{2m} - 1\right|. \tag{2.42}$$

To best simplify the computation, we can make other assumptions that will not invalidate the main result. First of all, since the SpaceTime appears more and more minkowskian as one goes far from the horizon, we can focus the narrow on the modes propagating from $\mathscr{I}_-$ to $\mathscr{I}_+$ close to the horizon when the black hole forms. Moreover, we can notice that the potential (2.41) vanishes both at $r \to +\infty$ ($r^\star \to +\infty$) and at the horizon $r \to 2m$ ($r^\star \to -\infty$). The last approximation comes from the observation that the modes reaching $\mathscr{I}_+$ passing close to the horizon suffer a very high redshift or, conversely, they had a very high frequency

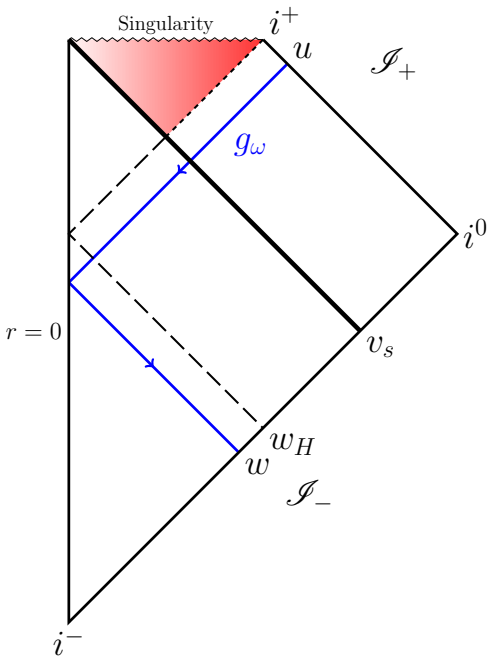


**Figure 2.1.** Penrose-Carter diagram of a collapsing star process in the thin shell Vaidya approximation. The black hole region is shaded. In the geometric optics approximation, a mode $g_\omega$ in the Fock space defined on $\mathscr{I}_+$ (and $H$) is ray-traced back to $\mathscr{I}_-$.

when they began their path from $\mathscr{I}_-$. Hence, we will follow null modes as they were light rays. In other words, we consider the bulk of the transmitted rays to be in the s-wake sector $l = 0$, since it is the one less affected by the potential, propagating in *geometric optics approximation*.

With these simplifications, the equations of motion reduce to

$$\left(-\frac{\partial^2}{\partial t^2}+\frac{\partial^2}{\partial r^2}\right)\phi(t,r)=0 \tag{2.43}$$

in the Minkowski sector, and

$$\left(-\frac{\partial^2}{\partial t^2}+\frac{\partial^2}{\partial r_\star^2}\right)\phi(t,r)=0 \tag{2.44}$$

in the Schwarzschild one, where the subscript $l = 0$ is implied and the path of propagation is described by ingoing null rays starting from $\mathscr{I}_-$, bouncing at the center $r = 0$ and reaching $\mathscr{I}_+$ as outgoing null rays. See Fig. 2.1. The solutions to these equations are better expressed in terms of double null coordinates:

$$u_{\rm m}=t-r \qquad w=t+r \qquad \text{(Minkowski sector)} \tag{2.45}$$

$$u=t-r_\star \qquad w=t+r_\star \qquad \text{(Schwarzschild sector)}\,, \tag{2.46}$$

from which the two metrics become

$$\begin{aligned} ds^2 &= -du_{\rm m}\,dw+r_{\rm m}^2\,d\Omega^2 \qquad \text{(Minkowski sector)}\\ ds^2 &= -\left(1-\frac{2m}{r_{\rm s}}\right)du\,dw+r_{\rm s}^2\,d\Omega^2 \qquad \text{(Schwarzschild sector)}\,. \end{aligned} \tag{2.47}$$

We want to define now the two Fock spaces on which apply the Bogolubov formalism. First of all, we need to find two stationary regions tailored to the double

null description. Thanks to asymptotically flatness of Schwarzschild SpaceTime, we can take one of them to be past null infinity $\mathscr{I}_-$. The positive frequency modes with respect to the natural time parameter on $\mathscr{I}_-$ are

$$f_\omega = \frac{1}{4\pi\sqrt{\omega}} \frac{e^{-i\omega\, w}}{r} \tag{2.48}$$

orthonormal with respect to scalar product

$$\langle f_\omega, f_{\omega'} \rangle = -i \int_{\mathscr{I}_-} dw\, r^2 d\Omega \, (f_\omega \partial_w f^\star_{\omega'} - f^\star_{\omega'} \partial_w f_\omega) = \delta(\omega - \omega') \, . \tag{2.49}$$

We can also associate a Fock space at future null infinity $\mathscr{I}_+$, where the set of positive frequency modes with respect to the natural time on it, is given by

$$g_\omega = \frac{1}{4\pi\sqrt{\omega}} \frac{e^{-i\omega\, u}}{r} \, . \tag{2.50}$$

These modes obey a similar normalization condition

$$\langle g_\omega, g_{\omega'} \rangle = -i \int_{\mathscr{I}_+} du\, r^2 d\Omega \, (g_\omega \partial_u g^\star_{\omega'} - g^\star_{\omega'} \partial_u g_\omega) = \delta(\omega - \omega') \, . \tag{2.51}$$

In this form it seems that we are picking $\mathscr{I}_+$ to be a Cauchy surface, which clearly is not. We must add the horizon $H$ to have a complete Cauchy surface. In the geometric optics approximation, indeed, the modes that reach $\mathscr{I}_+$ are only the ones that start on $\mathscr{I}_-$ before the collapse of the shell, namely for $w < v_s$. This means that the modes $g_\omega$ are not a basis because they are not complete. To construct a proper Fock space, we need to consider those modes $g^{BH}_\omega$ that start after the collapsing shell and cross the horizon ending in the singularity. However, the result is insensitive to the particular choice of these modes, because we are interested on light rays that reach future null infinity.

Indeed, the next step is to compute the Bogolubov coefficients $\beta_{\omega\omega'}$ relating $f$ modes to $g$ modes, namely

$$\beta_{\omega,\omega'} = -\langle g_\omega, f_{\omega'} \rangle = i \int_{\mathscr{I}_-} dw\, r^2 d\Omega \, (g_\omega \partial_w f^\star_{\omega'} - f^\star_{\omega'} \partial_w g_\omega) \, , \tag{2.52}$$

where, we choose $\mathscr{I}_-$ as Cauchy surface for convenience, since the scalar product doesn't depend on its particular choice. To evaluate this integral we need to know the behavior of modes $g_\omega$ on the 'initial data surface' $\mathscr{I}_-$. In the geometric optics approximation we are using, this is done by ray-tracing back the modes $g_\omega$ from $\mathscr{I}_+$ to $\mathscr{I}_-$. Since $w > v_s$ the mode remains unaltered. As marked in Section 1.1.3, gluing two patches of SpaceTimes is possible only by imposing regularity conditions on the gluing surface. One of these physical matching conditions (see Poisson [2004, p. 84-94]) is that the induced metric on the surface should not be discontinuous. In our case, from Eq. (3.17), this is translated by requiring the radius coordinates $r_{\rm m}$ and $r_{\rm s}$ to be equal on the surface $w = v_s$, namely

$$r_{\rm m}(v_s, u_{\rm m}) = r_{\rm s}(v_s, u) \, . \tag{2.53}$$

Here

$$r_{\rm m}(v_s, u_{\rm m}) = \frac{v_s - u_{\rm m}}{2} \tag{2.54}$$

and $r_{\rm s}(v_s, u)$ is implicitly defined by

$$r_{\rm s}(v_s, u) + 2m \log\left(\frac{r_{\rm s}(v_s, u)}{2m} - 1\right) = \frac{v_s - u}{2} \ . \tag{2.55}$$

Solving Eq. (2.53), we can find $u$ as a function of $u_{\rm m}$:

$$u(u_{\rm m}) = u_{\rm m} - 4m \log \frac{v_s - 4m - u_{\rm m}}{4m} \ . \tag{2.56}$$

Moreover, we need to impose a regularity condition in the origin for the fields satisfying Eq. (2.43). From Eq. (2.39), this means that $\phi_l(t, 0) = 0$. In our case, $r = 0$ is given by $u_{\rm min} = w$ and the previous condition forces the following form of the ray-traced back mode in the Minkowski part of the SpaceTime

$$g_\omega = \frac{1}{4\pi\sqrt{\omega}} \left(\frac{e^{-i\omega\, u(u_{\rm m})}}{r} - \frac{e^{-i\omega\, u(w)}}{r}\right) \tag{2.57}$$

where

$$u(w) = w - 4m \log \frac{v_s - 4m - w}{4m} \ . \tag{2.58}$$

We need to notice that the map above is defined only in the range $-\infty < w < v_s - 4m$. This is clear when looking at the diagram in Fig. 2.1: $w_H \equiv v_s - 4m$ is the traced back value on $\mathscr{I}_-$ of the null outgoing ray representing the horizon. Any mode starting from $\mathscr{I}_-$ after $w_H$ will not end on future null infinity, being lost inside the black hole. The map $w(u)$ is called the *canonical map* from $\mathscr{I}_+$ to $\mathscr{I}_-$ and will play a crucial role in Chapter 6.

Once bounced at the origin, the ray-traced back mode will follow a $w =$ const. ray, being therefore described by

$$g_\omega = -\frac{1}{4\pi\sqrt{\omega}} \frac{e^{-i\omega\,(w - 4m \log \frac{w_H - w}{4m})} \Theta(w_H - w)}{r} \ , \tag{2.59}$$

where the Heavise function $\Theta$ is to remark that we traced back only the modes coming from $\mathscr{I}_+$. We still have to implement one approximation, namely that the important physics is encoded in the light rays propagating close to the horizon. Therefore we can consider $w \simeq w_H$ finding

$$g_\omega \simeq -\frac{1}{4\pi\sqrt{\omega}} \frac{e^{-i\omega\,(w_H - 4m \log \frac{w_H - w}{4m})} \Theta(w_H - w)}{r} \ . \tag{2.60}$$

We are now ready to compute the Bogolubov coefficient inserting expressions (2.60) and (2.48) into the integral in Eq. (2.52). Performing a partial integration and discarding the boundary terms since $g_\omega(w)$ vanishes at $v \to \pm\infty$. Our starting point is then

$$\beta_{\omega\omega'} = 2i \int_{\mathscr{I}_-} dw\, r^2 d\Omega\, g_\omega \partial_w f_{\omega'} \ . \tag{2.61}$$

A similar expression can be computed for $\alpha_{\omega\omega'}$

$$\alpha_{\omega\omega'} = -2i \int_{\mathscr{I}_-} dw\, r^2 d\Omega\, g_\omega \partial_w f^\star_{\omega'}. \tag{2.62}$$

With the found expression (2.60) for the mode $g_\omega$ we obtain

$$\beta_{\omega\omega'} = \frac{-1}{2\pi}\sqrt{\frac{\omega'}{\omega}} \int_{-\infty}^{w_H} dw\, e^{-i\omega(w_H - 4M \ln \frac{w_H - w}{4M}) - i\omega' w}\ , \tag{2.63}$$

and

$$\alpha_{\omega\omega'} = \frac{-1}{2\pi}\sqrt{\frac{\omega'}{\omega}} \int_{-\infty}^{w_H} dw\, e^{-i\omega(w_H - 4M \ln \frac{w_H - w}{4M}) + i\omega' w}\ . \tag{2.64}$$

Changing variable $x = w_H - w$ one gets

$$\beta_{\omega\omega'} = \frac{-1}{2\pi}\sqrt{\frac{\omega'}{\omega}} (4M)^{-4M\omega i} e^{-i(\omega+\omega')w_H} \int_0^{+\infty} dx x^{4M\omega i} e^{i\omega' x}\ , \tag{2.65}$$

and

$$\alpha_{\omega\omega'} = \frac{-1}{2\pi}\sqrt{\frac{\omega'}{\omega}} (4M)^{-4M\omega i} e^{-i(\omega-\omega')w_H} \int_0^{+\infty} dx x^{4M\omega i} e^{-i\omega' x}\ , \tag{2.66}$$

The above integrals do not converge absolutely. The reason is that we are using another approximation, namely we are using pure plane waves. Let us be more precise. The computation of the Bogolubov coefficients is being done in order to evaluate the expectation value of the number operator of a mode $g_\omega$ on the initial vacuum state $|0_f\rangle$, namely the continuum version of Eq. (2.36):

$$\langle 0_f |\, N_{g_\omega}\, |0_f\rangle = \int_0^\infty dw' \, |\beta_{\omega\omega'}|^2\ . \tag{2.67}$$

This quantity will provide the mean particle number detected at $\mathscr{I}_+$ with definite frequency $\omega$. However, pure plane waves with a definite frequency $\omega$ are completely delocalized and the uncertainty in time is infinite. Therefore, expression (2.67) gives the number of particles detected at anytime $u$. In a physical situation we need to replace plane waves with non-completely-spread wave packets [Fabbri and Navarro-Salas 2005, Sec. 3.3.2]. Nevertheless, the final result doesn't change if we use a little trick in order to compute the integral (2.66). Let us pick a sort of Wick rotation, inserting into the exponent an infinitesimal negative real part $(-\epsilon)$ to force the integrals to converge. This way one 'imitates' the role of the wave packets. Using the properties of the Eulero gamma function $\Gamma(x)$

$$\int_0^{+\infty} x^a e^{-bx} = b^{-1-a}\Gamma(1+a), \tag{2.68}$$

where $a = 4M\omega i$ and $b = \pm\omega' i + \epsilon$, one finally obtains

$$\beta_{\omega\omega'} = \frac{-1}{2\pi}\sqrt{\frac{\omega'}{\omega}} (4M)^{-4M\omega i} e^{-i(\omega+\omega')w_H} (-i\omega' + \epsilon)^{-1-4M\omega i}\Gamma(1 + 4M\omega i) \tag{2.69}$$

and

$$\alpha_{\omega\omega'} = \frac{-1}{2\pi}\sqrt{\frac{\omega'}{\omega}}(4M)^{-4M\omega i}e^{-i(\omega-\omega')w_H}(i\omega'+\epsilon)^{-1-4M\omega i}\Gamma(1+4M\omega i)\ . \tag{2.70}$$

Note that $\beta_{\omega\omega'} = -i\alpha_{\omega(-\omega)}$. Taking into account that

$$\ln(-\omega' - i\epsilon) = -i\pi + \ln\omega'\ , \tag{2.71}$$

it is easy to find the following relation between the Bogolubov coefficients

$$\alpha_{\omega\omega'} = -e^{4\pi M\omega}e^{2i\omega' w_H}\beta_{\omega\omega'} \tag{2.72}$$

and

$$|\alpha_{\omega\omega'}| = e^{4\pi M\omega}|\beta_{\omega\omega'}|\ . \tag{2.73}$$

Inserting the above expressions in (2.67) to evaluate $\langle in|\, N_{g_\omega}\, |in\rangle$ one finds that, due to the factor $(\omega')^{-\frac{1}{2}}$ in the coefficients $\beta_{\omega\omega'}$, it diverges logarithmically. This means that the black hole produces at $\mathscr{I}^+$ an infinite number of particles of frequency $\omega$. However, this is another consequence of using plane waves instead of wave packets. The quantity $\langle in|\, N_{g_\omega}\, |in\rangle$, which has dimension of time, represents indeed the flux of radiation integrated for all times. The exact computation should consider wave packets peaked of the form

$$g_{jn} = \frac{1}{\sqrt{\epsilon}}\int_{j\epsilon}^{(j+1)\epsilon} d\omega\, e^{\frac{2\pi i\omega\, n}{\epsilon}} g_\omega \tag{2.74}$$

where $j \geq 0$ is an integer. These packets are peaked about the value $u = 2\pi\, n/\epsilon$ with width given by $2\pi/\epsilon$. When $\epsilon$ is small the modes are narrowly centered around $\omega \simeq \omega_j = j\epsilon$. In this framework the physical quantity to be computed is $\langle 0_f|\, N_{g_{jn}}\, |0_f\rangle$ which gives the *counts of a particle detector sensitive only to frequencies within $\epsilon$ of $\omega_j$ turned on for a time interval $2\pi/\epsilon$ at the time $u = 2\pi\, n/\epsilon$.* This quantity is finite. From Eq. (2.73) and the continuum version of Eq. (2.31)

$$\int_0^{+\infty} d\omega'(\alpha_{jn,\omega'}\alpha^\star_{j'n',\omega'} - \beta_{jn,\omega'}\beta^\star_{j'n',\omega'}) = \delta_{jj'}\delta_{nn'}. \tag{2.75}$$

For the particular values $j = j', n = n'$ we have

$$\int_0^{+\infty} d\omega'(|\alpha_{jn,\omega'}|^2 - |\beta_{jn,\omega'}|^2) = 1. \tag{2.76}$$

From the relation between the Bololubov coefficents, Eq. (2.73) can write

$$(e^{8\pi M\omega_j} - 1)\int_0^{+\infty} d\omega'|\beta_{jn,\omega'}|^2 = 1, \tag{2.77}$$

and, therefore, for late times $n \to +\infty$, we find the desired result

$$\langle 0_f|\, N_{g_{jn}}\, |0_f\rangle = \int_0^{+\infty} d\omega'|\beta_{jn,\omega'}|^2 = \frac{1}{e^{8\pi M\omega_j} - 1}. \tag{2.78}$$

This expectation value *coincides exactly with a* Planck distribution *of thermal radiation for bosons*

$$\frac{1}{e^{\hbar\omega/k_BT}-1} \tag{2.79}$$

with a temperature given by

$$T_H = \frac{\hbar}{8\pi k_B M} \ , \tag{2.80}$$

where the constants of Nature have been reintroduced and $k_B$ is Boltzmann's constant. The quantity $T_H$ is called *Hawking temperature* of a black hole with mass $m$, and it is usually written in Planck units as

$$T_H = \frac{\kappa}{2\pi} \tag{2.81}$$

where $\kappa = 1/4m$ is the so called *surface gravity* that will be soon introduced in (see Section 2.3).[3]

Despite the fact it has been derived in a very simplified way, this result coincides with the original Hawking [1975] one, and it remains correct for a generic and complicated process of gravitational collapse ending up in a black hole.

To be rigorous, Eq. (2.79) is not sufficient to conclude that particles are emitted with a Planck spectrum. One should show that the different one-particle modes are *uncorrelated*. This was done by Wald [1975], who found that the probability to observe $N$ particles with frequency $\omega$ is

$$P(N,\omega) = \frac{e^{-\beta N\omega}}{\prod_\omega\left(1-e^{-\beta\omega}\right)} \qquad \beta^{-1} = k_BT_H \tag{2.82}$$

in perfect accordance with thermal emission.

*We showed that a collapsing object settled down into a black hole will produce an uncorrelated thermal radiation with temperature given by $\kappa/2\pi$.*

### 2.2.2 Information-Loss Paradox

**Backreaction and evaporation** The main limitation in the derivation of the Hawking's effect is the fact that we consider the background metric to be *fixed*. Since the radiation carries energy, however, this approximation is not in agreement with energy conservation if the black hole doesn't reduce its mass at the same rate at which the energy is radiated out. This implies therefore a correction to the initial background geometry: the so called *backreaction* of the radiation on the metric. More precisely, if the initial metric $g_{ab}$ is solution of Einstein's equations for some energy-momentum tensor $T_{ab}$, i.e.

$$G[g_{ab}] = T_{ab} \ , \tag{2.83}$$

[3] For fermions a similar computation can be performed and it also gives a Planck distribution: $\langle 0_f|\, N_\omega\, |0_f\rangle = (e^{\hbar\omega_j/k_BT_H}-1)^{-1}$, but now with the corresponding Fermi statistic.

when particles creation takes place $T_{ab}$ changes and the metric $g_{ab}$ is not a solution anymore. However, for macroscopic black holes the temperature is very small

$$T_H \simeq 10^{-7} \frac{m_{\text{sun}}}{m} \ ^\circ K \tag{2.84}$$

and one can make the plausible assumption that the evaporation process is *quasi-static*, being very accurately described, for all its duration, by *thermal radiation* with temperature depending on the mass as $\sim 1/m$. The backreaction is then taken into account in the simplest possible way just allowing the mass parameter $m$ to be time-dependent: the evolution is described by a succession of static pictures at each instant of time, where the metric is the Schwarzschild metric with mass $m(t)$.

Assuming quasi-static approximation, one can estimate the mass loss rate of a Schwarzschild black hole by the Stephan-Boltzmann's law

$$\frac{dm}{dt} = -\sigma A T_H^4 \tag{2.85}$$

where $\sigma$ is the Stephan-Boltzmann's constant and $A = 2\pi(2m)^2$ the area of the black hole horizon. Inserting Eq. (2.81) and reintroducing the constants of Nature, we find

$$\frac{dm}{dt} = -\alpha \frac{m_{\text{planck}}^3}{t_{\text{planck}}} \frac{1}{m^2} \tag{2.86}$$

where $\alpha$ is a dimensionless constant of order $10^{-5}$. Integrating over $t$ we have the evolution law

$$m(t) = \left( m_0^3 - 3\alpha \frac{m_{\text{planck}}^3}{t_{\text{planck}}} t \right)^{1/3} \tag{2.87}$$

with $m_0$ the initial mass. Therefore the black hole completely disappears after a large amount of time

$$\Delta t = \frac{t_{\text{planck}}}{3\alpha} \left( \frac{m_0}{m_{\text{planck}}} \right)^3 . \tag{2.88}$$

The above argument cannot be trusted when the mass reaches Planck scale. However, since the rate of the radiation grows as the mass of the black hole decreases, for most of the time $\Delta t$ the black hole mass is much bigger than the Planck mass. Estimation (2.88), therefore, is likely to provide the correct order of magnitude. Furthermore, when the mass reaches Planck regime, the Hawking temperature is so high to 'unfreeze' a high number of fields, causing a final explosion of the black hole [Hawking 1974]. While Eq. (2.84) tells us that the radiation emitted by present-day black holes *does not* produce an observable effect because of its really small temperature, the effects of such a catastrophic end of the life of a black hole are believed to provide detectable signals. However, for a black hole of solar mass or higher, the evaporation time computed from Eq. (2.88) comes out to be greater then the life of the Universe. The upper bound on the mass of a black hole that has undertaken a complete evaporation up to now is $m_0 \simeq 5 \times 10^{14}\, g$. Celestial objects with this mass, however, are too 'light' and their gravitational collapses cannot form black holes. The only detectable signals, therefore, can arise from 'primordial' black holes created in the early stages of the Universe.

**Breakdown of predictability** Hawking [1976] pointed out another, perhaps dramatic, physical implication of the process of black hole evaporation: the so called *information-loss paradox*. To explain it, let us before consider the 'mere' formation of the black hole, without turn on Hawking's radiation. Because of the presence of the event horizon, an external observer at infinity, say Bob, does not know the full details of the star from which the black hole has been formed. However, and in general, the external observer can always argue that the remaining information is not lost, since it still lies inside the black hole, even if it is not accessible in the outer region. Although Bob loses the possibility of reconstructing the past (breakdown of 'postdictablity'), there is no problem at all for predicting the future. Notice that a breakdown of *classical* predictability could happen if a *naked singularity* is allowed. This observation leads Penrose [1973] to state the so called *cosmic censorship conjecture*: Nature abhors naked singularities and forces them to be covered by an horizon.

If quantum effects are taken into account, the situation is more complicated. Consider an initial pure state $|\psi_{in}\rangle$ prepared on a Cauchy surface $\Sigma_{in}$ before the formation of the horizon (for instance $\Sigma_{in} = \mathscr{I}_-$). Let it evolve in the (dynamical) collapsing SpaceTime, and consider the evolution unitary. This means that on any future Cauchy surface the state maintains its purity. When the horizon forms, any Cauchy surface $\Sigma$ is split into two regions $\Sigma = \Sigma_{BH} \cup \Sigma_{ext}$, respectively lying inside and outside the black hole. On such a surface, the evolved pure state $|\psi\rangle$ can be expanded as

$$|\psi\rangle = \sum_{k,l} c_{k,l} \, |k\rangle_{BH} \otimes |l\rangle_{ext} \ . \tag{2.89}$$

where $|k\rangle_{BH}$ and $|l\rangle_{ext}$ are orthonormal basis in the internal and external region. A local measurement in the external region associated with an operator $\mathcal{O}$ is then of the form

$$\begin{aligned} \langle\psi|\,\mathcal{O}\,|\psi\rangle &= \sum_{k,l,k',l'} \langle k'|_{BH} \langle l'|_{ext} \, c^\star_{k',l'} \, \mathcal{O} \, c_{k,l} \, |l\rangle_{ext} \, |k\rangle_{BH} = \\ &= \sum_{k,l,k',l'} c^\star_{k',l'} c_{k,l} \, \langle k' \,|\, k\rangle_{BH} \, \langle l'|\,\mathcal{O}\,|l\rangle_{ext} = \\ &= \sum_{k,l,l'} c^\star_{k,l'} c_{k,l} \, \langle l'|\,\mathcal{O}\,|l\rangle_{ext} = \\ &= \mathrm{Tr}\{\rho\,\mathcal{O}\} \end{aligned} \tag{2.90}$$

where we have introduced the *density matrix* $\rho$

$$\rho = \sum_{k,l,l'} c^\star_{k,l'} c_{k,l} \, |l\rangle \, \langle l'|_{ext} \tag{2.91}$$

obtained from $|\psi\rangle\,\langle\psi|$ by tracing over all the internal states. That is for an external observer the initial state is now seen as a mixed state, due to the fact that the degrees of freedom relative to the internal region of the Cauchy surface are inaccessible. If $|\psi\rangle_{in}$ is a vacuum Minkowski state prepared on $\mathscr{I}_-$ and the external part of the final Cauchy surface is taken to be $\mathscr{I}_+$, this mixed state is nothing but the thermal state of Hawking's radiation. However, up to now, this is

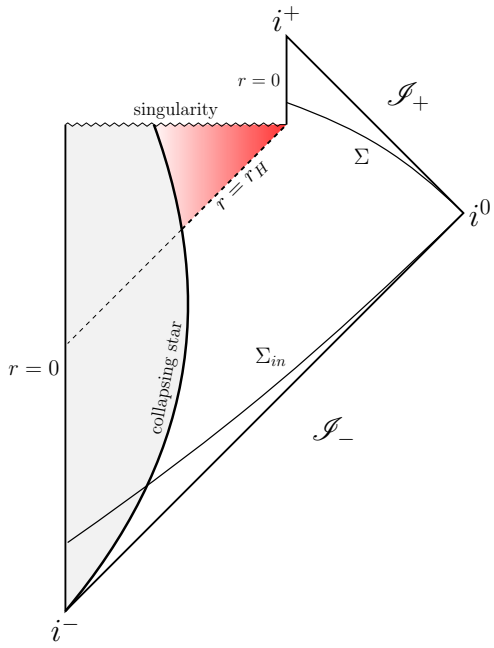


**Figure 2.2.** Penrose-Carter diagram of formation and complete evaporation of a black hole. The black hole region is red-shaded.

just the quantum mechanical version of the previous considerations. The external observer can again argue that the remaining information is not lost because it just lies inside the horizon. Nevertheless, we must consider now that the black hole will completely evaporate leaving nothing else but Hawking's radiation. See Fig. 2.2.

*The final state is necessarily a mixed state. Therefore, the fundamental principle of quantum mechanics stating that the evolution of a quantum system is unitary breaks down if a singularity forms. Information is lost inside it.*

Without changing the general relativistic framework, two solutions are possible. (*i*) The black hole doesn't evaporate completely, but settles in a either stable or exploding planckian-size remnant where information in stored. However, some arguments lying on holographic principles as the Bekenstein's and the Bousso's bounds strongly undermine this possibility, stating that a planckian-size object is 'too small' to contain such a huge amount of information. (*ii*) The other possibility is that in some way information starts escaping from the black hole well before it reaches Planck regimes and the purity of the final state is recovered. We will better examine this possibility in Section 2.4.1. However, this means that the event horizon can be crossed, allowing a violation of macroscopic causality.

The debate on if and how unitarity is recovered in gravitational collapse scenario is still open. Nowadays, new tolls from string theory as the AdS/CFT correspondence, as well as new ideas by Susskind, Thorlacius, and Uglum [1993] (complementarity) and Almheiri et al. [2013] (firewalls) strongly renewed the discussion. The lack of unitarity will be one of the main reasons for the next Parts of this work. Before addressing this topic, however, let us finish the discussion on the implication of Hawking's result.

When Hawking [1974] firstly presented it, its importance was amplified by the fact that it put on a solid physics ground the so called *law of black hole thermodynamics*. One year before, indeed, Hawking himself, together with Bardeen,

Carter [Bardeen, Carter, and Hawking 1973] and Bekenstein [1973], suggested that the mechanics of black hole SpaceTimes allows to formulate four laws in a strict analogy with the four well known laws of thermodynamics. However, this analogy was just a mathematical curiosity until Hawking's result. Let us explain why, starting from a brief review of black holes mechanics' laws.

## 2.3 Black Hole Thermodynamics

For a complete dissertation we refer to the classic paper by Bardeen, Carter, and Hawking [1973], and to Wald's book [Wald 1984, p. 330] and living review [Wald 2001].

**The 0th law** As seen in Section 2.1.2, the black hole geometry admits a Killing vector field $\chi^a$. Moreover, it comes out to be normal to the event horizon $H$ and null on it, i.e. $\chi^b\chi_b|_H = 0$. It follows that also the vector $\nabla^a(\chi^b\chi_b)$ is normal to the horizon and then it is proportional to $\chi^a$. This proportionality defines a function $\kappa$ on the horizon such that

$$\nabla^a(\chi^b\chi_b) \overset{H}{=} -2\,\kappa\,\chi^a \ . \tag{2.92}$$

For a stationary black hole, $\kappa$ comes out to be the acceleration, as exerted at infinity, needed to keep an object at the horizon, from which its name *surface gravity* of the horizon. The zeroth law of BH mechanics asserts that

*Given a stationary black hole, the surface gravity $\kappa$ is* constant *over each connected region of the black hole horizon.*

In the case of non-rotating, uncharged (in one word: Schwarzschild) black holes of mass $m$, this constant turns out to be

$$\kappa = \begin{cases} +\dfrac{1}{4m} & \text{on the future event horizon;} \\ -\dfrac{1}{4m} & \text{on the past event horizon.} \end{cases} \tag{2.93}$$

**The 1st law** The first law concerns what happens perturbing a black hole in equilibrium, for example throwing in it some amount of matter. If we suppose that, after a transient to absorb the perturbation, our SpaceTime settles in a new equilibrium state, then it is possible to relate the change in mass $m$ with the change in electric charge $Q$, in angular momentum $J$ and, overall, in area of the horizon's surface $A$ as

$$\delta m = \frac{\kappa}{8\pi}\,\delta A + \Omega_H\,\delta J + \Phi_H\,\delta Q \ . \tag{2.94}$$

where $\Omega_H$ is the *angular velocity* of the horizon, while $\Phi$ the electrostatic potential on it. In the Schwarzschild's case, it reduces to

$$\delta m = \frac{\kappa}{8\pi}\,\delta A \ , \tag{2.95}$$

assuming the perturbation to not give neither electric charge nor angular momentum to the hole.

**The 2nd law** Despite of the complicated mathematical proof of the second law, it can be phrased in a really simple way

*In any classical dynamical process, the area of the black hole horizon can never decrease:*

$$\delta A \geq 0 \,. \tag{2.96}$$

**The 3rd law** While the other laws are based on rigorous mathematical proof, the third and last law of BHs' mechanics was initially just postulated by Bardeen, Carter, and Hawking [1973] stating that

*Starting from a black hole with non-null surface gravity $\kappa \neq 0$, it is impossible to reduce $\kappa$ to zero in a finite amount of time (or steps).*

The "gedanken experiments to destroy a black hole" proposed by Wald [1974] were the first evidences of the validity of such a conclusion. He imagined to hit a black hole with particles whose mass, angular momentum and charge were calibrated in a way that $\kappa$ reduces; in this framework he showed that the decreasing rate of $\kappa$ becomes the more negligible the more $\kappa$ itself approaches zero. Only in 1986, Israel [1986] gave a first proof of the third law valid when the weak energy condition is satisfied.

Given in these forms, the relationship between this laws and the laws of thermodynamics is clear, as resumed in the following Table:

| Laws | Black holes' mechanics | Thermodynamics |
|---|---|---|
| 0th | $\kappa = \text{const.}$ | $T = \text{const.}$ |
| 1st | $\delta m = \frac{\kappa}{8\pi}\,\delta A + \Omega_H\,\delta J + \Phi_H\,\delta Q$ | $\delta E = T\,\delta S + p\delta W$ |
| 2nd | $\delta A \geq 0$ | $\delta S \geq 0$ |
| 3rd | It's impossible to reach $\kappa = 0$ | It's impossible to reach $T = 0$ |

### Entropy

The most fascinating and puzzling conclusion arising from these analogies is that *any black hole is endowed with an entropy proportional to its area.* The suggestion was formalized the same year by Bekenstein [1973] with the use of information theory; he treated the BH entropy $S_{BH}$ as the *measure of information inaccessible* to an outer observer. In particular, he computed the increase of the area of the horizon due to a particle falling into the hole crossing the event horizon: as it disappears some information is lost with it and the area of the black hole increases, confirming the relation: $A \sim S_{BH} \sim$ inaccessible information. At the same time he argued that, if an entropy is not associated to a black hole, the second law of thermodynamics can be violated. Indeed, since the in-falling particle carries a non-null entropy $S_{\text{body}}$ (the uncertainty in one's knowledge of the internal configuration of the body), the entropy $S_{\text{ext}}$ of the accessible universe decreases when it crosses the horizon. However, admitting the presence of the entropy associated to the black hole, we expect this entropy to increase *at least* of an amount $S_{\text{body}}$. "At least", we said. Effectively, the increase of $S_{BH}$ may be even larger because any information about the particle that was available is now

hidden by the horizon. This argument led Bekenstein to the formulation of the *generalized second law* of thermodynamics (GSL):

*For an isolated system, the sum of the black hole entropy with the common entropy in the exterior never decreases*

$$\delta(S_{BH} + S_{\text{ext}}) \geq 0 \,, \tag{2.97}$$

largely discussed the year after in a entirely dedicated paper [Bekenstein 1974].

If the variation of the area can be associated with a variation of entropy, therefore, by the 1st law of BHs' mechanics, we should associate to a black hole a temperature $T_{BH}$ proportional to the surface gravity $\kappa$. The black hole becomes a "hot" black body. However, from a purely classical point of view this is not possible. In fact, as pointed out by Bardeen, Carter, and Hawking [1973] themself, a black hole cannot be in thermal equilibrium with a black body radiation at any non-zero temperature because there is no way the black hole can emit radiation, whereas some radiation would always be absorbed by it: *the effective temperature of a black hole is absolute zero.*

Here we are! The importance of the existence of Hawking's radiation is now manifest. Going beyond the purely classical framework, there actually exists a way in which the black hole can emit radiation. The Hawking's result built a new fascinating bridge connecting General Relativity, Quantum Field Theory and Thermodynamics.

Restoring the physical constants of Nature, from. Eq. (2.81) one can say that a black hole possesses an associated entropy

$$S_{BH} = k_B \frac{c^3}{4G\hbar} A + \text{const.} \tag{2.98}$$

or in terms of the mass, since $A = 4\pi(2m)^2$:

$$S_{BH} = k_B \frac{4\pi c^3}{G\hbar} m^2 + \text{const.} \tag{2.99}$$

The question immediately arises: *What is the origin of this entropy? What is the physical mechanism behind it?* Although lots of proposal came in succession, up to now the debate is still open (see Bekenstein [1994] and Wald [2001, sec. 5, sec. 6.2]). By analogy with statistical physics, one would like to obtain Eq. (2.98) identifying and counting the quantum dynamical degrees of freedom of a black hole. In order to do that, however, it will be necessary to go beyond the classical and semiclassical considerations, describing the black hole geometry in a full quantum theory of gravity. In such a way one could in principle count the number of quantum internal states that macroscopically arise, via no-hair theorem,[4] in a black hole with given values of mass, angular momentum and electric charge.

[4]Roughly speaking, the no-hair theorem asserts that the more general electro-vacuum axisymmetric solution of Einstein's equations must belong to Kerr-Newmann family. It corresponds to a spherical charged rotating black hole, and is characterized by only three macroscopic parameters: the mass $m$, the electric charge $Q$ and the angular momentum $J$. See for example Poisson [2004, p. 205].

However, without a complete theory of quantum gravity the degrees of freedom responsible for the entropy cannot be identified.

Another interesting proposal arises from the seminal works by Bombelli et al. [1986] and Srednicki [1993]: in the context of (3+1)-dimensional QFT of a scalar field in Minkowski space, the so called *entanglement entropy (Ent.Ent.)* associated with the splitting of the space in two regions is *proportional to the area* of the splitting surface, as well as the Bekenstein's entropy is proportional to the horizon area. Since the horizon splits the Schwarzschild SpaceTime in two regions, it seems natural to think that a generalization of the Srednicki [1993] and Bombelli et al. [1986] result can allow to identify the entropy of the black hole with the entanglement entropy [Sorkin 1983]. However different difficulties, as the so called *species problem*, condemned the idea to remain only one of the interesting proposed solution to the puzzle (see Solodukhin [2011, sec. 8]).

On the other hand, the study of the entanglement entropy in BH-like scenarios shines several interesting aspects which help the understanding of the evaporation process and the information-loss paradox. As discussed in Section 2.2.2, one of the possible way-out of this paradox is to allow information to escape well before the complete evaporation of the black hole. This scenario was proposed by Page [1993b] and is based on the concept of Ent.Ent.. Moreover, the last original part of this thesis, Chapter 6, is entirely based on the definition of entanglement entropy and its production by BH-like SpaceTimes [Bianchi, De Lorenzo, and Smerlak 2014]. For these reasons, we dedicate the entire next Section to the presentation of the main results about entanglement entropy, and its classical applications to BH physics.

## 2.4 Entanglement Entropy

*Entanglement* ("Verschränkung" as originally named by Schrödinger in a letter sent to Einstein) is one of the most counterintuitive and controversial predictions of Quantum Mechanics. According to the Copenhagen interpretation, a pair of quantum systems may be described by a single wave function, which encodes the probabilities of the outcomes of experiments that may be performed on the two systems, whether jointly or individually. The origin of the entanglement comes from the fact that may be not possible to write the wave function of the two systems as the joint state of the two subsystems. More precisely, consider a quantum system described by states in an Hilbert space $\mathcal{H}$, an observer Alice who measures only a subset $A$ of a complete set of commuting observables defining the sub-Hilbert space $\mathcal{H}_A \subset \mathcal{H}$, and another observer Bob who may measure the remainder (with associated $\mathcal{H}_B \subset \mathcal{H}$). The whole Hilbert space $\mathcal{H}$ can be written as $\mathcal{H} = \mathcal{H}_A \otimes \mathcal{H}_B$ and any state $|\psi\rangle \in \mathcal{H}$ can be decomposed as

$$|\psi\rangle = \sum_{i,j} \lambda_{i,j} \, |u_i\rangle_A \, |u_j\rangle_B \ , \tag{2.100}$$

where $\{|u_i\rangle_A\}$ and $\{|u_j\rangle_B\}$ are bases of the subsystems. Now, if the coefficients $\lambda_{i,j}$ can be factorized into products, i.e. $\lambda_{i,j} = \alpha_i \beta_j$ then the state $|\psi\rangle$ is said to be *separable* (or *factorizable*).

Contrarily, the state is said to be *entangled*.

Roughly speaking, the latter case tells us that the two subsystems are *correlated* even if not directly interacting, as for example two particles that interact and then separate: if a measurement is done on one particle, the other instantly "knows" its outcome. Despite the strong opposition of Einstein, Podolsky, and Rosen [1935] and many other physicists, entanglement is nowadays accepted in quantum mechanics, finding application in almost any field of physics and supported by empirical evidences.

*How to measure entanglement?* The main subject of this Section, the entanglement *entropy* defined the first time by Schumacher [1995], is a suitable answer to this question. Although there are other measures of entanglement, the entropy is most readily suited to analytic investigation.

**Definition** Consider the same quantum system as before, described by a pure state $|\psi\rangle$ in an Hilbert space $\mathcal{H}$, together with the two observers Alice and Bob. Moreover, suppose $\dim\mathcal{H}_A = m$ and $\dim\mathcal{H}_B = n$ with $m \leq n$ ($\dim\mathcal{H} = N = m \cdot n$). Defining the density matrix associated to $|\psi\rangle$ by $\rho = |\psi\rangle\langle\psi|$, the reduced density matrices of each subsystem are found by tracing out the degrees of freedom related to the other, i.e.

$$\rho_A = \mathrm{Tr}_B\rho \qquad \text{and} \qquad \rho_B = \mathrm{Tr}_A\rho \ . \tag{2.101}$$

The *entanglement entropy* of $A$ is then defined as the von Neumann entropy associated to $\rho_A$, namely

$$S(A) = -\mathrm{Tr}_A\big[\rho_A \log\rho_A\big] \ . \tag{2.102}$$

This definition applies even in the case $|\psi\rangle$ is not a pure state, but a mixed one, namely $\rho^2 \neq \rho$.

**Non-extensive** Thanks to the *Schmidt decomposition*, any state $|\psi\rangle \in \mathcal{H}$ can be written as

$$|\psi\rangle = \sum_{k=1}^{m} \alpha_k \, |u_k\rangle_A \, |v_k\rangle_B \ , \tag{2.103}$$

where $\{|u_k\rangle_A\}$ and $\{|v_k\rangle_B\}$ are orthonormal sets respectively in $\mathcal{H}_A$ and $\mathcal{H}_B$, while the coefficients $\alpha_k$ are real, non-negative and uniquely determined by $|\psi\rangle$ as the square root of the eigenvalues of $\rho_A$ normalized such that $\sum_k \alpha_k = 1$. It strictly follows that

$$S(A) = S(B) \ : \tag{2.104}$$

*Ent.Ent. is not an extensive quantity.*

**Bounded** Moreover, Ent.Ent. is null for separable states and reaches a maximum (given by the log of the dimension of the space) when the state is *maximally entangled*, i.e. the density matrix $\rho_A$ has all non-zero equal eigenvalues:

$$0 \leq S(A) \leq \log m \ . \tag{2.105}$$

**Sub-additive** Finally, it has the remarkable property

$$S(A \cup B) + S(A \cap B) \leq S(A) + S(B). \tag{2.106}$$

This property, called *sub-additivity*, does not have a counterpart in classical information theory, where the entropy of a system can never be lower than that of its components.

The entanglement entropy gives a measure of the correlation between the two subsystems or, complementarily, of the *information shared* by Alice and Bob. Indeed, it is possible to define the amount of information $I$ as the discrepancy of the Ent.Ent. by its maximum, i.e.

$$\begin{aligned} I(A) = \log m - S(A) \qquad I(B) = \log n - S(B) \\ I(A \cup B) = \log N - S(A \cup B)\ . \end{aligned} \tag{2.107}$$

The shared information, or better the *mutual information* between Alice and Bob is defined as

$$\begin{aligned} I(A,B) = I(A \cup B) - I(A) - I(B) = \\ = S(A) + S(B) - S(A \cup B) \end{aligned} \tag{2.108}$$

which, thanks to the sub-additivity of the Ent.Ent., is non-negative. For a pure state $I(A,B) = 2S(A) = 2S(B)$.

As mentioned at the end of the last Section, Page [1993b] used these notions to investigate the evaporation process of a black hole. Let us review his line of reasoning.

### 2.4.1 Page's Curve

Consider a black hole which evaporates *via* Hawking's radiation. The radiation and the black hole can be considered as subsystems of an isolated quantum system in a pure state. As the black hole emits radiation, correlations are set up between the two subsystems and the Ent.Ent. associated with the radiation $S_{\text{rad}}$ grows. However, looking at Eq. (2.105) it is clear that requiring the final state to be pure implies the final Ent.Ent. to be zero; in particular, if the BH totally evaporates then $S_{\text{rad}}$ has to finally vanish. This means that $S_{\text{rad}}$ should have two regimes for unitarity to be preserved: a growing phase corresponding to the early Hawking-like stage of evaporation, and a decreasing phase corresponding to the release of information by the "old" black hole. The evolution of $S_{\text{rad}}$ is usually called *Page's curve* and the turning point, where then semiclassical analysis breaks down, is generally referred to as the *Page's time*. See Fig. 2.3. To estimate the Page's time, let us follow the original argument. It relies on a previous conjecture proposed by Page [1993a] himself and later proved by Foong and Kanno [1994].

**Theorem 2.1 Average entropy of a subsystem**
*Consider the same framework in the definition of Ent.Ent., namely a quantum system in a state of a $N$-dimensional Hilbert space $\mathcal{H}$, divided into two subsystems $A$ and $B$. Suppose $dim\mathcal{H}_A = m$ and $dim\mathcal{H}_B = n$ with $m \leq n$. If the system*

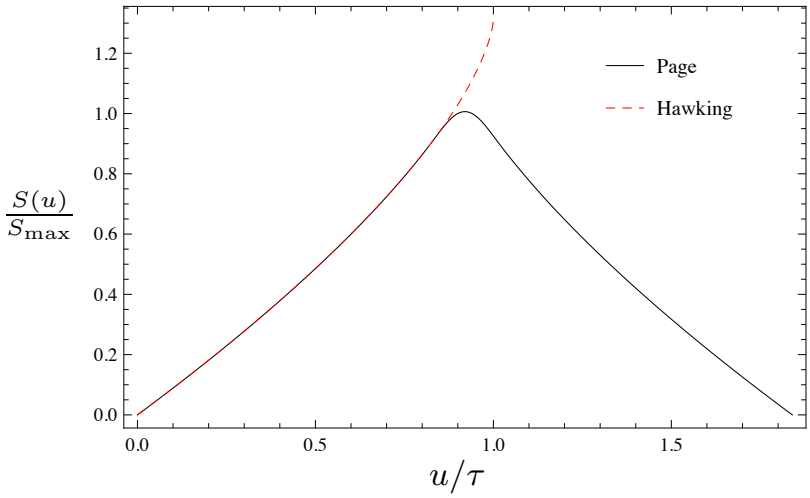


**Figure 2.3.** Page's curve as originally depicted by Page [1993b], compared to its totally semiclassical counterpart. $u$ is the affine parameter on future null infinity. Figure reproduced from Bianchi and Smerlak [2014a].

*is in a maximally entangled (or random) pure state* $|\psi\rangle \in \mathcal{H}$*, then the average entanglement entropy is given by*

$$\langle S_{m,n}\rangle = \sum_{k=n+1}^{nm} \frac{1}{k} - \frac{m-1}{2n} \tag{2.109}$$

*that in the case* $1 \ll m \leq n$ *becomes*

$$\langle S_{m,n}\rangle \simeq \log m - \frac{m}{2n}\,. \tag{2.110}$$

It follows that the information in the smaller subsystem

$$I(A) = \log m - \langle S_{m,n}\rangle = \frac{1}{2}\frac{m}{n} \tag{2.111}$$

is less than one bit of information: Alice would measure a nearly thermal state and she doesn't know anything about the purity of the joint state. The information for the bigger subsystem reads

$$I(B) = \log \frac{n}{m} + \frac{m}{2n} \tag{2.112}$$

while the mutual information is

$$I(A,B) = \log m^2 - \frac{m}{n}\,; \tag{2.113}$$

the sum of the three gives the correct result for the overall maximally entangled pure state: $I(A \cup B) = \log(mn) = \log N$. Reminding that we are working in the case $1 \ll m \leq n$, we can now distinguish two important limit cases:

$$I(A \cup B) \sim \begin{cases} I(B) & \text{if } m \ll n \\ I(A,B) & \text{if } m \simeq n \end{cases}\,: \tag{2.114}$$

the totality of the information is almost completely stored either in the larger subsystem $B$ or in the correlations between the two, depending on whether $B$ is much bigger than $A$ or they are comparable.

What happens when we apply this analysis to a black hole evaporation framework? At *early times*, the black hole's subsystem is much bigger than the radiation's one: Alice doesn't acquire any information and perceives a nearly thermal Hawking's radiation. On the opposite limit, when radiation has been emitted for a very long time, the situation is reversed: almost all the information is now stored in the radiation's subsystem which is much larger then the black hole's one. This means that *information must escape* from the BH, *via* quantum correlations. Now, the Page's time occurs when the shared information is maximum, namely when the two subsystems have the same dimension $n = m = \sqrt{N}$. To estimate the value of the turning point Page assumes that, when the black hole is still large, its Bekenstein's entropy $S_{BH}$ is given by

$$S_{BH} \sim \log d \tag{2.115}$$

where $d$ is the dimension of the Hilbert space associated to the black hole. Since at the beginning of the evaporation the dimension of the radiation's subsystem is negligible $d \sim N$, the initial entropy of the black hole is $S_{BH}(0) \sim \log N$. Furthermore, at the turning point $S_{BH}(t_{\text{page}}) \sim \log \sqrt{N} = \frac{1}{2} S_{BH}(0)$. Relating now this result with the Bekenstein entropy in terms of the mass, Eq. (2.99), follows that the black hole starts to release information when the mass is still large $m_{\text{page}} \sim \frac{m}{\sqrt{2}} \gg m_{\text{planck}}$.

This argument will be much more precise from a quantitative point of view in Chapter 6.

# Part II

# Original Results 1: Static Non-Singular Black Holes

*The presence of a singularity inside a black hole implies a breakdown of the predictability of the theory bringing, when dynamical evaporation is considered, to the information-loss paradox. Due to the Singularity Theorems, the formation of such a ill-defined region seems unavoidable in classical General Relativity. Nevertheless, the singularity is expected to be cured by quantum gravitational effects that become important in regions with high density of matter, as in the last stages of the life of a collapsing star. When matter reaches Planck density, quantum gravity generates pressure sufficient to counterbalance weight and the collapse stops, avoiding the formation of a singularity.*

# Summary



The two previous Chapters introduced the main aspects of classical black hole physics, each of them underlining one main problem. The first one is the unavoidable formation of a singularity in any gravitational collapse process that forms a trapped surface. Formalized by the proof of the *Singularity Theorems* in Section 1.4, it implies a breakdown of the theory of General Relativity. Strongly related to the first is the second problem arose when quantum mechanical effects are turned on in the framework of QFT in curved SpaceTimes. The astonishing result by Hawking [1976] that black holes radiate energy away with a Planck spectrum, indeed, implies the *information-loss paradox* (Section 2.2.2).

It is commonly believed that a resolution of the singularity in the deep interior of a collapsed star, will simultaneously solve the paradox. At the same time, since a star collapsing and forming a black hole will reach a phase in which the density becomes planckian, one expects pure quantum gravitational effects to dominate generating pressure sufficient to counterbalance weight avoiding the formation of the singularity, exactly as in a hydrogen atom [Ashtekar and Bojowald 2006; Modesto 2004, 2006]. In the absence of a full theory of quantum gravity, it is possible to start from the hypotheses of the singularity theorems and ask which one could be relaxed, as consistently as possible with physical requirements, in order to mimic background-independent quantum gravity effects that allow the avoidance of the singularity. This approach leads to an interesting area of research: that of *non-singular (or regular) black holes*. The idea is to build effective metrics solutions the Einstein's Equations such that the resulting SpaceTime is Schwarzschild-like in the outer region and, at the same time, singularity-free in the deep interior (see for example [Bardeen 1968; Dymnikova 1992; Hayward 2006; Hossenfelder, Modesto, and Premont-Schwarz 2010; Mazur and Mottola 2001; Nicolini 2005]).

The aim of this Part is to deeply analyze the statical features of this kind of metrics, starting, in the first Chapter, from the proof of a theorem presented by Dymnikova [2002] asserting that, if such non-singular black holes exist, they must have a rather universal causal structure. This structure is better studied focusing on the particular example proposed by Hayward [2006] and recently reconsidered by many authors [Bardeen 2014; Frolov 2014; Rovelli and Vidotto 2014].

The second Chapter contains the first original results. We point out some *before unnoticed problems* affecting this picture for which a relatively easy *solution* is proposed (Modified Hayward's Metric).

Chapter 3

# What is Known about Non-Singular BHs

From an historical point of view, the first regular solution of Einstein Equations having an event horizon and a regular center was obtained by Bardeen in his (really hard to find) paper [Bardeen 1968]. On the other hand, as said in the introduction to this Chapter, this metric belongs to a family of solutions having the same causal structure. The proof of this assertion is given by citedymnikova2002cosmological and is here re-proposed.

## 3.1 Dimnikova's Theorem

Let us assume that the SpaceTime of a spherically symmetric gravitationally collapsed object can still be described (at least within an approximation) by a static effective metric. Thanks to Birkhoff's theorem (see Weinberg [1972, Sec. 11.7] for a simple proof), the most general static spherically symmetric line element reads

$$ds^2 = -e^{\mu(r)}dt^2 + e^{\nu(r)}dr^2 + r^2 d\Omega^2 \,. \tag{3.1}$$

From the Einstein equations

$$R_{\mu\nu} - \frac{1}{2}g_{\mu\nu}R = 8\pi T_{\mu\nu} \tag{3.2}$$

we find the only non-null components of the stress energy tensor to be

$$8\pi T^0_0 = -8\pi\rho(r) = e^{-\nu}\left(\frac{1}{r^2} - \frac{\nu'}{r}\right) - \frac{1}{r^2} \tag{3.3a}$$

$$8\pi T^1_1 = 8\pi p_r(r) = e^{-\nu}\left(\frac{1}{r^2} + \frac{\mu'}{r}\right) - \frac{1}{r^2} \tag{3.3b}$$

$$8\pi T^2_2 = 8\pi T^3_3 = 8\pi p_\perp(r) = e^{-\nu}\left(\frac{\mu''}{2} + \frac{\mu'^2}{4} + \frac{\mu' - \nu'}{2r} - \frac{\mu'\nu'}{4}\right) \,, \tag{3.3c}$$

where $\rho(r)$ is the energy density, while $p_r(r)$ and $p_\perp(r)$ are respectively the radial and the transversal pressures. Combining Eqs. (3.3), we can rewrite Eq. (3.3c) as

$$p_\perp = p_r + \frac{r}{2}p_r' + (\rho + p_r)\frac{M(r) + 4\pi\, r^3 p_r}{2(r - 2\, M(r))} \tag{3.4}$$

which is a generalization of the Tolman-Oppenheimer-Volkoff equation ([Wald 1984, p. 127]) in the case of different pressures. Integration of Eq. (3.3a) yields

$$e^{-\nu} = 1 - \frac{2M(r)}{r} \tag{3.5}$$

with

$$M(r) = 4\pi \int_0^r dx \rho(x) x^2 \ . \tag{3.6}$$

**Theorem 3.1 Dymnikova's theorem**
*Under the following assumptions:*

1. *Dominant energy condition (DEC);*
2. *Asymptotic flatness;*
3. *Finiteness of $m$;*
4. *Finiteness of $\rho(r)$ for all $r$;*
5. *Regularity of the metric in $r = 0$;*

*the resulting restrictions on the functions $\mu(r)$ and $\nu(r)$ hold:*

1. $\lim_{r\to\infty} \mu(r) = 0$;
2. $\nu(0) = 0$;
3. $\mu'(r) + \nu'(r) \geq 0 \ \forall\, r$, *with* $\mu'(0) = \nu'(0) = 0$.
4. $\mu(0) \leq 0$;

*Proof.* Eqs. (3.3) tells that the energy momentum tensor is, following the classification exhibited in Appendix B, clearly of *Type I*. Therefore DEC holds if and only if

$$\rho(r) \geq |p_i| \qquad \text{for } i = 1, 2, 3 \ , \tag{3.7}$$

and regularity of the density implies regularity of the pressures.

In the limit $r \to \infty$, Eq. (3.5) becomes

$$e^{-\nu(r)} = 1 - \frac{2m}{r} \qquad \text{with} \qquad m = 4\pi \int_0^\infty dr \rho(r) r^2 \ . \tag{3.8}$$

Condition of finiteness of $m$ forces the density $\rho(r)$ to vanish at infinity quicker the $r^{-3}$. Consequently, Eq. (3.7) requires pressures to vanish in this limit, leading,

through Eq. (3.3c), to $\mu' \to 0$ and so $\mu \to const.$ Asymptotic flatness directly implies the first restriction: $\mu \to 0$ as $r \to \infty$.

From Eq. (3.6) and requirement of finiteness of $\rho(r)$ follows that $M(r) = 0$ at $r = 0$ and then the second restriction $\nu(r = 0) = 0$.

Subtracting Eq. (3.3a) to Eq. (3.3b) we have

$$T_1^1 - T_0^0 = p_r(r) + \rho(r) = \frac{1}{8\pi}\frac{e^{-\nu(r)}}{r}(\nu'(r) + \mu'(r)) \; ; \tag{3.9}$$

since, as said before, pressures and density are finite thanks to the DEC, Hypothesis 5 ($e^{\nu}(r) < \infty$) and the above equation lead to $\nu'(0) + \mu'(0) = 0$. Similarly, Eq. (3.3c) tells us $\nu'(0) - \mu'(0) = 0$. Then, $\mu'(0) = \nu'(0) = 0$.

The last effort is to show that the sum $\mu'(r)+\nu'(r)$ is non-negative everywhere, since, as we will see, restriction 4 strictly follows from the previous ones. To do that, let us consider two different cases: $e^{-\nu(r)} \geq 0$ and $e^{-\nu(r)} < 0$. In the former, $\mu'(r) + \nu'(r) \geq 0$ simply follows by Eq. (3.9). The same argument seems to show that in the second case $\mu'(r) + \nu'(r) < 0$. However, where $e^{-\nu(r)} < 0$, the radial coordinate $r$ becomes timelike while $t$ becomes spacelike. Consequently the roles of the coordinates are exchanged, and now $T_0^0$ represent a tension, $p_r = T_0^0$, along the axes of the spacelike three cylinders of constant 'time' $r = const$, as well as $-T_1^1$ determines the 'density profile'.[1] It follows that $T_1^1 - T_0^0 = -(p_r + \rho)$ and the combination of Eq. (3.9) and the DEC still demands the sum $\mu'(r) + \nu'(r)$ to be non negative.

The last restriction is now trivial. From the showed results, the function

$$A(r) \equiv \mu(r) + \nu(r) \tag{3.10}$$

is a monotonically increasing function from $A(0) = \mu(0)$ to $A(\infty) = \nu(\infty) = 0$ (for the finiteness of $m$ and Eq. (3.8)). As a result $\mu(0) \leq 0$.

□

From the proof is evident that requiring the DEC is needed only to ensure, thanks to $\rho(r) < \infty$, the finiteness of the pressures. The same results are therefore emerging just postulating the validity of the WEC and the finiteness of the pressures ($p_i(r) < \infty$ for $i = 1, 2, 3$ everywhere).

The value $\mu(0)$ plays the role of family parameter and, as will be shown, the choice of it will be crucial concerning the physical plausibility of the model.

### 3.1.1 The case A(0) = 0

The simplest choice is clearly to take $A(0) = \mu(0) = 0$, such that $A(r) = 0$ everywhere. In this case the line element reduces to

$$ds^2 = -F(r)dt^2 + \frac{1}{F(r)}dr^2 + r^2 d\Omega^2 \tag{3.11}$$

with

$$F(r) = 1 - \frac{2M(r)}{r} \; . \tag{3.12}$$

[1] Actually the identification of $T_0^0$ with $\rho$ and $T_1^1$ with $p_r$ has been a little abuse of notation.

Since $A(r) = 0$ (i.e. $\rho(r) = -p_r(r)$ from Eq. (3.9)), Eq. (3.4) simplifies to

$$p_\perp = -\rho - \frac{r}{2}\rho' \qquad \Longrightarrow \qquad \rho' = -\frac{2}{r}(p_\perp + \rho) \; . \tag{3.13}$$

Because of the DEC, $p_i + \rho \geq 0$, the energy density $\rho$ is then a monotonically decreasing function of $r$ ($\rho' \leq 0$). Moreover, regularity of the pressures forces $|\rho'|$ to be non divergent, leading to $p_\perp(0) = -\rho(0)$. It follows that the equation of state in the origin is the one of a deSitter vacuum (see Hawking and Ellis [1973, Sec. 5.2])

$$p_i = -\rho \qquad \text{in } r = 0 \; , \tag{3.14}$$

which in turn implies the violation of the strong energy condition, as we expected. The line element in the origin becomes

$$ds^2 \overset{r\to 0}{\longrightarrow} -\left(1 - \frac{r^2}{L^2}\right) dt^2 + \left(1 - \frac{r^2}{L^2}\right) dr^2 + r^2 \, d\Omega^2 \tag{3.15}$$

where the physics is completely determined by an effective cosmological constant $\Lambda$ defined by

$$L^2 \equiv \frac{3}{\Lambda} \; . \tag{3.16}$$

Of course, the specific form of the line element depends on the function $M(r)$. This family includes most of the metrics so far proposed in the literature, as for example,

$$M(r) = \begin{cases} \dfrac{m\, r^3}{(r^2 + a^2)^{\frac{3}{2}}} & \text{Bardeen [1968];} \\ m\left(1 - e^{-\frac{r^3}{2m\, L^2}}\right) & \text{Dymnikova [1992];} \\ \dfrac{m\, r^3}{r^3 + 2mL^2} & \text{Hayward [2006];} \\ \dfrac{2m}{\sqrt{\pi}}\gamma\left(\dfrac{3}{2}; \dfrac{r^2}{4L^2}\right) & \text{Nicolini [2005],} \end{cases} \tag{3.17}$$

where $\gamma(a; b) \equiv \int_0^b t^{a-1} e^t \, dt$ is the incomplete Euler gamma. Since the structure and the principal features of this SpaceTimes are the same, it's easier to focus the narrow on the simplest one, i.e. the Hayward's one, in order to deeply analyze their physical plausibility. In the open debate about the information-loss paradox, this metric was recently reconsidered by different authors [Bardeen 2014; Frolov 2014; Rovelli and Vidotto 2014].

## 3.2 Hayward's Metric

As said before, the particular choice of the function $M(r)$ in the Hayward case is given by

$$M(r) = \frac{m\, r^3}{r^3 + 2mL^2} \qquad \text{that is} \qquad F(r) = 1 - \frac{2mr^2}{r^3 + 2mL^2} \tag{3.18}$$

where $L$ is the same as in Eq. (3.16).

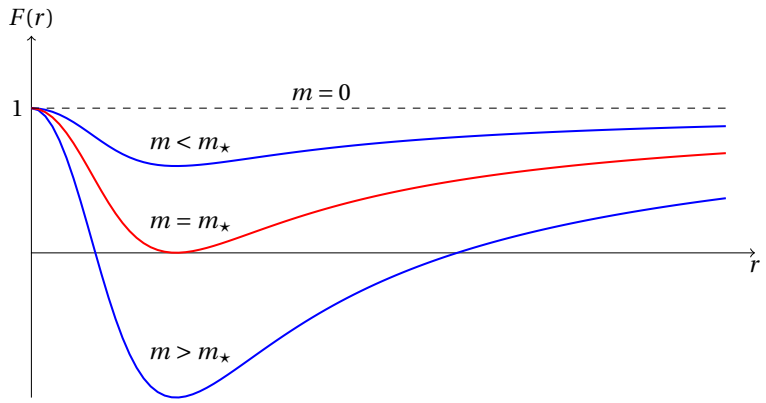


**Figure 3.1.** Redshift factor $g_{00}$ of the Hayward's metric as a function of the radius for different values of the mass $m$.

### 3.2.1 General Features

**Horizons** The horizons $r_H$ are given by the solutions of the equation

$$F(r) = 0 \tag{3.19}$$

that solved for $m$ gives

$$m(r_H) = \frac{r_H^3}{2(r_H^2 - L^2)} \,. \tag{3.20}$$

It follows the existence of a critical mass $m_\star = \frac{3\sqrt{3}}{4} L$ such that horizons are not present for values of $m$ below $m_\star$ and a pair of them ($r_+$ and $r_-$) appears above this threshold. The extremal case $m = m_\star$ corresponds to one degenerate horizon with radius $r_\star = \sqrt{3}\, L$ (see Figure 3.1).

Furthermore, defining

$$\cos x := 1 - \frac{27L^2}{8m^2} \,, \tag{3.21}$$

it is possible to write the solutions of Eq. (3.19) in the following, before un-noticed, explicit analytical expressions

$$r_+ = \frac{2m}{3}\left[1 + 2\cos\left(\frac{x}{3}\right)\right] \tag{3.22a}$$

$$r_- = \frac{2m}{3}\left[1 - 2\cos\left(\frac{x+\pi}{3}\right)\right] \,. \tag{3.22b}$$

In the extremal case $m = m_\star$, $x = \pi$ and then the two horizons join at $r_+ = r_- = 4/3\; m_\star = \sqrt{3}L = r_\star$. The other interesting limit is $m/L \gg 1$: in this case

$$\begin{aligned} r_+ &\simeq \frac{2m}{3}\,[1+2] = 2m \\ r_- &\simeq \frac{2m}{3}\left[1 - 2\left(\frac{1}{2} - \frac{3}{4m}L\right)\right] = L \,, \end{aligned}$$

as expected analyzing Figure 3.2 and as pointed out in Hayward [2006].

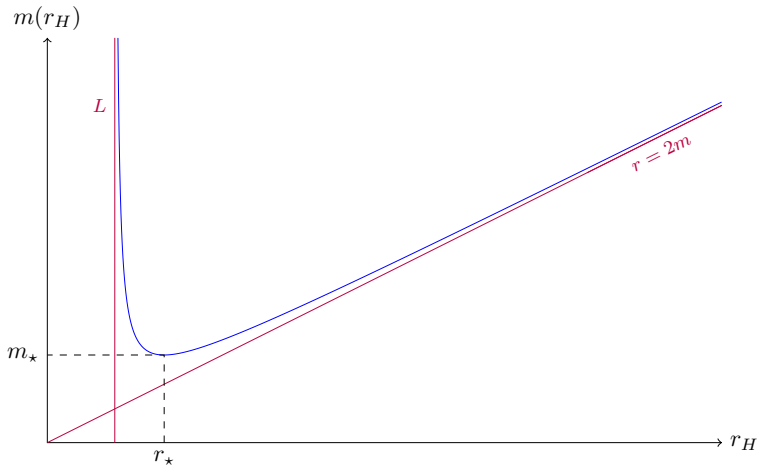


**Figure 3.2.** The relation between horizons radius and mass for the Hayward's metric.

**Causal structure** In order to explore the causal structure of this picture it is useful to solve the null geodesics equation. To do that, let us introduce Eddington-Finkelstein-like coordinates $(v, r, \theta, \varphi)$ (see Pag. 1.1.1). In these coordinates the metric (3.11) reads

$$ds^2 = -F(r)dv^2 + 2dvdr + r^2 d\Omega^2 \tag{3.23}$$

and the radial null geodesics equations can be found imposing

$$g_{\mu\nu}u^\mu u^\nu = 0 = -F(r)\,\dot{v}^2 + 2\,\dot{v}\,\dot{r}\ , \tag{3.24}$$

where dot denotes the derivative with respect to an affine parameter. This equation has two solutions: the first is $\dot{v} = 0$ and then $v = const$, while the second is obtained integrating the differential equation

$$\frac{dv}{dr} = \frac{2}{F(r)}\ . \tag{3.25}$$

Since the integral is not analytically solvable, we found a numerical solution using the software Wolfram Mathematica®. In Figure 3.3 solutions for different initial conditions are represented in the plane $v$-$r$. The most important feature to notice is the behaviour of the light cones in comparison with the one of the Schwarzschild case illustrated in Figure 1.1(a) of Section 1.1. In the region outside the outer horizon $r_+$, the behaviour is basically the same of the Schwarzschild outer region $(r > 2m)$. In the region inside $r_+$, on the other hand, the situation is drastically different: while in the Schwarzschild case the light cones are the more tilted the more the radius $r$ approaches the origin forcing lightlike (or null) and timelike geodesics to fall into the singularity, in the Hayward case the inner horizon plays a role opposite to the outer one, allowing the light cones to be un-tilted as they approach it. Time-like observers are not obliged to reach $r = 0$.

The complete causal structure is, as said in Appendix A, easily visualized by drawing the Penrose-Carter diagram associated to the SpaceTime. In our case, it is similar to the one of the Reissner-Nordström metric, with the fundamental difference that the singularity at the center is replaced by a regular timelike line. The diagram for the non-degenerate case is shown in Fig. 3.4.

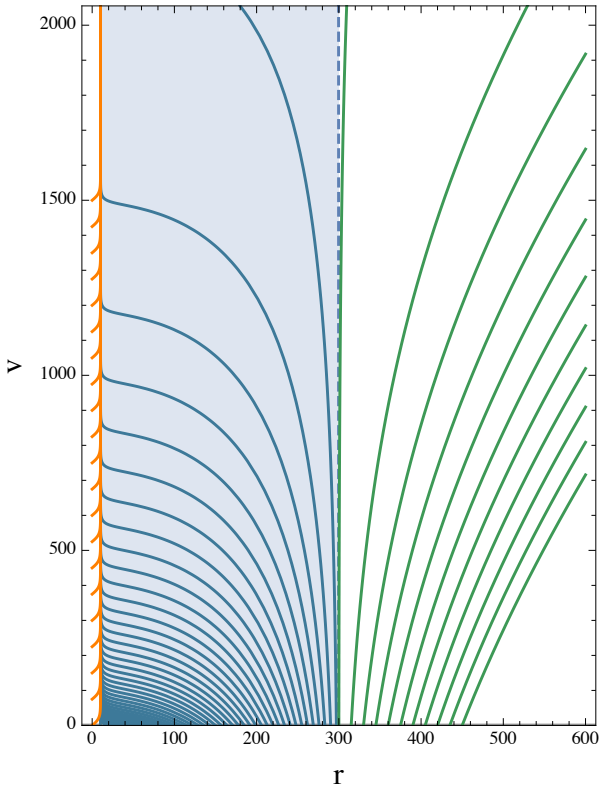


**Figure 3.3.** Numerical solutions for the outgoing null geodesic equation in the Hayward SpaceTime. Geodesics starting outside the outer horizon have a Schwarzschild-like behavior. Inside the trapping region (shaded) the inner horizon plays as an attractor and the light cone are un-tilted. The ingoing solutions are $v$ =const. lines, here non reproduced. We used $L = 10$ and $m = 150$ (Planck units).

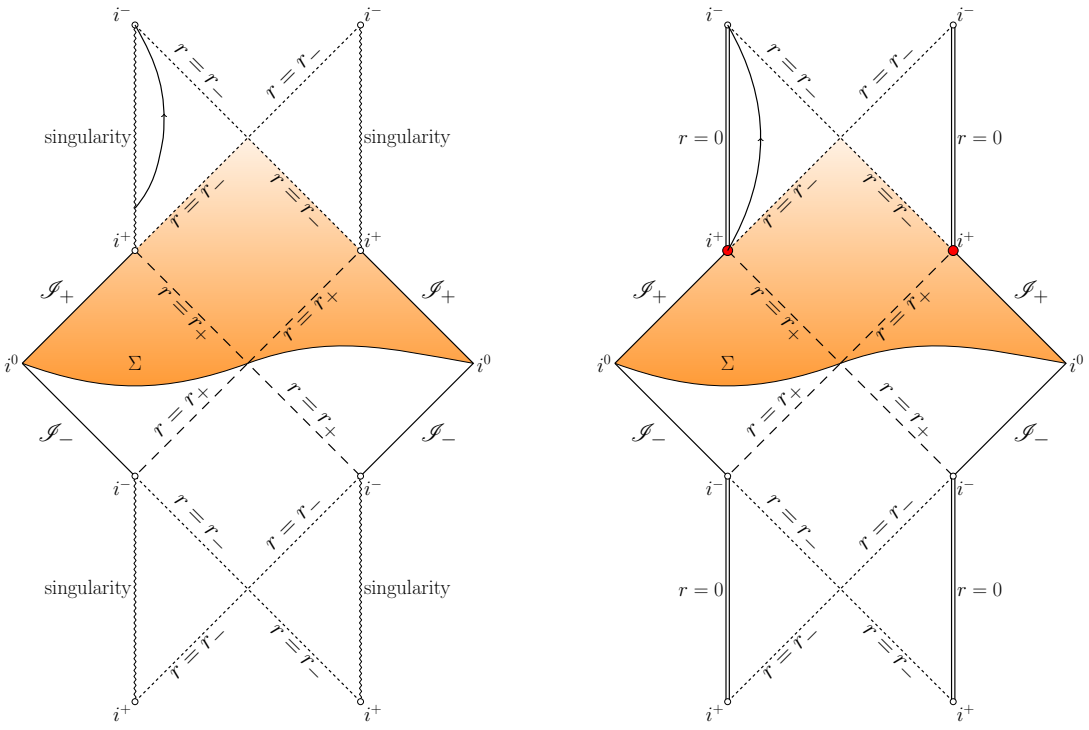


**Figure 3.4.** Penrose-Carter diagram for the non-degenerate Hayward SpaceTime (a) compared to the Reissner-Nordström one (b). Both of them repeat themselves infinitely in both up and down directions. However, in the Hayward's case, the timelike singularity at $r = 0$ is replaced by a regular center. Future Cauchy developments of the surface $\Sigma$ are shaded.

### 3.2.2 How Did We Avoid Singularity Theorems?

As explained in Section 1.2, Singularity Theorems' results come from three different types of hypotheses: (*i*) the validity of some conditions on the matter content of the SpaceTime (energy conditions), (*ii*) the validity of some geometrical properties of the SpaceTime (the presence of horizons or trapping surfaces), and (*iii*) the validity of some hypothesis on the causal structure of the system (global hyperbolicity).

*Which one of these hypotheses is relaxed in the Dynmikova's theorem framework?* Most of the Singularity Theorems we just sketched are avoided simply requiring the Strong Energy Condition to do not hold. On the other hand, the violation of the only Theorem we completely proved, Theorem 1.8 (Penrose 1965), is more subtle. The Weak Energy Condition, indeed, is postulated to be valid in the Dymnikova's Theorem, leading us to look to a violation of either hypotheses (*ii*) or (*iii*). To do that it is simpler to focus our attention on the Hayward's metric, where an event horizon is known to form. The answer to the main question is then straightforward: the avoidance of the Singularity Theorems has to be implied by *a lack of global hyperbolicity*.[2]

This sentence, even if subtle, is confirmed by looking at the conformal diagram in Fig. 3.4. We remind (see Section 1.2.2) that a SpaceTime is globally hyperbolic if it admits a Cauchy surface. A Cauchy surface is a closed achronal surface such that the union of its past and future Cauchy developments covers the entire SpaceTime. Finally, the future (resp. past) Cauchy development of a hypersurface $S$ is the set of points $x$ for which every inextensible past (resp. future) directed causal curve through $x$ intersects $S$ at least once. Roughly speaking, the set of points *completely* determined by initial data on $S$.

From Fig. 3.4, therefore, it is clear that, for the Reissner-Nordström SpaceTime, the lack of global hyperbolicity comes from the fact that past directed causal curves starting from points in the region inside the inner horizon $r_-$ ends in the singularity. The shaded future Cauchy development of a possible Cauchy surface $\Sigma$ does not cover the entire SpaceTime and the null surface $r = r_-$ is called a *Cauchy horizon*. In the Hayward case, however, the situation is more subtle. The singularity is now replaced by a regular core, and every past directed causal curves starting from points in the inner region seems to reach $\Sigma$ by 'bouncing' at the origin. Nevertheless, this is not correct. Indeed, we are not considering the causal curves represented as arrow lines that end at $i^+$. Since $i^+$ is a point of non-extensibility, those geodesics cannot be extended from $i^+$ to $\Sigma$ that therefore does not represent a Cauchy surface. Since there are not other possibilities to built a Cauchy surface, we conclude that the SpaceTime is not globally hyperbolic. In Borde [1997] the lack of globally hyperbolicity is explained by a *topology change* from compact to non-compact regions. See also Pacilio and Balbinot [2014] for a complete discussion.

**Degenerate case** In the degenerate case $m = m_\star$, the two horizons merge; the SpaceTime is again non-globally hyperbolic, as illustrated in the conformal diagram of Fig. 3.5.

[2] For a more precise discussion about it, see Hawking and Ellis [1973, p. 265].

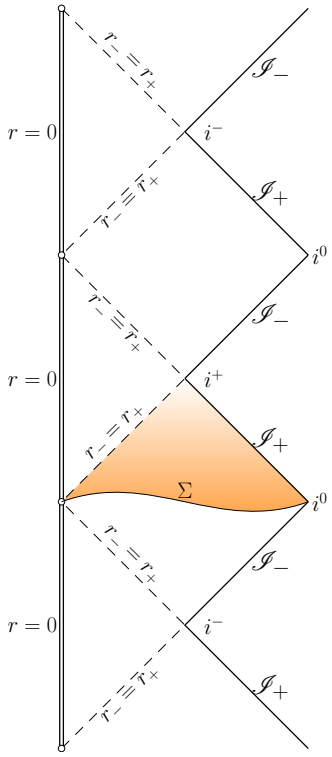


**Figure 3.5.** Penrose-Carter diagram of the degenerate Hayward SpaceTime. It repeats itself infinitely in both up and down directions. The future Cauchy development of the surface $\Sigma$ is shaded.

**Sub-planckian curvature** Violation of some classical energy conditions is not a problem, but rather a natural consequence of the fact that the singularity-free metric is supposed to include some quantum gravity effects. On the other hand, if we want the description of SpaceTime in terms of a classical metric to be meaningful, the curvature should always be sub-planckian, so that quantum details of the SpaceTime do not matter.

What about the curvature in the Hayward case? As shown in Fig. 3.6, the Kretschmann scalar turns out to be smoothly decreasing from a maximum value at the origin given by the expansion

$$\mathcal{K}^2 = R_{abcd}R^{abcd} = \frac{24}{L^4}\left(1 - 2\frac{r^3}{mL^2}\right) + o(r^5) \tag{3.26}$$

to zero, where $R_{abcd}$ is the Riemann tensor. The physical requirement of having a sub-planckian curvature, i.e. lower than unity in Planck units, fixes a lower bound for the value of $L$: $L \gtrsim 3$ in Planck units.

The compelling picture presented up to now is undermined by two before un-noticed shortcomings presented in the next Chapter, together with a straightforward but non-trivial solution.

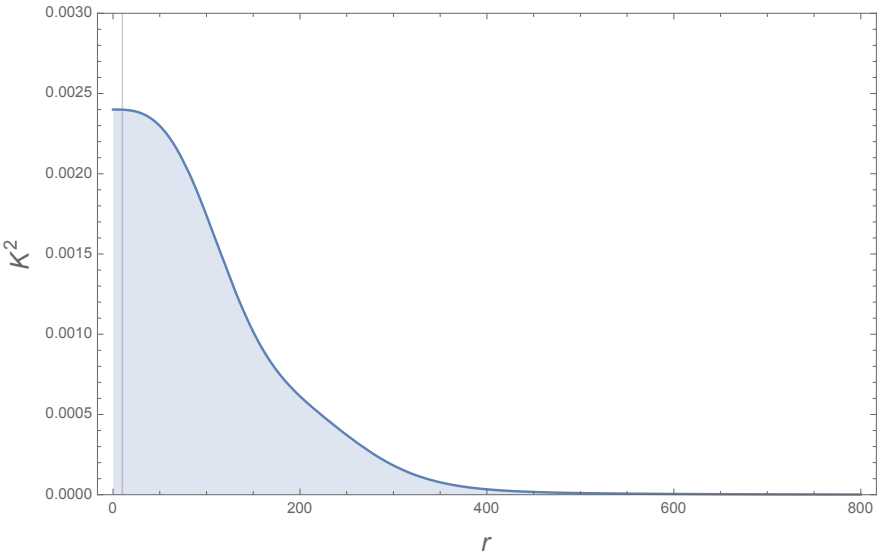


**Figure 3.6.** Kretschmann scalar curvature as a function of the radius for the Hayward metric; here $m = 10^5$ and $L = 10$ (Planck units). The vertical line represents the inner horizon $r_-$.

Chapter 4

# Modified Hayward's Metric

Together with the restriction on the maximum value of the scalar curvature discussed in the previous Chapter, we can require other two physical properties to a plausible metric describing a non-singular black hole.

## 4.1 Shortcomings

Gravitational time dilatation slows down clocks in a gravitational potential well, compared to clocks in an asymptotically flat region. A clock kept in the center of a dust cloud, for example, shows an elapsed time shorter than that of a clock at infinity, when the two clocks are moved together and compared. Since the Hayward's metric is regular at the origin, we can imagine a clock sitting at the center of the collapsing object, during the entire process of collapse, evaporation and explosion of the hole. The time measured by this clock is easy to compute: since $F(r) = 1$ at $r = 0$, Eq. (3.11) shows that this is equal to the coordinate time $t$. The same argument can be applied for a clock at infinity, finding an identical result. Therefore a clock at the center of the star suffers no time delay with respect to a clock at infinity. This is physically unreasonable. Therefore the fact that $F(r) = 1$ at $r = 0$ appears as a physically unmotivated restriction, shared, *via* Eq. (3.15), by all the models we presented in Eq. (3.17) and most of the others proposed in the literature. We need to notice an exception given by the *gravastars'* model proposed by Mazur and Mottola [2001].

The second difficulty we point out concerns the fact that an effective metric that supposes to mimic quantum effects should capture the 1-loop quantum corrections to the Newton's potential obtained using effective field theory [Bjerrum-Bohr, Donoghue, and Holstein 2003; Donoghue 1994], that is (reintroducing constants of Nature)

$$\Phi(r) = -\frac{G\,m}{r}\left(1 + \beta\,\frac{l^2_{\text{planck}}}{r^2}\right) + o\left(\frac{1}{r^4}\right), \tag{4.1}$$

where $\beta = \frac{41}{10\pi}$. The standard derivation of the Newton's limit from the metric components in the Schwarzschild case [Weinberg 1972, Sec. 3.4] reads

$$\Phi(r) = -\frac{1}{2}(1 + g_{00}). \tag{4.2}$$

For the Hayward's metric $g_{00} = -F(r)$ is given by Eq. (3.18), which expanded for large $r$ gives

$$g_{00} = -F(r) = -1 + \frac{2m}{r} - \frac{4L^2m^2}{r^4} + o\left(\frac{1}{r^5}\right) . \tag{4.3}$$

Large scale corrections, proportional to $L$, start at $o(r^{-4})$ instead of $o(r^{-3})$ as required by Eq. (4.1). It is worth mentioning that the metric proposed by Bardeen [1968] does well reproduce the required behavior of the newtonian potential. On the other hand, as well as the other line elements proposed, it suffers for the time delay problem.

In the next Section we introduce a minimal generalization of Hayward's metric that allows to fit in these two requests.

## 4.2 Solution

Let us parametrize the most general static spherically symmetric metric (3.1) by adding an arbitrary function $G(r)$ to (3.11), namely

$$ds^2 = -G(r)F(r)dt^2 + \frac{1}{F(r)}dr^2 + r^2d\Omega^2. \tag{4.4}$$

Written in this form, it explicitly underlies the slight difference from the Hayward's metric.

Following the discussion in Section 4.1, we want the function $G(r)$ to be such that the following physical requirements are satisfied:

($i$) the Schwarzschild behavior is preserved at large $r$;

($ii$) the first order correction to the Newton's potential matches the 1-loop result (4.1);

($iii$) a time dilation between the center and infinity is allowed. In particular, we define

$$\epsilon \equiv -g_{00}(r = 0) \ll 1 = -g_{00}(r = \infty), \tag{4.5}$$

so that $(\delta t_\infty - \delta t_0)/\delta t_\infty = 1 - \sqrt{|g_{00}(0)|} = 1 - \sqrt{\epsilon}$.

As we said in Section 4.1, the original Hayward's metric fails to recover 1-loop corrections because of a missing $o(1/r^3)$ term, Eq. (4.3). Therefore, the first two conditions are satisfied when $G(r)$ acquires the asymptotic behavior

$$\lim_{r\to\infty} G(r) = 1 - \beta\, \frac{m\, l^2_{\text{planck}}}{r^3} \tag{4.6}$$

where $\beta$ is the same of Eq. (4.1). At the origin $r = 0$, on the other hand, the last condition imposes

$$G(0) = \epsilon \equiv 1 - \alpha \,, \tag{4.7}$$

where we introduced a new parametrization for $\epsilon$ which make the following discussion more easily treatable. From the restriction on $\epsilon$ follow $0 < \alpha < 1$ and $\alpha \simeq 1$. An additional $(iv)$ useful restriction – albeit not mandatory – is to demand that near the center, the equation of state of the derived energy-momentum tensor is still deSitter. Since the expansion near $r = 0$ of $g_{00}(r)$ gives now

$$g_{00}(r) = -G(0)\left(1 - \frac{r^2}{L^2}\right) - G'(0)\, r - \frac{G''(0)}{2}\, r^2 + o(r^3) \,, \tag{4.8}$$

matching the de Sitter behavior (3.15) gives

$$G'(0) = G''(0) = 0 \,. \tag{4.9}$$

$G(0)$ can be absorbed rescaling $t$, introducing in this way the desired time delay. Conditions $(i)$ and $(iv)$ then suggest to look for solutions as rational functions of $r^3$. Taking the simplest case, and using $(ii)$ and $(iii)$ to fix the coefficients, we can propose the following explicit function:

$$G(r) = 1 - \frac{\beta\, m}{r^3 + \frac{\beta\, m}{\alpha}}. \tag{4.10}$$

This example shows how *it is possible to improve the metric proposed by Hayward to take into account the 1-loop quantum corrections and a time delay in the central core.* Notice that, since $G(r)$ is always positive, the horizons remain unchanged with respect to the Hayward's case. Therefore, they are still determined by Eqs. (3.22).

**Bounds** Next, we check what restrictions arise on the new metric coming from physical arguments. In particular, we will see that it is not possible to arbitrarily lower the coefficient $\epsilon$ or, in other words, arbitrarily increase the time delay between the center and infinity.

These bounds come from the physical requirement we already imposed on the Hayward's metric: in order for such metric to make sense the curvature should stay sub-planckian at all scales.

The Kretschmann invariant associated with (4.10) has a rather long expression which prevents a purely analytic study of its properties. However, numerical investigations are possible. The main point is that lowering $\epsilon$ too much introduces a trans-planckian peak of curvature near – but not at – the central core that can exceed the planckian value by many order of magnitude. See Fig. 4.1.

To investigate the nature of this peak, let us study the usual decomposition of the Kretschmann scalar

$$\mathcal{K}^2 = R_{abcd}R^{abcd} = \mathcal{W}_{abcd}\mathcal{W}^{abcd} + 2R_{ab}R^{ab} - \frac{1}{3}R^2 \,, \tag{4.11}$$

where $\mathcal{W}_{abcd}$ is the Weyl's tensor, while $R_{ab}$ and $R$ are respectively the Ricci's tensor and the Ricci's scalar. The direct evaluation depicted in Fig. 4.2 shows that

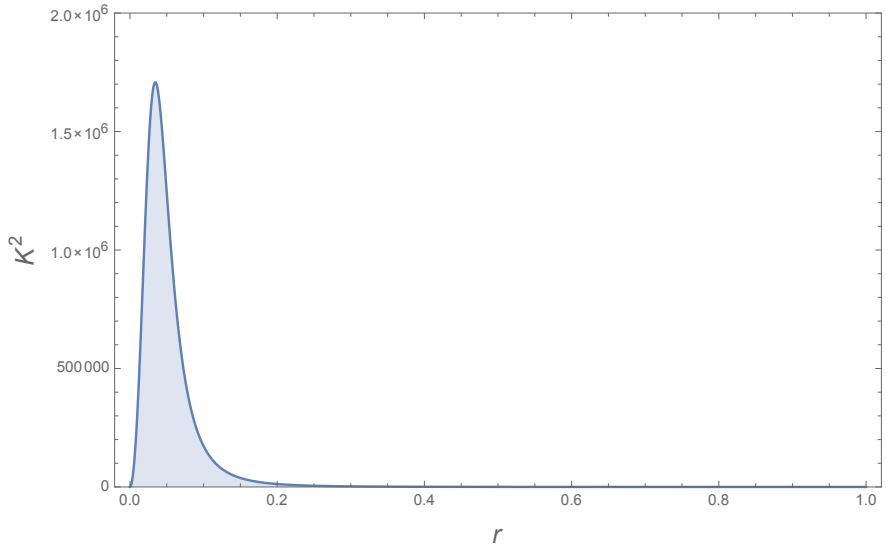


**Figure 4.1.** Kretschmann scalar curvature as a function of the radial coordinate $r$ for the corrected Hayward's metric. A too small value of the parameter $\epsilon$ provokes the violation of sub-planckianity request by many orders of magnitude. Here $\epsilon = 10^{-9}$, with $m = 10^5$ and $L = 10$ (Planck units).

Weyl's tensor contribution is always small, thus the origin of the bad behavior is in the energy momentum-tensor uniquely.

Let us now call $\mathcal{K}^2_{\rm max}$ the maximum value of the Kretschmann scalar curvature; in general it will be a function of the three free parameters of the model, i.e. $m$, $L$ and $\epsilon$ (or equivalently $\alpha$). At fixed $m$ and $L$, it is possible to numerically compute the behavior of $\mathcal{K}^2_{\rm max}$ with respect to $\alpha = 1 - \epsilon$. The result for $m = 10^5$ and $L = 10$ is plotted in Fig. 4.3, revealing the monotonically increasing behavior of $\mathcal{K}^2_{\rm max}$ in $\alpha \in [0, 1]$. Therefore, we can impose a bound on $\alpha$ (and then on $\epsilon$) by requiring the maximum curvature to be smaller than unity, say 0.1. Let us call $\alpha_{\rm planck}$ the bound value, namely

$$\mathcal{K}^2_{\rm max}(\alpha_{\rm planck}) = 0.1 \tag{4.12}$$

at fixed $m$ and $L$.

*What happens now varying $m$ and $L$?* To explore these dependences, let us fix one of the two parameters, and varying the other. For instance, let us firstly fix $L$, say $L = 10$. A numerical analysis show that the monotonically increasing behavior of $\mathcal{K}^2_{\rm max}$ as a function of $\alpha$, is valid for all the values of $m \in [m_\star, \infty)$. This means that for each value of $m$ we can found the correspondent bound value $\alpha_{\rm planck}$, such that, for each $0 < \alpha \leq \alpha_{\rm planck}$, $\mathcal{K}^2$ is sub-planckian everywhere. In Fig. 4.4 is represented the dependence of $\alpha_{\rm planck}$ on the mass $m$. The behavior is monotonically increasing, appraoching asymptotically one. The more the mass is bigger then $L$, the more we are allowed to low the coefficient $\epsilon$, increasing the time delay between the origin and infinity.

Moreover, let us now vary $L$. Fig. 4.5 is the equivalent of Fig. 4.4 for different values of $L$. It reveals that, in good approximation, the bound value $\alpha_{\rm planck}$ does not depend on $L$, in particular in the regime $m \gg L$. *What does 'good*

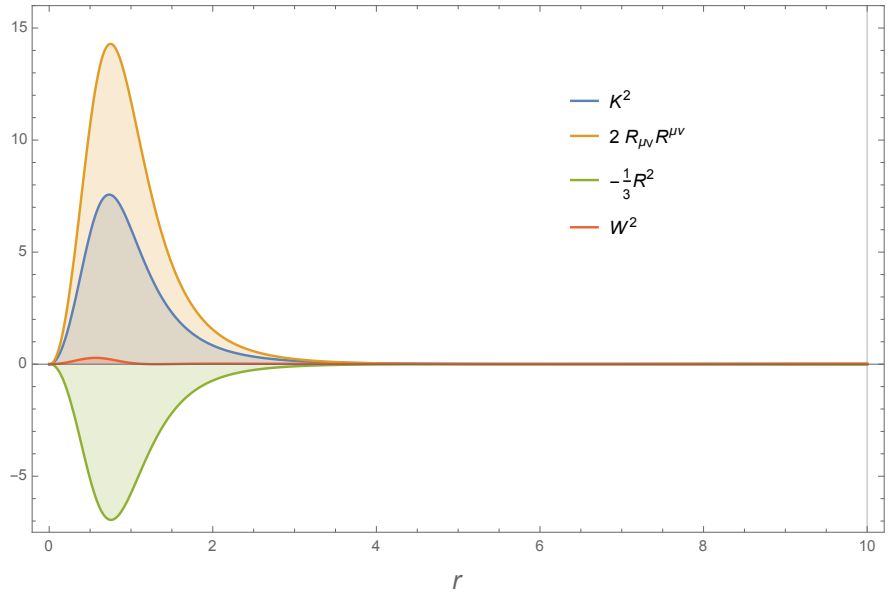


**Figure 4.2.** Comparison between the different factor contributing to the Kretschmann scalar $\mathcal{K}^2$. The Weyl's tensor contribution is always small. Here $m = 10^5$, $L = 10$ and $\epsilon = 10^{-5}$ (Planck units).

*approximation' mean?* Choosing $m = 10^8$, the value of $\alpha_{\text{planck}}$ as a function of $L$ is plotted in Fig. 4.6, finding that they are in good agreement up to $10^{-5}$.

*Given these conditions on the parameters, the simple introduction of the function $G(r)$ resolves the before un-noticed problems of the Hayward's metric; the line element* (4.4) *together with Eq.* (4.10)*, therefore, provides a more realistic description of a non-singular black hole.*

### Energy Conditions

We need to stress that the modification (4.10) introduces a violation of the weak energy condition. Indeed, as shown in Fig. 4.7, the sum of the density profile with the tangential pressures fails to be non-negative. Unlike the violation of the sub-planckian condition, this violation is strongly dependent on $L$.

While a violation of the weak energy condition is *per se* not a problem in a model which is supposed to include quantum gravity effects, it is interesting to remark that this is *a priori* avoidable. Let us go back to Dymnikova's theorem in Section 3.1; we said that the value in the origin of the function $\mu(r)$ plays the role of a family parameter. The Hayward's metric and the others we mentioned belong to the family characterized by $\mu(0) = 0$. Since $g_{00}(0) = \exp(\mu(0))$, it is clear that the time-delay problem comes exactly from this unphysical un-motivated restriction. Relaxing this condition by allowing $\mu(0) < 0$ is equivalent to choose a metric of the type we considered in Eq. (4.4). Since in the Dymnikova's theorem the validity of the WEC is taken as an hypothesis, we expect that it is possible to find an explicit function $G(r)$ that satisfies the physical requirements we imposed in this Chapter and, at the same time, does not to violate the weak energy condition.

A possible approach is to reverse the way of reasoning taking a general $G(r)$

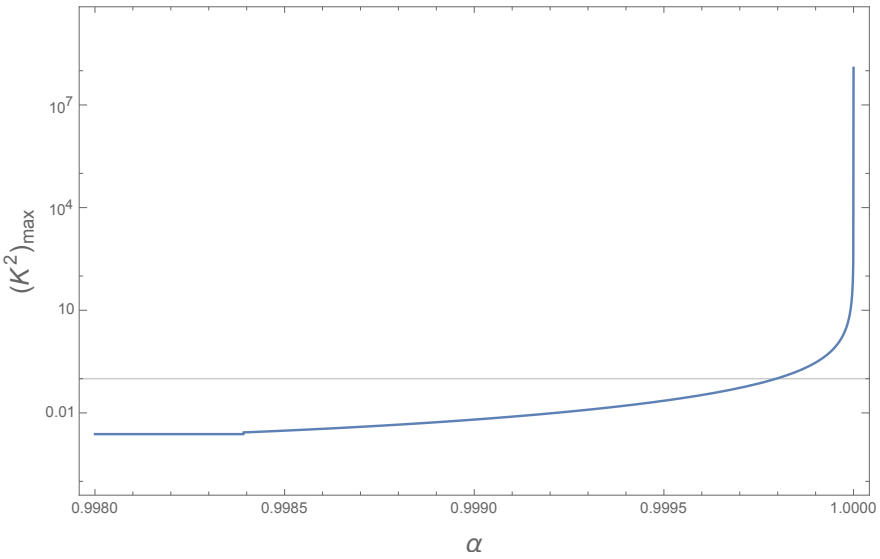


**Figure 4.3.** Maximum value of the Kretschmann scalar curvature as a function of the parameter $\alpha$ for the corrected Hayward's metric; here $m = 10^5$ and $L = 10$ (Planck units and logarithmic scale).

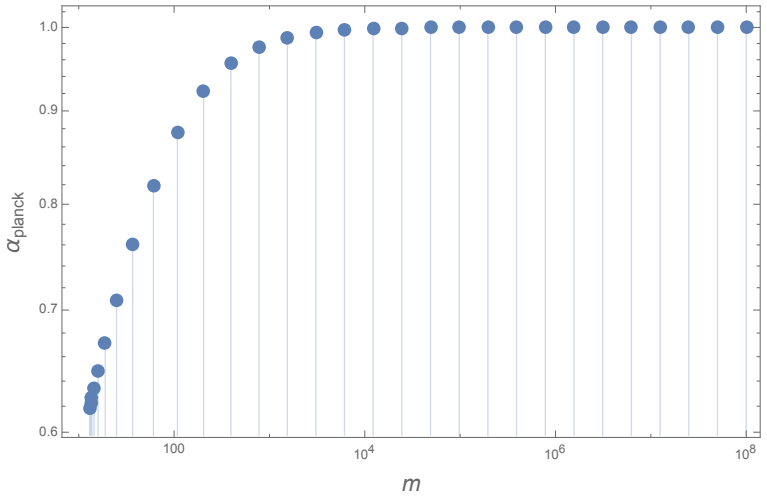


**Figure 4.4.** $\alpha_{\text{planck}}$ as a function of the mass $m$, at fixed $L = 10$ (Planck units).

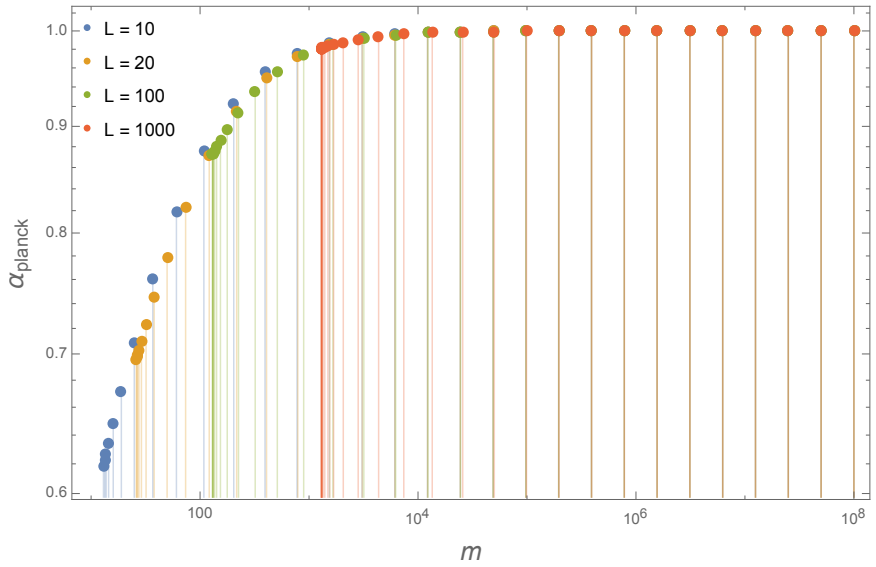


**Figure 4.5.** $\alpha_{\text{planck}}$ as a function of the mass $m$ for different values of $L$ (Planck units).

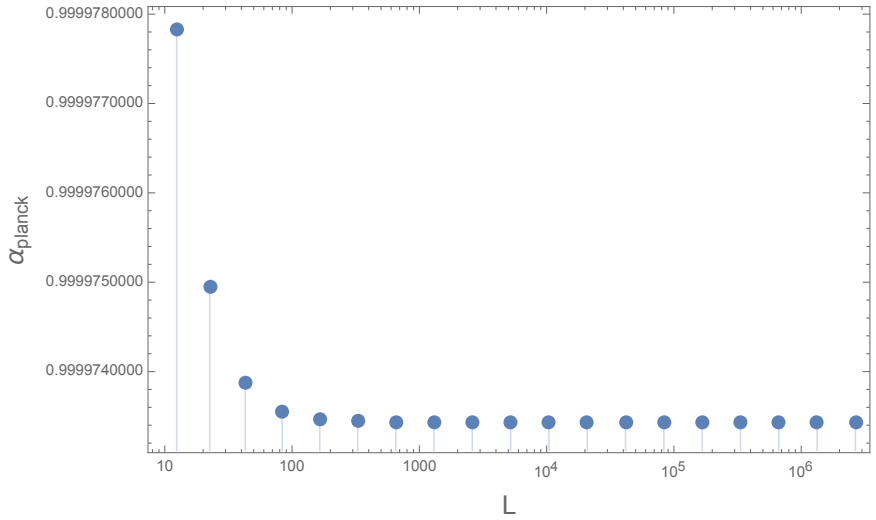


**Figure 4.6.** $\alpha_{\text{planck}}$ as a function of the parameter $L$ at fixed value of $m = 10^8$ (Planck units, x-axis in logarithmic scale).

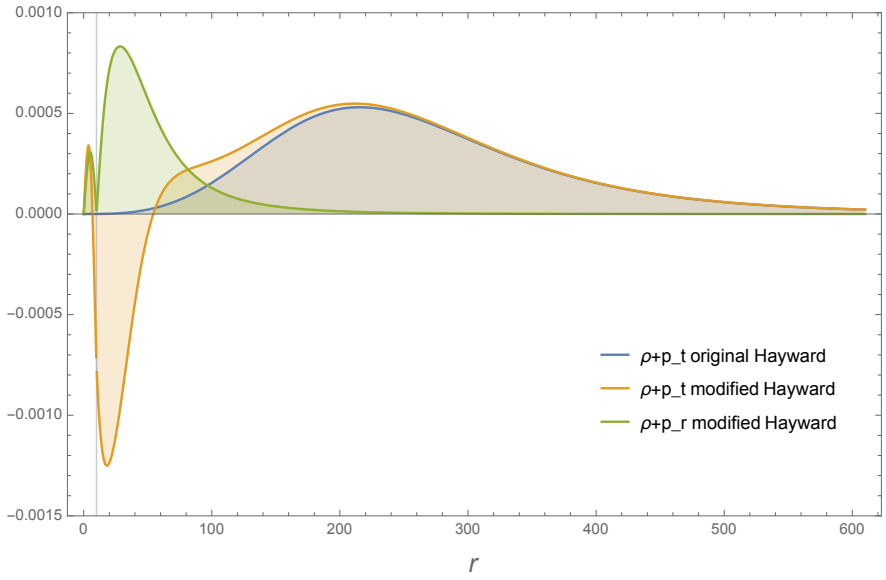


**Figure 4.7.** Violation of the weak energy condition in the transversal part (orange) of the modified Hayward's metric, compared with the transversal contribution for the original Hayward's metric (blue). The original radial contribution $\rho + p_r$ is null everywhere, while it is green depicted for the modified Hayward's metric. Here $m = 10^5$, $L = 10$ and $\epsilon = 0.99$ (Planck units).

and looking for conditions on it such that WEC is satisfied, namely $\rho \geq 0$ and $\rho + p_i \geq 0$. To do that we must distinguish the inner core and the exterior ($r < r_-$ and $r > r_+$), where $\rho = -T^0_0$ and $p_r = T^1_1$, from the trapping zone ($r_- < r < r_+$) where $\rho = -T^1_1$ and $p_r = T^0_0$. As said before, taking $G(r) > 0$ ensures that the position of the horizons is unchanged, still determined by $F(r) = 0$. The condition $\rho \geq 0$ is given by

$$\begin{aligned} -\frac{-1 + F(r) + r\,F'(r)}{8\pi r^2} &\geq 0 \qquad \text{for } r < r_- \text{ and } r > r_+ \,; \\ -\frac{G(r)\big(-1 + F(r) + rF'(r)\big) + rF(r)G'(r)}{8\pi\, r^2 G(r)} &\geq 0 \qquad \text{for } r_- < r < r_+ \,, \end{aligned} \tag{4.13}$$

as well as $\rho + p_r \geq 0$ becomes

$$\begin{aligned} \frac{F(r)G'(r)}{8\pi\, r\, G(r)} &\geq 0 \qquad \text{for } r < r_- \text{ and } r > r_+ \,; \\ -\frac{F(r)G'(r)}{8\pi\, r\, G(r)} &\geq 0 \qquad \text{for } r_- < r < r_+ \,. \end{aligned} \tag{4.14}$$

The function $G(r)$ proposed in Eq. (4.10) actually satisfies these conditions. The

non-trivial requirement comes from the transversal part $\rho \geq p_\perp$:

$$\begin{aligned}
&\frac{1}{32\pi\, r^2 G(r)^2}\Bigg[ - r^2 F(r) G'(r)^2 + G(r)^2 \Big(4 - 4F(r) + 2r^2 F''(r)\Big) + rG(r)\times \\
&\times \Big(3r\, F'(r) G'(r) + 2F(r)\big(G'(r) + r\, G''(r)\big)\Big)\Bigg] \geq 0 \qquad \text{for } r < r_- \text{ and } r > r_+ \,; \\
&\frac{1}{32\pi\, r^2 G(r)^2}\Bigg[ - r^2 F(r) G'(r)^2 + G(r)^2 \Big(4 - 4F(r) + 2r^2 F''(r)\Big) + rG(r)\times \\
&\times \Big(3r\, F'(r) G'(r) - 2F(r)\big(G'(r) - r\, G''(r)\big)\Big)\Bigg] \geq 0 \qquad \text{for } r_- < r < r_+ \,.
\end{aligned} \tag{4.15}$$

Unfortunately, from these differential equations on a function is really hard to find an explicit solution which also fulfills the physical requirements $(i)$-$(iii)$.

The metric proposed in this Chapter can be considered a new, more realistic description of a static non-singular black hole, keeping in mind the theoretical possibility to construct a similar one that could also satisfy the weak energy condition.

In the next Chapters we'll study what happens when Hawking's radiation and therefore evaporation is turned on. The main question is: can a similar effective metric solve the information-loss paradox?

# Part III

# Original Results 2: Dynamic Non-Singular Black Holes

*Black holes evaporate. Any collapsing object forming a trapping region evaporates. Therefore, the evolution of a non-singular black hole after its formation is dynamical: the mass loss allows the shrinking of the region between outer and inner horizon which, in a finite amount of time, merge and eventually disappear. Unitarity is preserved and no information is lost in the process.*

# Summary



In the previous Chapters we studied the properties of a non-singular black hole settled by the gravitational collapse of a spherical body and remaining in its static configuration. However an event horizon forms and then, as in the singular black hole case in Chapter 2, we expected Hawking's radiation and consequent evaporation to take place and the after-formation system to become *dynamic*. As seen in Chapter 2, the study of the *evaporation process* is subtle because of the non-clear backreaction contribution of the Hawking's radiation on the metric, in particular in the late stages of the life of the black holes. However, useful informations can be found considering quasi-statical approximation to hold during the entire evaporation process. The aim of this last Part is to apply this analysis to non-singular black hole models, in order to explore their physical plausibility.

To do this we will start with an introductory brief Chapter presenting some first insights on the problem. As in the Hawking's evaporation case discussed in Section 2.2.2, the dynamics will be simply encoded allowing the mass of the black to decrease in time. Different scenarios are shortly discussed.

The main results, however, are presented in the last Chapter. Here the plausibility of evaporation processes is studied through the investigation of their *Page's curve*. This analysis is made quantitative possible thanks to a new covariant definition of entanglement entropy developed by Bianchi and Smerlak [2014a]. From this definition, presented in Section 6.1, follows the possibility to give a precise characterization of entanglement entropy production and to analytically compute the Page's curve associated to any SpaceTime. In particular, applied to the Hayward's metric, this analysis confirms the recover of unitarity, but at the same time shines a light on two non-easily solvable problems, undermining the physical validity of the dynamical Hayward's metric itself (and, because of the Dymnikova's theorem, of almost all the metrics so far proposed).

Chapter 5

# Dynamic Hayward's Metric

According to Section 2.2.2, the simplest way to take into account the backreaction of the Hawking's radiation on a BH-like geometry is to allow the parameter $m$ to be time-dependent. The result is a *generalized Vaidya metric* (see Section 1.1.3) that, for the modified Hayward metric and in Eddington-Finkelstein coordinates, reads

$$ds^2 = -G(r,v)\,F(v,r)\,dv^2 + 2\sqrt{G(r,v)}\,dv\,dr + r^2\,d\Omega^2\ , \tag{5.1}$$

where $F(v,r)$ and $G(v,r)$ are the same in Eqs. (3.18) and (4.10) with the substitution $m \to m(v)$. We can model the formation process, as in Section 1.1.3, by a thin null shell collapsing at $v = v_s$ and settling to a (modified) Hayward black hole of mass $m_0$. Moreover, for $v > v_s$, since Hawking's evaporation is taking place, we expect a SpaceTime of the form in Eq. (5.1) with a decreasing $m(v)$,[1] i.e. $m'(v) < 0$.[2] In Fig. 5.1, the solutions of the radial null geodesics equation are plotted for the Hayward's metric before and after the slight modification of Chapter 4. We used a simple toy-model where $m(v)$ is assumed to vary linearly, namely

$$m(v) = \begin{cases} 0 & \text{for } v < v_s\ ; \\ m_0 - \dfrac{v}{\alpha} & \text{for } v_s \le v < v_\star\ ; \\ 0 & \text{for } v \ge v_\star\ , \end{cases} \tag{5.2}$$

where $\alpha > 1$ is a parameter and $v_\star$ is the advanced time at which the horizons merge, i.e. $m(v_\star) = m_\star$. As we expected, the qualitative behavior is the same a part from the region inside the inner horizon. Indeed, the time-delay factor $G(r)$ modifies the components of the metric only near the origin. For the purpose of this Chapter, therefore, we can work with the non-modified Hayward's metric

[1] This is only an intuitive expectation. Indeed, Bianchi and Smerlak [2014a] showed that, under some physical requirements, the mass loss rate cannot be monotonically decreasing.

[2] As in the Hawking dynamical case, all the energy conditions are violated in the evaporation framework. See Appendix B.1 for a simple proof.

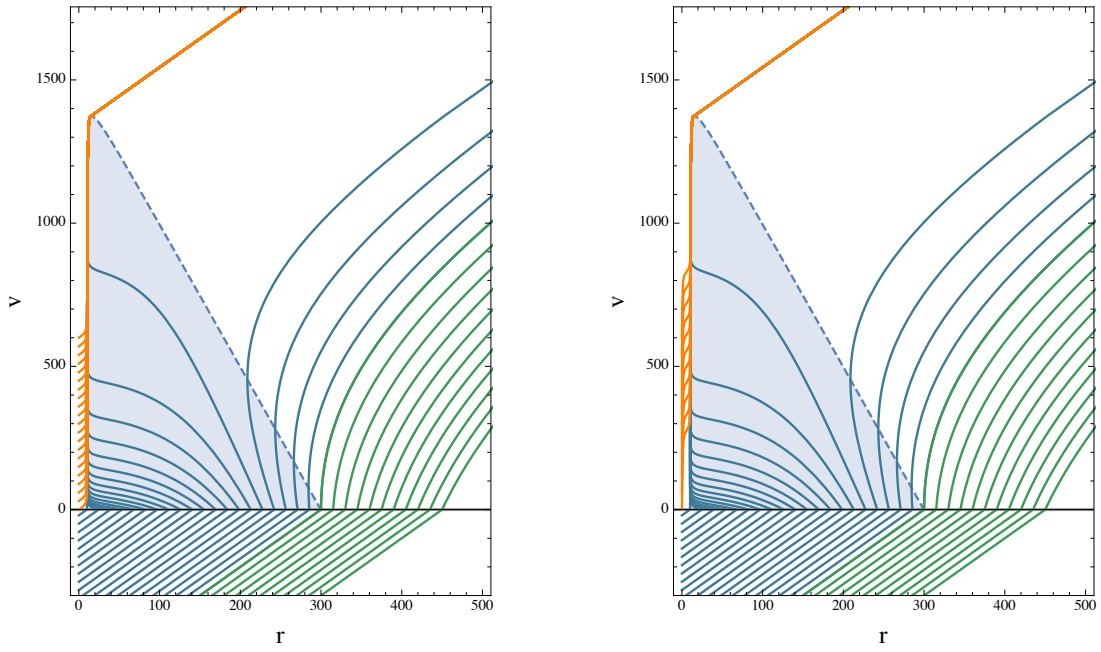


(a) Hayward's metric.

(b) Modified Hayward's metric.

**Figure 5.1.** Numerical solutions for the outgoing null geodesic equation in the dynamical (modified and non) Hayward's SpaceTime. Geodesics starting outside the outer horizon have a Schwarzschild-like behavior. Inside the trapping region (shaded) the inner horizon plays as an attractor. The timelike nature of the apparent horizon is manifest. The ingoing solutions are $v$ =const. lines, here non reproduced. We used the simple toy-model of Eq. 5.2 with $L = 10$, $m = 150$, $\alpha = 10$, $\epsilon = 0.99$. Before the ingoing shell collapse at $v_s = 0$ the SpaceTime is flat.

making the discussion much more easily treatable. Namely we use the metric in Eq. (5.1) with

$$G(v,r) = 1 \qquad \text{and} \qquad F(v,r) = 1 - \frac{2m(v)\,r^2}{r^3 + 2m(v)L^2}\,. \tag{5.3}$$

**Apparent horizon** The first clear difference between the static and the dynamic case is the merging and consequent disappearance of the horizons; being the solution of $F(v,r) = 0$, $r = r_H$ hypersurfaces are now dynamic themselves. Therefore, $r_+(v) \simeq 2m(v)$ is not an event horizon anymore becoming an *apparent (or trapping) horizon*, namely the boundary of the trapping surfaces (see 1.2 for the definition). Being a timelike surface, moreover, it can be crossed by causal geodesics and loses the characterization of the event horizon as a no-escape surface (that's why "apparent"). In one of his last papers, Frolov [2014] introduced a new notion — the *quasi-horizon*, and, using his own words, "demonstrated that it is much better generalization of the event horizon for time-dependent 'black holes' than the apparent horizon". However, different complicated generalizations of event horizon for a dynamical case have been introduced so far in the literature (for example the *Ashtekar's dynamical horizon*, see Ashtekar and Krishnan [2004] for a review), and it can be interesting to investigate their relationships with the Frolov's quasi-horizon. In any case, for our purpose this is just a curiosity.

**Two scenarios** The scenario represented in Fig. 5.1(a) is the one considered originally by Hayward [2006] and re-proposed by Frolov [2014] and Rovelli and Vidotto [2014]: the horizons merge and disappear. What left is a remnant of mass less then the critical value $m_\star$ that can remain stable or, more likely for possible phenomenological consequences [Barrau and Rovelli 2014], explode. Nevertheless, another fate for the black hole is possible, advocated by Hossenfelder, Modesto, and Premont-Schwarz [2010] and Alesci and Modesto [2014] by studying a different model of non-singular black hole: the horizons approach each other asymptotically in an infinite time. The conformal diagrams of the two scenarios (reintroducing a collapsing body instead of a thin shell) are represented in Fig. 5.2. In both cases is important to remark that restoration of unitarity is possible. Indeed, in the first case the information fallen into the black hole can go back to null infinity when the horizons disappear; in the second, on the other hand, information cannot escape to infinity, but, since the black hole never disappears, correlations are stored inside of it, even if unaccessible to external observers [Alesci and Modesto 2014]. Therefore, both of them represent a possible solution to the information-loss paradox.

**Surface gravity and third law** The plausibility of the two scenarios is explored by studying the evolution of the *surface gravity* defined in Section 2.3, Eq. (2.92). In the static Hayward's case, $\kappa$ can be analytically computed (see Appendix C), finding

$$\kappa = \frac{3}{4m} - \frac{1}{r_+} \tag{5.4}$$

where $r_+$ is the outer horizon in Eq. (3.22a). In Fig. 5.3 the surface gravity is plotted as a function of $m$. We can see that for large values of $m$ its behavior

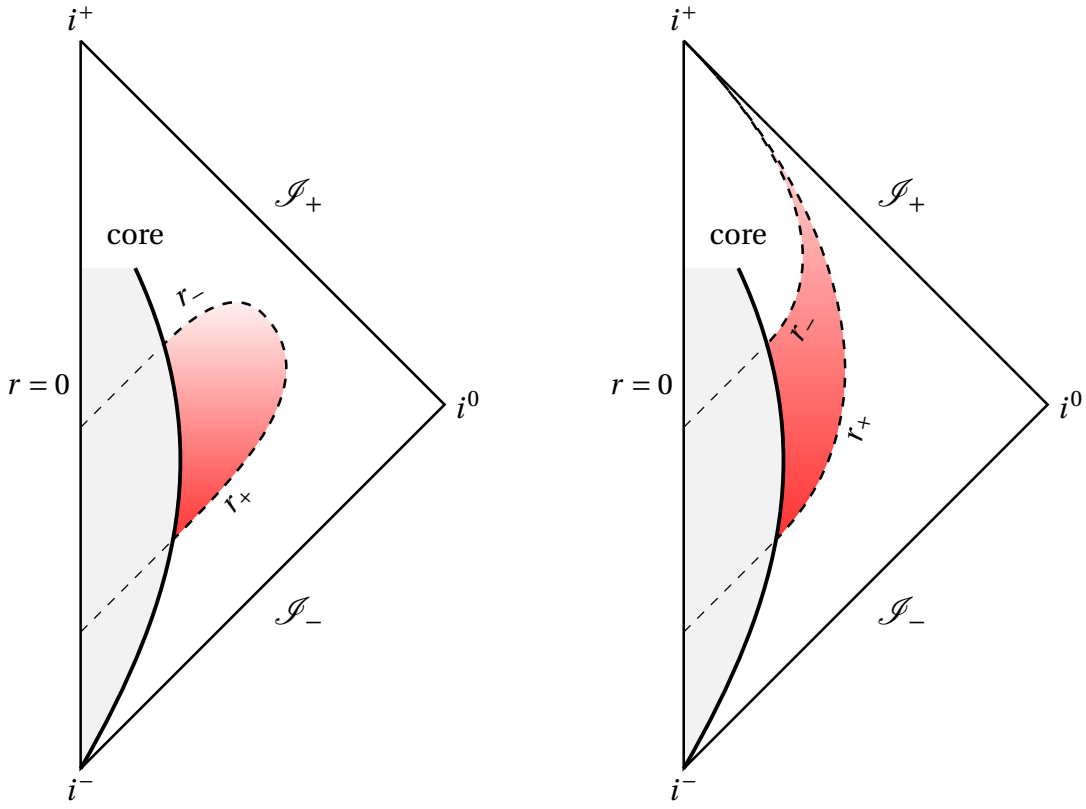


**Figure 5.2.** Conformal Carter-Penrose diagram for evaporating non-singular black holes scenarios. The trapping region is shaded. In (a) the evaporation ends in a finite amount of time, while in (b) the horizons approach asymptotically. In both cases restoration of unitarity is possible. The thick line represents the collapsing mass.

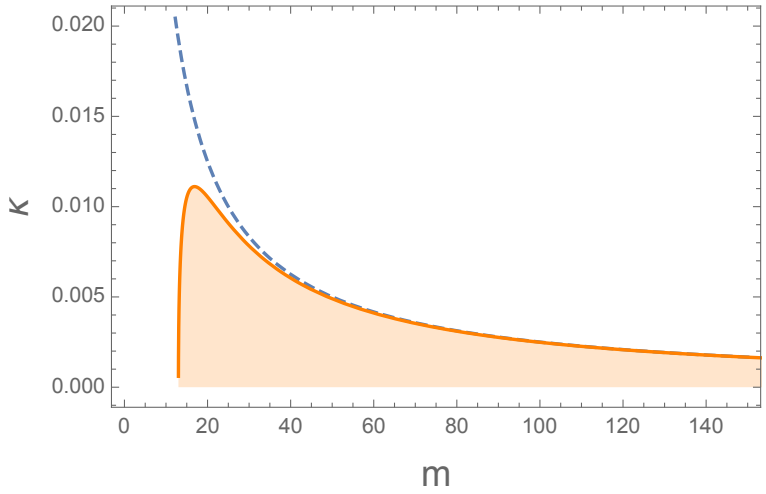


**Figure 5.3.** The surface gravity $\kappa$ for the Hayward's metric compared with the classical surface gravity $\frac{1}{4m}$ (dashed line), as a function of the mass $m$. The maximum arises for $m = \frac{27}{16}L$. Here $L = 10$ (Planck units).

is similar to the classic Hawking's one. How the mass decreases, however, it strongly deviates from $\frac{1}{4m}$, reaching a maximum at $m = m_{\text{crit}}$ and dropping down to vanish at $m = m_\star = \frac{3\sqrt{3}}{4}L$. The maximum occurs for $m_{\text{crit}} = \frac{27}{16}L$, as analytically computed in Appendix C. The curve suggests that the evaporation of the non-singular black hole takes place when $\kappa = 0$. The third law of black hole thermodynamics discussed in Section 2.3, however, tells us that the extremal case cannot be reached in a finite amount of time. Taking seriously this analysis, therefore, the second scenario, where the horizons approach asymptotically, seems to be more realistic. We need to stress that to reach such a conclusion we used a *quasi-static approach*: namely, we assumed the dynamics to be a succession of static pictures at each instant of time. Strong backreaction effects in the last stages of the evaporation, on the other hand, can underline the validity of this approximation.

Moreover, even when these strong effects due to the backreaction of the Hawking's radiation on the metric are neglected, the outcomes can be totally different from our naïve expectation. In the next, last Chapter of this work, the analysis of the evaporation process will become more quantitatively precise. A new definition of entanglement entropy tailored for curved SpaceTimes, indeed, allows a precise study of the Page's curve (introduced in Section 2.4.1) of different evaporation pictures.

Chapter 6

# Entanglement Entropy Production in Dynamical SpaceTime

This last Chapter contains the work done during the 'Undergraduate summer project' conducted at 'Perimeter Institute for Theoretical Physics' in Canada, flowed into the paper Bianchi, De Lorenzo, and Smerlak [2014] on which the discussion is largely based. *All the figures of this Chapter, except for Fig. 6.1, are reproduced from that paper.*

*Entanglement entropy* as a measure of correlations in a bipartite quantum system has been introduced in Section 2.4. In a relativistic QFT, it generally refers to correlations, at a given time, between modes of the field supported respectively in a spatial region and its complement [Bombelli et al. 1986; Srednicki 1993]. A quantitative study of the Ent.Ent. in a general relativistic context, however, cannot be based on a definition associated to non-covariant objects, as spatial regions are. Let us therefore present the covariant definition given by Bianchi and Smerlak [2014a].

## 6.1 Covariant Entanglement Entropy

**Preliminary** Consider a $(1+d)$-dimensional globally hyperbolic SpaceTime, and a set of points $S$. The set of points space-like separated from all points of $S$ is called *the causal complement* $\overline{S}$ *of* $S$. Consider now a Cauchy surface $\Sigma$, a spatial region $R \subset \Sigma$ and the Cauchy development $\mathcal{D}$ of $R$ calling it $D \equiv \mathcal{D}(R)$ (see Appendix A for definition). From Fig. 6.1 it easy to see that the causal complement of $D$ coincides with the Cauchy development of the complementary region $\overline{R} = \Sigma - R \subset \Sigma$, namely $\overline{D} = \mathcal{D}(\Sigma - R)$. Let us also define the corner of the causal domain $D$ as $C_D \equiv \partial R$.

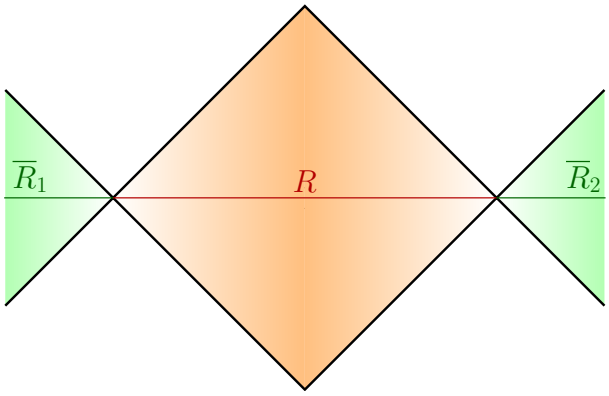


**Figure 6.1.** Pictorial representations of a region $R$ of a surface $\Sigma$, its complementary region $\overline{R} = \Sigma - R$ and their Cauchy developments.

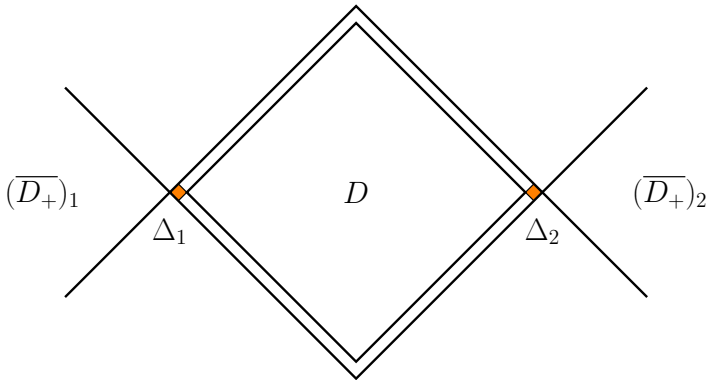


**Figure 6.2.** Entanglement entropy in the *causal splitting regularization* of a diamond $D$, defined as (one half) the mutual information between $D$ and $\overline{D_+} = (\overline{D_+})_1 \cup (\overline{D_+})_2$. The covariant cutoff $\mu$ is the SpaceTime volume of the splitting region $\Delta = \Delta_1 \cup \Delta_2$ (shaded).

**Definition** Take $D_+$ to be a causal domain that contains $D$ and call it a *smearing of* $D$. Since the domains $D$ and $\overline{D_+}$ are causally disconnected, we can define the *splitting region* as

$$\Delta \equiv \overline{D \cup \overline{D_+}}\,, \tag{6.1}$$

which comes out to be a causal domain as well. The construction is clear the $(1+1)$-dimensional picture in Fig. 6.2.

At every point of the corner $C_D$ of the domain $D$ there are two null geodesics $\ell = \partial_v$ and $n = \partial_w$ that lie on the boundary of $\Delta$. In the limit $D_+ \to D$ the SpaceTime volume $\mathcal{V}_{(d+1)}$ of $\Delta$ is given by the integral over $C_\Delta$ of the transversal SpaceTime area of $\Delta$, i.e.

$$\mu \equiv g_{\alpha\beta}\ell^\alpha n^\beta\, \delta v\, \delta w. \tag{6.2}$$

We require the smearing $D_+$ to be such that the transversal area $\mu$ is constant. As a result the splitting region has finite SpaceTime volume given by

$$\mathcal{V}_{(d+1)}(\Delta) \;=\; \mu\, \mathcal{A}_{(d-1)}(C_D)\,, \tag{6.3}$$

where $\mathcal{A}_{(d-1)}$ is the area of the $(d-1)$-dimensional corner $C_D$, and $\mu$ is a cut-off with dimensions of *length*$\times$*time*. Moreover, for $d = 1$ (as in Fig. 6.2) we define

$\mathcal{A}_{(0)} = 1$ and impose $\mathcal{V}_{(1+1)}(\Delta_i) = \mu$ for each connected component of $\Delta$.

We are now ready to define the entanglement entropy in the *causal-splitting regularization* $S_+(D)$ as half of the mutual information between the domain $D$ and the complement of its smearing $D_+$, namely

$$S_+(D) \equiv \frac{1}{2} I(D, \overline{D_+}) \tag{6.4}$$

This quantity depends on the cut-off $\mu$: it is finite if the cut-off is finite while diverges in the limit $\mu \to 0$ since the causal domains $D$ and its smearing $D_+$ coincide and the mutual information diverges. The idea is that $\mu$ is a physical cut-off, fixed for instance at the Planck scale

$$\mu = \frac{G\hbar}{c^4} , \tag{6.5}$$

or at the scale below the point where the effective field theory considered breaks down. More importantly, it is defined in a covariant way by the curved SpaceTime volume of the splitting region $\Delta$, Eq. (6.3).

In our path toward a covariant definition of entanglement entropy, we need one more step: we must connect the expression of $S_+(D)$ to the standard definition, Eq. (2.102), namely:

$$S_\epsilon(D) = -\mathrm{Tr}_D\big[\rho_D \log \rho_D\big] . \tag{6.6}$$

From the definition of mutual information, Eq. (2.108) and using the fact that for a pure global state $S_\epsilon(D) = S_\epsilon(\overline{D})$, Eq. (6.4) reduced to the simple form

$$\begin{aligned} S_+(D) &= \frac{1}{2}\Big(S_\epsilon(D) + S_\epsilon(\overline{D_+}) - S_\epsilon(D \cup \overline{D_+})\Big) = \\ &= \frac{1}{2}\Big(S_\epsilon(D) + S_\epsilon(D_+) - S_\epsilon(\Delta)\Big) . \end{aligned} \tag{6.7}$$

The subscript $\epsilon$ is to stress the fact entanglement entropy is usually UV divergent. Expression (6.7) depends on two cut-offs, $\mu$ and $\epsilon$. The covariant regularized entropy $S_+(D)$ is defined by the limit $\epsilon \to 0$ with $\mu$ finite. In the opposite limit, $\mu \to 0$ and $\epsilon$ finite, since $D_+ \to D$ and $S_\epsilon(\Delta) \to 0$, the right-hand-side of Eq. (6.7) reduces to the ordinary entropy $S_\epsilon(D)$.

In standard QFT in Minkowski space, the entanglement entropy has been found to be computable in $(1+1)$-dimensional SpaceTime thanks to a formula due to Holzhey, Larsen, and Wilczek [1994]. This formula can be rewritten in terms of the new covariant definition. As we can expect, the result is an analogue expression where the cut-off $\epsilon$ is replaced by the covariant volume cut-off $\mu$. More importantly, the generalization to curved SpaceTimes becomes straightforward.

### 6.1.1 Entanglement entropy in 2D SpaceTimes

**Minkowski SpaceTime** Consider $(1+1)$-dimensional Minkowski SpaceTime written in a double-null coordinate set $(v, w)$, that is

$$ds^2 = -dv\, dw \; ; \tag{6.8}$$

two spacelike separated points $p_1$ and $p_2$ can be seen as the corners of a causal domain $D$ (called *diamond*), where $p_1 = (v_1, w_1)$, $p_2 = (v_2, w_2)$ with $w_1 < w_2$ and $D = [v_2, v_1] \times [w_1, w_2]$. In the highly correlated vacuum state, the entanglement entropy of a massless scalar field is given by the already mentioned Holzhey, Larsen, and Wilczek [1994] formula

$$S_\epsilon(D) = \frac{1}{6} \log \frac{\Delta v \, \Delta w}{\epsilon^2} \,, \tag{6.9}$$

where $\Delta v \equiv v_1 - v_2$, $\Delta w \equiv w_2 - w_1$.

To find an expression for the covariant entanglement entropy, let us introduce a smearing $D_+$ of the diamond $D$ as $D_+ \equiv [v_2 - \delta v_2, v_1 + \delta v_1] \times [w_1 - \delta w_1, w_2 + \delta w_2]$, with $\delta v_1, \delta v_2, \delta w_1, \delta w_2$ all positive. The causal complement of $D \cup \overline{D_+}$ is a domain $\Delta$ consisting of two (small) disconnected diamonds,

$$\Delta = \Delta_1 \cup \Delta_2 \,, \tag{6.10}$$

with $\Delta_1 = [v_1, v_1 + \delta v_1] \times [w_1 - \delta w_1, w_1]$ and $\Delta_2 = [v_2 - \delta v_2, v_2] \times [w_2, w_2 + \delta w_2]$, see again Fig. 6.2. Therefore, the sought result can be found combining Eqs. (6.7)-(6.9) with the fact that the entanglement entropy of the union of two diamonds is additive in the limit of diamonds that are small compared to their separation, $S(\Delta_1 \cup \Delta_2) \to S(\Delta_1) + S(\Delta_2)$ [Calabrese, Cardy, and Tonni 2009; Casini and Huerta 2009]. This results in

$$S_+(D) = \frac{1}{12} \log \frac{(\Delta v)^2 (\Delta w)^2}{\delta v_1 \, \delta w_1 \, \delta v_2 \, \delta w_2} \,. \tag{6.11}$$

The physical cut-off $\mu$ can be identified with the SpaceTime volume of the splitting regions $\Delta_1$ and $\Delta_2$, namely, by Eq. (6.3), $\delta v_1 \delta w_1 = \delta v_2 \delta w_2 = \mu$.

Up to now, Eq. (6.11) is just another way to write the well known Holzhey, Larsen, and Wilczek [1994] formula. Nevertheless, the UV cut-off $\epsilon$ is now substituted by the covariant cut-off $\mu$, allowing a straightforward but non trivial generalization to QFT in $(1+1)$ curved SpaceTime.

**Curved SpaceTimes** Consider a conformal curved line element

$$ds^2 = -C^2(v, w) \, dv \, dw \,. \tag{6.12}$$

Klein-Gordon equation for a massless scalar field on this background is $C^{-2} \, \partial_v \partial_w \varphi = 0$. It follows that in terms of the coordinates $v$ and $w$ the solutions of the wave equation are the same as in Minkowski space. If we restrict the discussion to SpaceTimes with the same past asymptotic structure as Minkowski space, moreover, the global state $|0\rangle_-$ defined by the Minkowski vacuum at past null infinity $\mathscr{I}_-$ is also a global state of the quantum theory on the curved SpaceTime.

The main result is that its entanglement entropy has the same expression as in Minkowski space, given by the previous result Eq. (6.11).

On the other hand, the geometry is now non-trivial and the metric relation between the points $(v_1, w_1)$ and $(v_2, w_2)$, together with the relation between the

splittings $\delta v_1, \delta v_2, \delta w_1, \delta w_2$ and the covariant cut-off $\mu$ given by the volume of the splitting region are changed. In particular, by Eq. (6.3), we have

$$\mu = -C^2(v_1, w_1)\,\delta v_1 \delta w_1 \;=\; -C^2(v_2, w_2)\,\delta v_2 \delta w_2\,, \tag{6.13}$$

which, put in Eq. (6.11), gives

*the entanglement entropy of a causal domain $D$ with corners $p_1 = (v_1, w_1)$ and $p_2 = (v_2, w_2)$ in the Minkowski vacuum state prepared at $\mathscr{I}_-$ of a QFT in a (past-asymptotically-flat) $(1+1)$-dimensional curved SpaceTime.*

$$S_+(D) = \frac{1}{12}\log\frac{(\Delta v)^2(\Delta w)^2\, C^2(v_1,w_1)\, C^2(v_2,w_2)}{\mu^2} \tag{6.14}$$

We are closer and closer to the main objective of this Chapter: computing the Page's curves of evaporating black hole-like geometries. For this purpose, we need two more steps: the definition of *entanglement entropy production*, and of a *tailored coordinates set* for a collapse geometry.

# 6.2 Ent. Ent. Production

Up to now, we considered the entanglement entropy associated with a diamond $D$. Otherwise, Eq. (6.14) allows to compute the difference $\Delta S \equiv S_+(D) - S_+(D')$ of entanglement entropy between two diamonds: $D$ with corners $p_1$ and $p_2$, and $D'$ with corner $p_1'$ and $p_2'$. If now $p_1'$ (resp. $p_2'$) is the 'time'-evolved of the initial corner $p_1$ (resp. $p_2$), the diamond $D'$ is the diamond $D$ evolved in time, and the difference $\Delta S$ can be interpreted as the *entanglement entropy production* in the diamond during the evolution from $D$ to $D'$.

More precisely, consider a one-parameter family of diamonds $D_\lambda$ labeled by the trajectory of the two spacelike separated corners $p_1(\lambda) = \big(v_1(\lambda), w_1(\lambda)\big)$ and $p_2(\lambda) = \big(v_2(\lambda), w_2(\lambda)\big)$. Given a reference 'time' $\lambda_0$, we define the *entanglement entropy production* (or *excess Ent.Ent.*), in $D_\lambda$ as

$$\Delta S(\lambda) \equiv\; S_+(D_\lambda) - S_+(D_{\lambda_0}) \tag{6.15}$$

that can be computed using Eq. (6.14). Since $\mu$ is a physical cut-off that is kept *fixed* in the evolution, the result turns out to be $\mu$-independent and reads

$$\Delta S(\lambda) = \frac{1}{12}\log\frac{(\Delta v)^2(\Delta w)^2\, C_1^2\, C_2^2\big|_\lambda}{(\Delta v)^2(\Delta w)^2\, C_1^2\, C_2^2\big|_{\lambda_0}}\,. \tag{6.16}$$

where $\Delta v|_\lambda \equiv v_1(\lambda) - v_2(\lambda)$, $\Delta w|_\lambda \equiv w_1(\lambda) - w_2(\lambda)$, and $C_i^2|_\lambda \equiv C^2\big(v_i(\lambda), w_i(\lambda)\big)$ with $i = 1, 2$.

## 6.2.1 Shadow Coordinates

Given a pair of double-null coordinates $(v, w)$ in the time-radius plane, the metric of a general spherically symmetric SpaceTime can be written as [Roman and Bergmann 1983]

$$ds^2 = -C^2(v, w)\, dv\, dw + r^2(v, w)\, d\Omega^2\;; \tag{6.17}$$

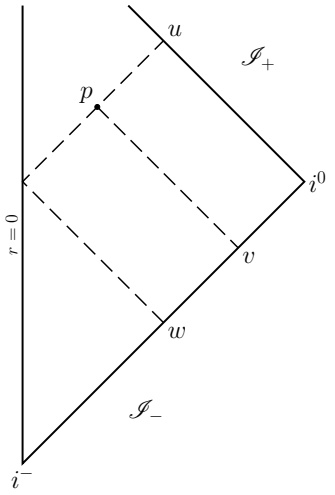


**Figure 6.3.** Definition of the shadow coordinates $(v, w)$. Here $u$ and $v$ are affine coordinates on $\mathscr{I}_+$ (resp. $\mathscr{I}_-$), with $u = f(w)$.

see for instance Eq. (1.14) for the Schwarzschild geometry.

In a past-asymptotically flat SpaceTime, we can choose the null coordinates as follows: take a point $p$ and an affine parameter on $\mathscr{I}_-$, we define the *shadow coordinates* $v(p)$ and $w(p)$ as the affine parameters of the two radial null rays which meet at $p$, with $w(p)$ the coordinate of the null ray bouncing at the centre.[1] See Fig. 6.3. By construction, the shadow coordinates are such that $w \leq v$ and the center $r(v, w) = 0$ has equation $w = v$, while past (resp. future) null infinity corresponds to $w \to -\infty$ (resp. $v \to +\infty$). Furthermore, past-asymptotic flatness requires that $\lim_{w\to-\infty} C^2(v, w) = 1$. Note that, being defined using data at $\mathscr{I}_-$, $v$ and $w$ are well-defined also in the presence of a future event horizon.

Moreover, outgoing null geodesics that reach future null infinity provide a canonical map $u = u(w)$ between $\mathscr{I}_-$ and $\mathscr{I}_+$, where $u$ as an affine parameter on $\mathscr{I}_+$. The ambiguity in $u$ is fixed by requiring that the null vectors $l = \partial_v$ and $n = \partial_u$ are canonically normalized at spatial infinity $i^0$, i.e. $l \cdot n \to -1$ there, and $u(0) = 0$. Calling $w(u)$ the inverse function of $u(w)$, we can rewrite the line element in Eq. (6.17) as

$$\begin{aligned} ds^2 &= -C^2(v, w(u))\, dv\, \frac{dw(u)}{du}\, du + r^2(v, w(u))\, d\Omega^2 = \\ &\equiv -\Theta^2(v, u)\, dvdu + R^2(v, u)\, d\Omega^2 \,, \end{aligned} \tag{6.18}$$

where the new conformal factor depends on the previous one as

$$\Theta^2(v, u) \equiv C^2(v, w(u))\, \dot{w}(u) \tag{6.19}$$

and the dot denotes the derivative with respect to $u$. If we now require also *future-asymptotic flatness*

$$\lim_{v\to\infty} \Theta^2(v, u) = 1 \,, \tag{6.20}$$

[1] There is of course a two-parameter family of such coordinates, following from the ambiguity of the affine parametrization of $\mathscr{I}_-$.

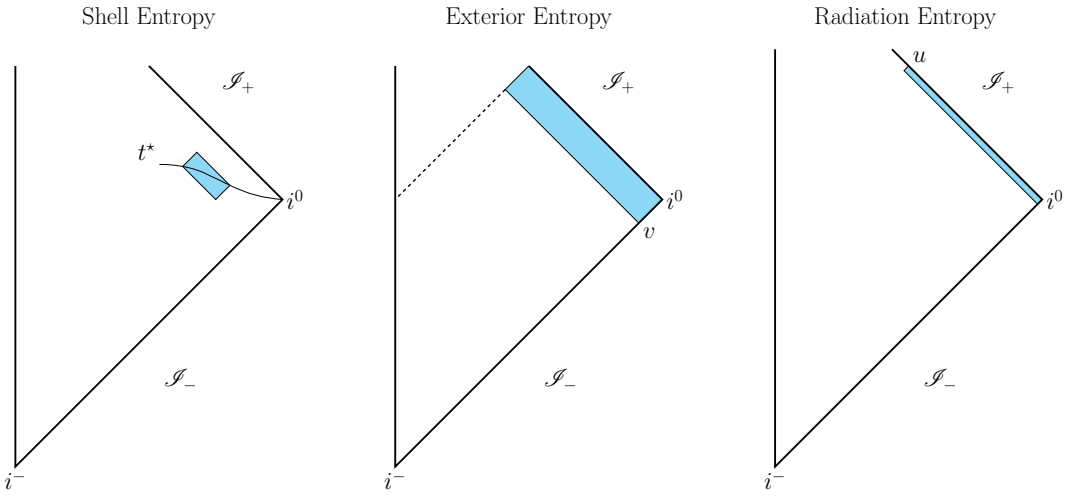


**Figure 6.4.** Diamonds $D_\lambda$ involved in the definition of the shell, exterior and radiation entropies, with $\lambda = t^*, v, u$ respectively.

the map $u(w)$ takes the form

$$u(w) = \int_0^w C^2_{\mathscr{I}_+}(w')\, dw' \tag{6.21}$$

where $C^2_{\mathscr{I}_+}(w) \equiv \lim_{v\to\infty} C^2(v,w)$ is the conformal factor at $\mathscr{I}_+$.

We finally have all the tools to define the radiation entropy and compute the Page's curve in different models of black hole evaporation. To do that we will consider a massless scalar field prepared in the Minkowski vacuum $|0_-\rangle$ at $\mathscr{I}_-$ evolving in time-dependent backgrounds describing gravitational collapses. This is the same framework as in the Hawking's particle production process described in Section 2.2: the scalar field at $\mathscr{I}_+$ is found in an excited state.

### 6.2.2 Page's Curves

Consider the various types of causal domains in Fig. 6.4. In the framework of a gravitational collapse and consequent evaporation, Bianchi, De Lorenzo, and Smerlak [2014] gave precise definitions of three different notions of entropy: the *thermal entropy of Hawking quanta*, the Sorkin [1983] *exterior entropy*, and the Page [1993b] *radiation entropy*. Despite the fact that the one we are interested in is the third, the study of the others two is intriguing in order to show how powerful is this method. In the case of a Vaidya collapse, indeed, they perfectly fit with the expected thermal behavior of Hawking's radiation and with the second law of thermodynamics (see Bianchi, De Lorenzo, and Smerlak [2014, Sec. 4.2-4.3]).

Let us focus the narrow on *radiation entropy. To which 'time' evolving diamond does it correspond?* Take a point $p_u \in \mathscr{I}_+$ with coordinate $u$ that represents an ideal observer, say Bob, on future null infinity. Consider now a diamonds formed by two corners $p$ and $p_0$. If we consider the limit in which $p_0$ goes to spacelike infinity $i^0$ and $p$ goes to $p_u$, the diamond 'degenerate' to a segment on $\mathscr{I}_+$. See the right picture in Fig. 6.4. Now, imagine the point $p$ (resp. $p_0$) to be the 'right' (resp. 'left') corner of our evolving diamond. Let $p_0$ be fixed at $i^0$, while $p$ evolves

from $i^0$ to $p_u$. In this way, the reference 'time' of definition (6.15) is spacelike infinity $i^0$ and the entropy associated to this diamond can be interpreted as the *excess* entropy perceived by Bob in the state at time $u$ with respect to the one perceived in the state at $i^0$.

**Definition** More precisely, we define the *radiation entropy* at retarded time $u$ as the limit

$$\Delta S_{\text{rad}}(u) \equiv \lim_{p\to p_u}\lim_{p_0\to i_0}\lim_{r\to i_0}\Big(S_+(D_{p,r}) - S_+(D_{p_0,r})\Big). \tag{6.22}$$

This gives

$$\Delta S_{\text{rad}}(u) = \frac{1}{12}\log\, C^2_{\mathscr{I}_+}\big(w(u)\big)\ , \tag{6.23}$$

and from Eq. (6.21)

$$\Delta S_{\text{rad}}(u) = -\frac{1}{12}\log\, \dot{w}(u)\ . \tag{6.24}$$

Thus, radiation entropy is nothing but the *logarithmic redshift* of outgoing rays.

We can notice that such a radiation entropy is defined independently from the presence of an event horizon. As explained by Barcelo et al. [2011], indeed, "an exponential relation between the affine parameters on past and future null infinities is a necessary and sufficient condition for generating a Hawking flux", whether or not an event or trapped horizon ever forms. Moreover, they showed that the salient features of the Hawking flux are controlled by the so called *peeling function* $\kappa(u)$, defined as[2]

$$\begin{aligned}\kappa(u) &\equiv -\frac{\ddot{w}(u)}{\dot{w}(u)} = \\ &= -\frac{d}{du}\log \dot{w}(u)\ .\end{aligned} \tag{6.25}$$

In terms of this function, Eq. (6.24) becomes

$$\Delta S_{\text{rad}}(u) = \frac{1}{12}\int_{-\infty}^{u}\kappa(u')\,du', \tag{6.26}$$

as found in Bianchi and Smerlak [2014a,b].

The evolution of the so-defined radiation entropy $\Delta S_{\text{rad}}(u)$ provides the *Page's curve* of any non-trivial (asymptotically flat) curved SpaceTime.

Written as in Eq. (6.26) the Page's curve assumes an intuitive geometric interpretation often discussed in the black hole literature: $\Delta S_{\text{rad}}(u)$ grows when the separation between neighboring outgoing geodesics increases, i.e. they are *peeled* ($\kappa(u) > 0$), and decreases when their separation decreases, i.e. they are *squeezed* ($\kappa(u) < 0$).

[2]The name $\kappa$ for the peeling function is not causal. In a specific limit, indeed, it coincides with the *surface gravity*. See Barcelo et al. [2011, Eq. (24)].

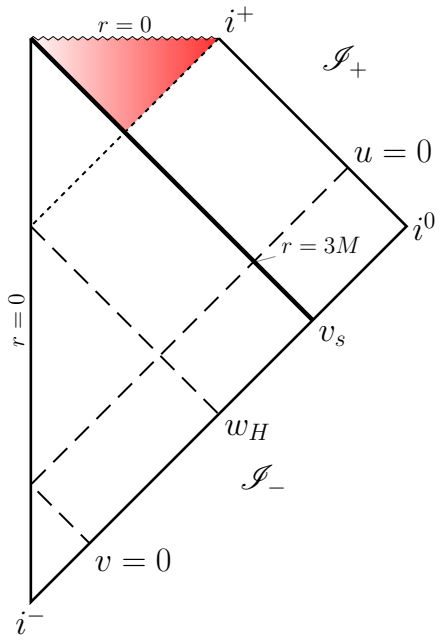


**Figure 6.5.** Penrose-Carter diagram for the Vaidya SpaceTime, with the black hole region shaded.

Equations (6.21) and (6.24) provide the working expressions which allow to compute the Page's curve in almost any SpaceTime describing a collapsing star. In the next Section, we firstly give a proof of the validity of this approach performing the computation in the Vaidya-Schwarzschild case. The results come out to be perfectly compatible with the standard Hawking's radiation framework. Thereafter, the same calculation is made for an evaporating Hayward's metric.

### 6.2.3 Hawking Flux in Vaidya SpaceTime

Consider the Vaidya's model of black hole formation discussed in Section 1.1.3 and used for the derivation of the Hawking's result in Section 2.2. The metric in advanced Eddington-Finkelstein coordinates reads

$$ds^2 = -\left(1 - \frac{2m}{r}\Theta\big(v - v_s\big)\right) dv^2 + 2\, dv\, dr + r^2\, d\Omega^2 \,. \tag{6.27}$$

Let us set $v = 0$ to be the ray that crosses the in-falling shell at $r = 3m$. The associated Carter-Penrose diagram is depicted in Fig. 6.5.

In order to compute the Page's curve, we need to obtain the peeling function $\kappa(u)$ or equivalently the canonical map $w(u)$. To do that, we need to write the Vaidya metric (6.27) in double null coordinate $(v, w)$. As we know, the coordinate $v$ labels in-falling null geodesics. By definition of shadow coordinates, an in-falling null geodesic with advanced time $v = w$ is reflected at the centre $r = 0$ and results in an outgoing null geodesic $r(v, w)$ with $v \geq w$. We use the coordinate $w$ to label outgoing null geodesic. The trajectory $r(v, w)$ is obtained by solving the null geodesic equation

$$\frac{dr}{dv} = \frac{1}{2}\left(1 - \frac{2m}{r}\Theta\big(v - v_s\big)\right). \tag{6.28}$$

with initial condition $r(w,w)=0$. The solution is

$$r(v,w)=\begin{cases}\dfrac{v-w}{2} & \text{for } v<v_s\,,\\[2ex] 2m\left\{1+W\Big(\left(\dfrac{v_s-w}{4m}-1\right)\exp\left[\dfrac{v-w}{4m}-1\right]\Big)\right\} & \text{for } v\geq v_s\,.\end{cases} \tag{6.29}$$

where $W$ is the Lambert function.[3] The conformal factor in (6.17) in shadow coordinates $(v,w)$ is obtained from Eq. (6.27) as follows:

$$\begin{aligned} ds^2 &= -\left(1-\frac{2m}{r}\Theta\big(v-v_s\big)\right)dv^2+2dv\ \left[\partial_v r(v,w)\,dv+\partial_w r(v,w)\,dw\right]+\\ &\qquad +r^2(v,w)\,d\Omega^2= \\ &=2\partial_w r(v,w)\,dvdw+r^2(v,w)\,dw^2= \\ &\equiv -C^2(v,w)\,dvdw+r^2(v,w)\,d\Omega^2\,, \end{aligned} \tag{6.30}$$

where Eq. (6.28) has been used in the first step. The conformal factor is then just $C^2(v,w)=-2\partial_w r(v,w)$, which explicitly reads

$$C^2(v,w)=\begin{cases}1 & \text{for } v<v_s\,,\\[2ex] \dfrac{w-v_s}{w-v_s+4m}\,\dfrac{W\Big(\big(\frac{v_s-w}{4m}-1\big)\exp[\frac{v-w}{4m}-1]\Big)}{1+W\Big(\big(\frac{v_s-w}{4m}-1\big)\exp[\frac{v-w}{4m}-1]\Big)} & \text{for } v\geq v_s\,.\end{cases} \tag{6.31}$$

Using formula (6.21) and the value of the conformal factor at $\mathscr{I}_+$,

$$C^2_{\mathscr{I}_+}(w)=\lim_{v\to+\infty}C^2(v,w)=\frac{w-v_s}{w-v_s+4m}\,, \tag{6.32}$$

we find the canonical map $u(w)$ to be

$$u(w)=w-4m\,\log\frac{v_s-4m-w}{v_s-4m}\,. \tag{6.33}$$

It is important to notice that the map $u=u(w)$ is defined only for $w\leq v_s-4m$ which identifies the presence of an event horizon $H$ at

$$w_H\equiv v_s-4m\,. \tag{6.34}$$

We obtained in a more elegant way the same canonical map we found in Section 2.2.1 in the computation of Hawking's radiation.

Equations (6.29), (6.31) and (6.33) contain the geometric information required for the evaluation of the shell, exterior and radiation entropies in the Vaidya model of gravitational collapse.

[3]The Lambert $W$-function is defined for $x\geq -e^{-1}$ as the unique solution of the equation $W(x)e^{W(x)}=x$.

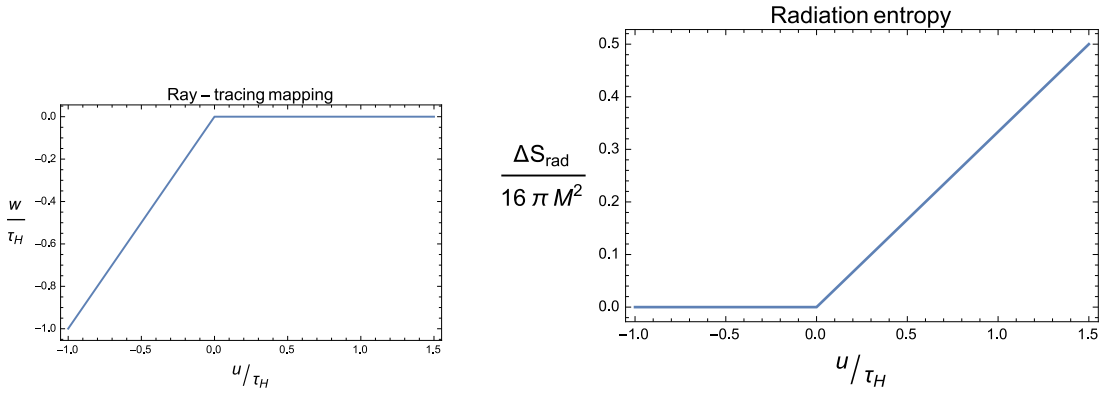


**Figure 6.6.** Ray-tracing mapping $w = w(u)$ (left) and radiation entropy $\Delta S_{\rm rad}(u)$ (right) in a Vaidya SpaceTime with $m = 10 m_P$.

**Monotonic Page's curve** Inverting Eq. (6.33) we find

$$w(u) = v_s - 4m \left\{ 1 + W\left( \frac{v_s - 4m}{4m} \exp\left[ -\frac{u - v_s + 4m}{4m} \right] \right) \right\}. \tag{6.35}$$

In the end, plugging this expression into Eq. (6.24), we are able to compute the radiation entropy:

$$\Delta S_{\rm rad}(u) = \frac{1}{12} \log \left( \frac{1 + W\left( \frac{v_s - 4m}{4m} \exp\left[ -\frac{u - v_s + 4m}{4m} \right] \right)}{W\left( \frac{v_s - 4m}{4m} \exp\left[ -\frac{u - v_s + 4m}{4m} \right] \right)} \right). \tag{6.36}$$

Thanks to the limiting property of the Lambert-W function,[4] the radiation entropy goes to zero at early times: $\Delta S_{\rm rad}(u) \to 0$ when $u \to -\infty$. The choice of the reference point $v = 0$ as the ray that crosses the in-falling shell at $r = 3m$ was not casual. Indeed, the associated retarded time $u = 0$ (the retarded time when the in-falling shell reaches radius $r = 3m$), is approximately the time when the entropy starts growing monotonically. Finally, for late times $u \to +\infty$, the Page's curve behavior is

$$\Delta S_{\rm rad}(u) \sim \frac{u}{48m}. \tag{6.37}$$

That is, the radiation entropy of a Vaidya black hole grows linearly and without bounds, corresponding to the monotonic Page's curve shown in Fig. 6.6. Such linear growth is completely consistent with the Vaidya black hole acting — from the perspective of asymptotic observers at $\mathscr{I}_+$ — as a steady source of thermal radiation.

What happens if we now consider the usual minimal back-reaction of the Hawking's radiation, allowing the parameter $m$ to decrease and finally reach zero? This is the evaporation scenario originally proposed by Hawking [1976] and discussed in Section 2.2. The evaporation time came out to be finite and given by

$$\tau_H \simeq \alpha \frac{m^3}{m_P^2}. \tag{6.38}$$

[4] The Lambert-W function satisfies $W(x) \sim x$ as $x \to 0$, $W(x) \to \infty$ as $x \to \infty$, and $W'(x) = W(x)/[x(1 + W(x))]$.

**Singular evaporation** To answer the question, it is possible to re-do the previous calculation in an analytically solvable simplified toy model of gravitational collapse and subsequent evaporation. In this model, after the usual Vaidya formation at advanced time $v_s$, the mass of the black hole remains constant and equal to $m$ for a time $\sim \tau_H$ after the onset of Hawking evaporation, and then instantaneously vanishes. Following Hiscock [1981a,b] the evaporation is modeled in the following way. At the advanced time $\overline{v}_s$ and at distance $r = \overline{R}_s > 2m$ (for instance $\overline{R}_s = 3m$) two null shells are produced: an out-going shell of mass $m$ and an in-going shell of mass $-m$. The out-going shell models the back-reaction on the metric of the positive energy flux brought by the Hawking's radiation, the in-going shell models the mass loss of the black hole.

The metric defining this model has the usual form

$$ds^2 = -F(v,r)\,dv^2 + 2\,dv\,dr + r^2\,d\Omega^2 \tag{6.39}$$

with

$$F(v,r) = \begin{cases} 1 & \text{for } v < v_s\ ; \\ 1 - \dfrac{2m}{r} & \text{for } v_s \leq v < \overline{v}_s\ ; \\ 1 - \dfrac{2m}{r} & \text{for } v \geq \overline{v}_s \text{ and } r > r_0(v, \overline{w}_s)\ ; \\ 1 & \text{for } v \geq \overline{v}_s \text{ and } r \leq r_0(v, \overline{w}_s)\ . \end{cases} \tag{6.40}$$

Here $r_0(v,w)$ is the same of Eq. (6.29),

$$r_0(v,w) = 2m\left\{1 + W\left(\frac{v_s - 4m - w}{4m}\exp\left[\frac{v-w}{4m} - 1\right]\right)\right\}, \tag{6.41}$$

while $(\overline{v}_s, \overline{w}_s)$ is the point where the production of the pair of null shells modeling the evaporation happens. The model has only three parameters $m$, $\overline{R}_s$ and $\Delta v \equiv \overline{v}_s - v_s$, and can be visualized looking at the conformal diagram in Fig. 6.7. The geometry presents the spacelike singularity at $r = 0$, a trapping horizon $TH$ and an event horizon $H$ inside the trapping region.

Without deeply analyzing the details (that one can find in Section 5.2 of the paper on which this Chapter is based) let us just give the main results. *Via* the analytical explicit form of the canonical map from $\mathscr{I}_-$ to $\mathscr{I}_+$ and Eq. (6.24), one can compute the *Page's curve* shown in Fig. 6.8. Looking at the conformal diagram Fig. 6.7, it is clear that for retarded times $u \leq \overline{u}_s$ the behavior has to be the same as in the non-evaporating case shown before. Therefore, light rays started on $\mathscr{I}_-$ before the advanced time $\overline{w}_s$ bounce at the center and reach future null infinity evolving in a perfectly Vaidya SpaceTime. This rays are not afflicted by the evaporation process: for them, the black hole is eternal as in the previous case. For this reason, the Page's curve in Fig. 6.8 grows exactly as in the Vaidya case up to the time $\overline{u}_s$.

After a discontinuity due to an artifact of the background metric chosen to model the evaporation process (outgoing null rays with $u < \overline{u}_s$ are more redshifted than outgoing null rays with $u > \overline{u}_s$), at later times, when $u \to u_H$, $\Delta S_{\rm rad}(u)$ presents a divergent behavior. Such null *entanglement singularities* would be the manifestation of *information loss* in singular black hole evaporation.

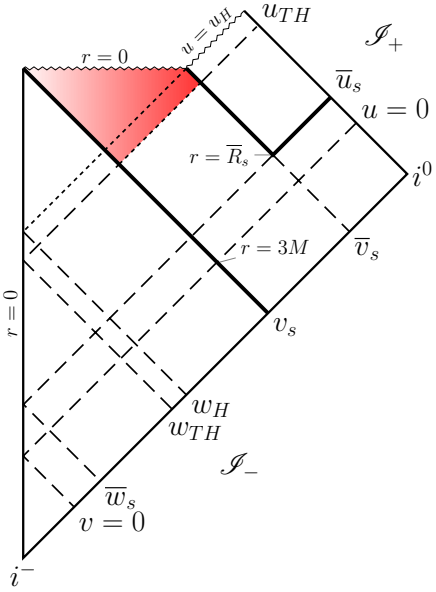


**Figure 6.7.** Penrose-Carter diagram for the singular evaporation toy model defined by Eqs. (6.39)- (6.40), with the trapped region shaded. It shows the three shells (thick line), the event horizon (thin dotted line) and the trapping horizon (thick dotted line). Note the difference between the event and trapping horizons, and the existence of (quantum) null singularity along $u = u_H$.

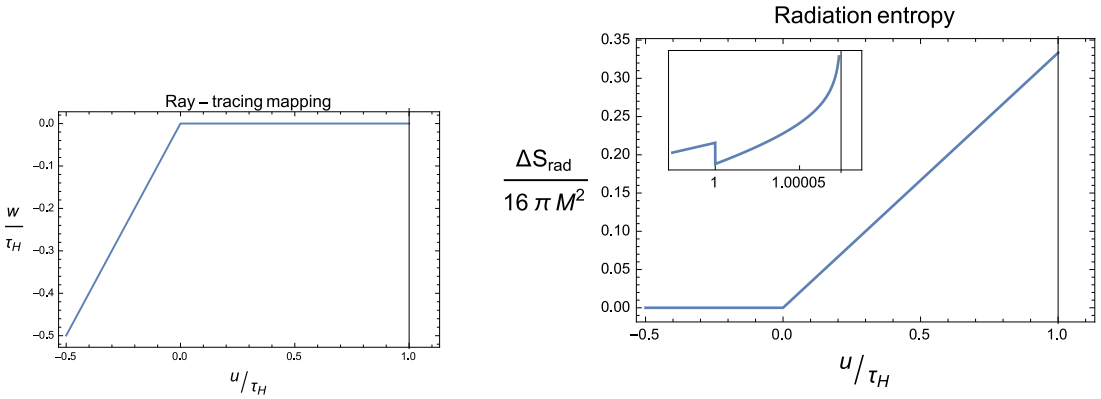


**Figure 6.8.** Ray-tracing mapping $w = w(u)$ (left) and radiation entropy $\Delta S_{\rm rad}(u)$ (right) in the singular evaporation model with $m = 10 m_P$ and $\overline{R}_s = 3m$. Inset: late-time behavior of the radiation entropy, showing the $\mathcal{O}(1)$ discontinuity and the divergence at $u = u_H$.

Once understood the validity of this method, we can address the main goal of this Chapter, that is studying Page's curve for an evaporating Hayward's metric.

### 6.2.4 Hayward-Like Black Hole Evaporation

As largely discussed in the previous Chapters, the Hayward's metric, as well as the other non-singular black hole metric proposed, exhibits two asymptotic regions. Far from the outer horizon, the SpaceTime is essentially the one of a Schwarzschild black hole; on the other hand, near to the origin $r = 0$, the behavior is essentially deSitter. Therefore, we can sketch our SpaceTime in a analytically solvable one. In particular, we consider an evaporating line element of the form in Eq. (6.39), with the function $F(v, r)$ given by

$$F(v,r) = \begin{cases} 1 & \text{for } v < v_s \ ; \\ 1 - \dfrac{2m}{r} & \text{for } \{v_s \leq v < \overline{v}_s,\ r > \overline{R}_s\} \ ; \\ 1 - \dfrac{r^2}{L^2} & \text{for } \{v_s \leq v < \overline{v}_s,\ r \leq \overline{R}_s\} \ ; \\ 1 - \dfrac{2m}{r} & \text{for } \{v \geq \overline{v}_s,\ r > r_0(v, \overline{w}_s)\} \ ; \\ 1 & \text{for } \{v \geq \overline{v}_s,\ 0 \leq r \leq r_0(v, \overline{w}_s)\} \ . \end{cases} \tag{6.42}$$

In such a way, we have the usual Vaidya's shell collapsing at $v = v_s$: inside it the SpaceTime is flat. The outside-the-shell region in the slab $v_s \leq v \leq \overline{v}_s$, consists of a Schwarzschild patch with mass $m$ for $r > R_m$ and a de Sitter patch with cosmological constant $\Lambda \equiv 1/L^2$ for $r \leq R_m$. The (spacelike) matching surface $R_m$ is assumed to lie within the trapped region. The evaporation process is the same as in the previous model. At $v = \overline{v}_s$ a positive and a negative mass shell are originated at $r = \overline{R}_s > 2m$. Even if more complicated then its precedents, the Penrose-Carter diagram depicted in Fig. 6.9 can more clearly shine the situation.

*Which are the relevant advanced times for this metric?* As before we call $w_1 \equiv \overline{w}_s$ the time when the two shells modeling the evaporation process are produced, i.e. $r_0(\overline{v}_s, \overline{w}_s) = \overline{R}_s$. Moreover we define $w_2$ as the advanced time when the negative-energy shell reaches the matching surface, i.e. $r_0(\overline{v}_s, w_2) = R_m$, $w_3$ and $w_4$ as the times when the positive-energy shell reaches respectively the matching surface, $r_0(v_s, w_3) = R_m$, and the inner horizon, $r_0(v_s, w_4) = L$. Finally we call $w_5 = v_s$ and $w_6 = \overline{v}_s$. As before we denote

$$w_{TH} \equiv v_s - 4m \tag{6.43}$$

the position of the outer trapping horizon and $\Delta v \equiv \overline{v}_s - v_s$.

Once fixed the notation, we can start out path toward the Page's curve. The

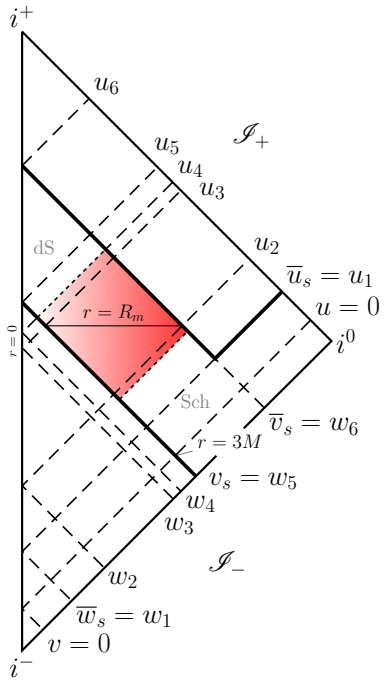


**Figure 6.9.** Penrose-Carter diagram of a non-singular black-hole evaporation model, with the trapped region (shaded) and a matching surface (horizontal line) between the de Sitter core (dS) and the Schwartzschild region.

canonical map $u \mapsto w(u)$ comes out to be analytically computable:

$$
w(u) = \begin{cases}
w_{TH} - 4m\, W\Big(\dfrac{w_{TH}}{4m} \exp[-\dfrac{u - w_{TH}}{4m}]\Big) & \text{for } u < u_1 \ ; \\
w_{TH} - 4m\, W\Big(\dfrac{\overline{u}_s - u + 2\overline{R}_s - 4m}{4m} \times & \\
\qquad \times \exp\left[-\dfrac{u - \overline{u}_s - 2\overline{R}_s + 4m + \Delta v}{4m}\right]\Big) & \text{for } u_1 \le u < u_2 \ ; \\
w_{TH} - 4m\, W\Big(\dfrac{R_m - 2m}{2m} \times & \\
\qquad \times \exp\left[-\dfrac{J(u - u_6) - 2R_m + 4m + \Delta v}{4m}\right]\Big) & \text{for } u_2 \le u < u_3 \ ; \\
v_s + 2L \coth\left[\dfrac{\Delta v}{2L} + \coth^{-1}\left[\dfrac{u - u_6}{2L}\right]\right] & \text{for } u_3 \le u < u_4 \ ; \\
v_s + 2L \tanh\left[\dfrac{\Delta v}{2L} + \tanh^{-1}\left[\dfrac{u - u_6}{2L}\right]\right] & \text{for } u_4 \le u < u_5 \ ; \\
\overline{v}_s + 2L \tanh^{-1}\left[\dfrac{u - u_6}{2L}\right] & \text{for } u_5 \le u < u_6 \ ; \\
u + 4m \log\Big(\dfrac{u - u_6 + 2\overline{R}_s - 4m}{v_s - 4m}\Big) & \text{for } u \ge u_6 \ .
\end{cases}
\tag{6.44}
$$

where the function $J(u)$ is

$$
J(u) \equiv 2L\left(\coth^{-1}\left[u/2L\right] + \coth^{-1}[R_m/L]\right) \tag{6.45}
$$

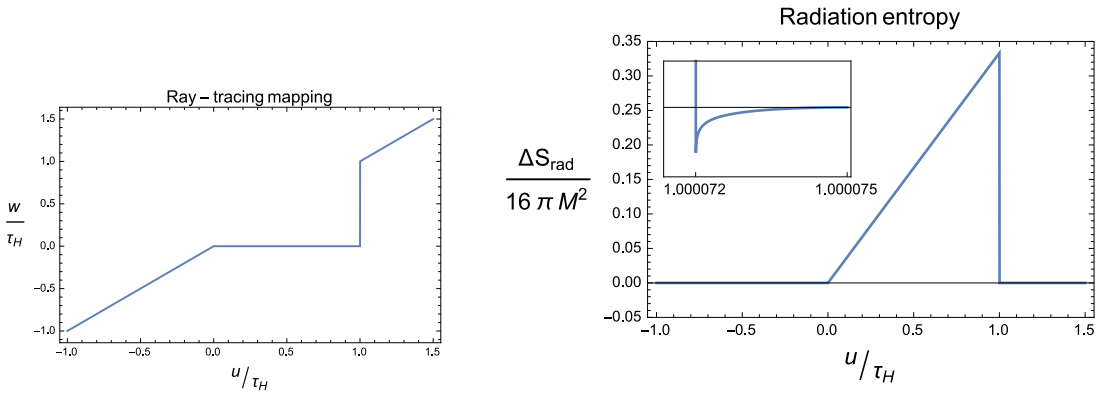


**Figure 6.10.** Ray-tracing mapping $w = w(u)$ (left) and radiation entropy $\Delta S_{\rm rad}(u)$ (right) in the nonsingular evaporation model, with $m = 10m_P$, $L = m/10$ and $\overline{R}_s = 3m$. Inset: late-time behavior of the radiation entropy, showing that $\Delta S_{\rm rad}(u) < 0$ in phase C.

and we defined the retarded times corresponding to $w_1, \ldots, w_5$:

$$\begin{aligned}
u_1 &= \overline{u}_s \ ; \\
u_2 &= \overline{u}_s + 2(\overline{R}_s - R_m) \ ; \\
u_3 &= \overline{u}_s + 2\overline{R}_s - 2L \coth\left[\frac{\Delta v}{2L} + \coth^{-1}\left[\frac{R_m}{L}\right]\right] \ ; \\
u_4 &= \overline{u}_s + 2\overline{R}_s - 2L \ ; \\
u_5 &= \overline{u}_s + 2\overline{R}_s - 2L \tanh\left[\frac{\Delta v}{2L}\right] \ ; \\
u_6 &= \overline{u}_s + 2\overline{R}_s . \ .
\end{aligned} \tag{6.46}$$

The Page's curve of the radiation emitted by the non-singular black hole can be again computed using Eq. (6.24). The result is plotted in Fig. 6.10, where we fixed

$$R_m \equiv (2mL^2)^{1/3} \ . \tag{6.47}$$

We distinguish four phases of the evolution of such a non-singular black hole, phase $A$, $B$, $C$ and $D$.

The behavior at early times, phase $A$, is the same as the entire singular evaporation scenario, but doesn't present the entanglement singularity since another phase starts after it: those light rays responsible for this phase are not affected by the presence of the deSitter core. This phase lasts for a retarded time $\Delta u_A$ approximately given by

$$\Delta u_A \equiv u_2 \approx \alpha\, m^3/m_p^2 \, . \tag{6.48}$$

$\Delta S_{\rm rad}(u)$ grows monotonically and reaches a maximum at

$$S_{\rm max} \equiv \Delta S_{\rm rad}(u_2) \approx \frac{\alpha}{48}\frac{m^2}{m_P^2} + \frac{1}{12}\log\frac{2m}{R_m} \, . \tag{6.49}$$

Phase $B$ is determined by outgoing rays that have been trapped by the null shell falling at $v_s$: they have entered de Sitter core and then been expelled when

the black hole terminates its evaporation (see also Fig 5.1(a) of Chapter 5). The duration of this phase is really *short*:

$$\Delta u_B \equiv u_5 - u_2 \approx 2R_m - 2L\,. \tag{6.50}$$

In this phase the entropy 'falls' monotonically and reaches its minimum at the negative value

$$S_{\min} \equiv \Delta S_{\rm rad}(u_5) \approx -\frac{\alpha}{12}\frac{m^3}{L\,m_P^2}\,. \tag{6.51}$$

*What does the fact that $\Delta S_{rad}(u)$ of the radiation becomes negative means?* As said at the beginning of Section 6.2.2, this quantity represents the *excess* of entanglement entropy at the time $u$ with respect to a $i^0$ where, thanks to asymptotic flatness, the state of the field is the Minkowski vacuum. Therefore, a negative value of $\Delta S_{\rm rad}(u)$ simply means that the state at that time $u$ is *less correlated* than the Minkowski vacuum state.

After the decreasing phase $B$, phase $C$ presents a monotonically increasing behavior. This phase is determined by the outgoing radiation that has entered the black hole after it formed at $v_s$ and before it disappeared completely at the time $\overline{v}_s$. This radiation traveled through the de Sitter core, bounced at the center and is expelled at the end of the evaporation. This phase lasts a finite time

$$\Delta u_C \equiv u_6 - u_5 \approx 2L\,. \tag{6.52}$$

in which the entanglement entropy of the radiation grows monotonically from its minimum and *approaches zero* from below, quadratically for $u \to u_6$

$$\Delta S_{\rm rad}(u) \sim -\frac{(u-u_6)^2}{48\,L^2}\,. \tag{6.53}$$

At the end of phase $C$ the black hole has disappeared and the entropy of radiation vanishes. Note however that this is not yet the end of the process.

Phase $D$ corresponds to late outgoing radiation that that has never entered the black hole as it fell in after its disappearance at $\overline{v}_s$. Therefore this radiation travels through Schwarzschild space (for $u < \overline{u}_s$), then through flat space, and it reaches $\mathscr{I}_+$ at a time $u > u_6$, see Fig. 6.9. The entanglement entropy for this phase is

$$\Delta S_{\rm rad}(u) = -\frac{1}{12}\log\left(1 + \frac{4m}{u - u_6 + 2\overline{R}_s - 4m}\right). \tag{6.54}$$

In particular at the beginning of phase $D$ the entanglement entropy is negative and equal to $\Delta S_{\rm rad}(u_6) \simeq -0.1$ for $\overline{R}_s = 3m$, while at late times it goes as

$$\Delta S_{\rm rad}(u) \sim -\frac{1}{12}\,\frac{4m}{u - u_6} \tag{6.55}$$

to finally vanish in the limit $u \to +\infty$, see Fig. 6.10. Even if the discussion has been made for a simplified model, it shares the main features of the Dyminikova-like metrics as the Hayward one, for which a numerical integration is needed.

As in the Page's argument discussed in Section 2.4.1, the entanglement entropy comes back to zero at the end of the process. That is, *in the process of evaporation of a Hayward-like non-singular black hole, unitarity is preserved and no information is lost.* As expected.

Up to now, therefore, this approach seems to confirm the goodness of the Hayward's model as resolution of the information-loss paradox. However, as we will show in the next Section, the same analysis shine a light on some un-noticed problems. Contrary to the difficulties arose in Section 4.1, those new problems come out to be not straightforwardly solvable.

## 6.3 Problems: Energy and Purification Time

**Energy** As explained by Bianchi and Smerlak [2014a], the radiation entropy can be related to the energy flux at future null infinity $\mathscr{I}_+$ carried by the radiation. Indeed, while the energy momentum tensor $T_{ab}$ of the out-vacuum $|0_+\rangle$ is null on $\mathscr{I}_+$, for the in-vacuum $|0_-\rangle$ it has a non-trivial component. The expression for the related energy flux $F = T_{\mu\nu}(d/du)^\mu(d/du)^\nu$ is a result of QFT in curved SpaceTime due to Davies, Fulling, and Unruh [1976]

$$F_{|0_-\rangle}(u) = -\frac{1}{24\pi}\left(\frac{\dddot{w}(u)}{\dot{w}(u)} - \frac{3}{2}\frac{\ddot{w}^2(u)}{\dot{w}^2(u)}\right) . \tag{6.56}$$

In terms of the radiation entropy, Eq. (6.24), it reduces to

$$F_{|0_-\rangle}(u) = \frac{1}{2\pi}\left(6\dot{S}^2(u) + \ddot{S}(u)\right) , \tag{6.57}$$

where, to simplify the notation, we called $S(u) \equiv \Delta S_{\text{rad}}(u)$. That is, the energy flux at future null infinity is completely determined by the radiation entropy. This puts constraints on the asymptotical behavior of $S(u)$. Indeed, since by construction $S(-\infty) = 0$, the physical requirement on the *total radiated energy* to be finite, i.e. $\int_{\mathscr{I}_+} du\, F_{|0_-\rangle}(u) < \infty$, implies

$$\dot{S}(u) \to 0 \qquad \text{for } u \to \pm\infty , \tag{6.58}$$

namely an asymptotical smooth behavior of the radiation entropy. Notice that we don't impose the radiation entropy to vanish at infinity. This doesn't imply a non-unitary evolution, but for instance the fact that information is trapped in a stable remnant settled after the evaporation. The condition (6.58) is clearly violated by the singular evaporation process studied in Section 6.2.3; therefore, the discussed 'entanglement singularity' (Pag. 88) can be related with a divergence of the energy radiated.

The non-singular black hole scenario, on the other hand, has an asymptotically vanishing radiation. The total energy radiated is then finite. Moreover, we can

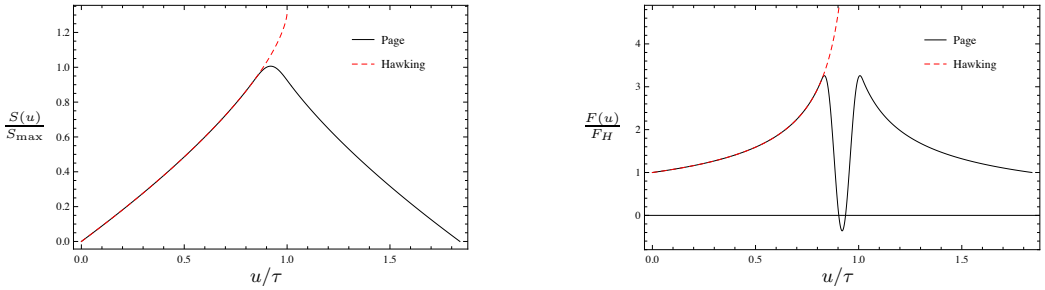


**Figure 6.11.** Left: Original entanglement entropy behavior proposed by Page [1993b]. Right: The corresponding flux function (normalized to the Hawking flux $F_H \sim ?? \frac{1}{m^2}$) derived by Eq. (6.57) (The Hawking thermal entropy and mass law (dashed line) are for reference, and $\tau \sim m^3$ denotes the Hawking evaporation time). Figure reproduced from Bianchi and Smerlak [2014a].

compute the energy flux plugging the analytical result for $S(u)$ into Eq (6.57). Integrated over all future null infinity, it results in a total radiated energy

$$\int_{\mathscr{I}_+} du\, F_{|0_-\rangle}(u) \sim e^{m^3} \,. \tag{6.59}$$

It is actually finite, but at the same time much greater then the initial energy of the SpaceTime represented by the ADM mass $m$. This result is completely un-physical. The Hayward (as well as any deSitter-Schwarzcshild-like non-singular black hole) metric seems to suffer of what we will call the *energy problem*.[5]

Moreover, another shortcoming can be found. Before analyzing it, it is interesting to remark that the particular shape of $S(u)$ for the Hayward's metric results also in a *negative energy flux* to infinity. States with local negative energy densities are well known in quantum field theory, as for example in *moving-mirror* scenarios, and in particular in particle production by black holes [Davies and Fulling 1977; Hawking 1975]. Fortunately, it turns out that pulses of negative energies cannot survive for too long, bounded by the so called *quantum inequalities* (see Ford [2010] for a review): if a pulse with negative energy $E$ is spread over a time $\delta t$, these inequalities require that $|E|\,\delta t \lesssim 1$. Since by the uncertainty principle $\delta E \delta t \gtrsim 1$, this means that $|E| \lesssim \delta E$: negative energies are fundamentally quantum fluctuations (without a classical interpretation).[6] Thank to the covariant definition of entanglement entropy, Bianchi and Smerlak [2014a] showed that any unitary evaporation process must be radiate some amount of negative energy. This is what they call the *last 'gasp'* the black hole makes "before dying a unitary death" [Bianchi and Smerlak 2014b]. As shown in Fig. 6.11, also the simple qualitative shape of the original entanglement entropy behavior proposed by Page [1993b] admits negative energies.

[5] The discussed paragraph and the following one are based on a private discussion with E. Bianchi, M. Smerlak, C. Rovelli, S. Speziale and C. Pacilio.

[6] Another consequence has been recently discussed by Ford and Roman [1999] under the name *quantum interest conjecture*: an energy 'loan' (negative energy $-E$) must always be 'repaid' (by positive energy $(1+\epsilon)E$) before 'term' $T$ with an 'interest' $\epsilon$ which depends on the magnitude $E$ and duration $T$ of the loan.

**Purification time** Let us now define *purification phase* the interval $\Delta u_p$ in which the early radiation is purified. This phase starts when the entanglement entropy reaches its maximum and ends when information is recovered. In the Page's argument, it starts at the *Page's time* to end when the Page's curve vanishes. In the Hayward-like scenario in Section 6.2.4, on the other hand, it corresponds to the interval $\Delta u_p \equiv u_6 - u_2$. Under some general physical assumptions on unitary black hole evaporation, it is possible to show that the purification time $\Delta u_p$ is bounded from below. Let us be more precise.

Take a black hole formation and evaporation scenario, and make the following assumptions:

1. *Energy conservation.* The total radiated energy is less the the initial ADM mass $m$;

2. *No information-loss.* The radiation entanglement entropy $S(u)$ is a smooth function of $u \in (-\infty, +\infty)$;

3. *Adiabatic Hawking phase.* Semiclassical gravity in the adiabatic approximation is correct at early times.

Define the *retarded mass* of the hole

$$m(u) = m - \int_{-\infty}^{u} du' \, F_{|0_-\rangle}(u') \ . \tag{6.60}$$

First hypothesis then implies

$$\lim_{u \to +\infty} m(u) \geq 0 \ . \tag{6.61}$$

Moreover, define the extremities of the purification interval as $\Delta u_p = [u_\star, u_f]$. Hypothesis two assures the process to be unitary. The third hypothesis, on the other hand, tells us that at early time, any black hole is seen as a Schwarzschild one, as observations in our Universe suggest.

From Eq. (6.37), Hypothesis 3 can be written as

$$\begin{cases} \dot{S}(u) \simeq \dfrac{1}{48\, m(u)} \\ \dot{m}(u) \simeq -\dfrac{1}{768\pi m^2(u)} \end{cases} \quad \text{for } u \leq u_\star \ . \tag{6.62}$$

From Eq. (6.57) and the fact that $\dot{S}(u_\star) = \dot{S}(u_f) = 0$, the energy radiated in the purification phase reads

$$E_p = \frac{1}{2\pi} \int_{u_\star}^{u_f} \dot{S}^2(u) du \ . \tag{6.63}$$

The RHS can be thought of as the Lagrangian of a free particle in two dimensions, so it is minimized by the 'straight line' $\dot{S} = const$:

$$E_p \geq \frac{1}{4\pi} \frac{S(u_\star)^2}{\Delta u_p} \ . \tag{6.64}$$

This equation together with energy conservation $E_p \leq m(u_\star)$ finally gives

$$\Delta u_p \geq \frac{1}{4\pi}\frac{S(u_\star)^2}{m(u_\star)} \,. \tag{6.65}$$

That is, *the purification time is bounded from below by the ratio between the square of the radiation entropy and the retarded mass evaluated at the end of the early Hawking phase.*

Moreover, from assumptions (6.62)

$$S(u_\star) \simeq 8\pi\big(m^2 - m^2(u_\star)\big)\,, \tag{6.66}$$

and therefore we find the bound on the purification time $\Delta u_p$ to be

$$\Delta u_p \gtrsim \frac{16\pi\big(m^2 - m^2(u_\star)\big)^2}{m(u_\star)} \,. \tag{6.67}$$

As Page's argument suggests, semiclassical approximation breaks down when the mass of the black hole is still macroscopic, namely $m_\star \sim \frac{m}{\alpha}$. In this case, $\Delta u_p \sim m^3$: purifying information is released in a very long interval of time.

Coming back to our result for the Hayward-like metric, from Eqs. (6.50)-(6.52) and Eq. (6.47), follows

$$\Delta u_p = u_6 - u_2 \simeq 2(2m\,L^2)^{1/3} \tag{6.68}$$

much smaller then expected.

*This inconsistency, together with the energy problem, undermines the validity of the Hayward's metric as a good semi-classical approach to the resolution of the singularity inside a black hole.*

**Possible solutions** In Chapter 4, we proposed a modification to the Hayward's metric, introducing the time-delay factor $G(r)$. One can think that the resulting line element can solve the shortcomings found in the previous paragraphs. However, since the slight modification in terms of metric influences only the interior of the black hole, the phase $(-\infty, u_4]$ of the Page's curve in Fig. 6.10 remains unchanged, in particular the huge slope in the decreasing phase. Since the energy flux depends on $\dot{S}^2(u)$ and $\ddot{S}(u)$, the enormous amount of energy radiated can be associate with a 'burst' in this 'falling' phase. The energy problem, therefore, seems to be not solved by the *modified Hayward's metric.*

Another observation has to be made about the model of evaporation used in the computation of the radiation entropy. Indeed, it has been assumed that the Hayward black hole totally disappears in a finite time. However, this is just one of the two evaporation scenarios discussed in Chapter 5. It could be then interesting to see if and how it is possible to analyze the Page's curve in the case the evaporation takes an infinite time as the horizons asymptotically merge.

Beyond these two *conservative* solution attempts, one can of course discard Hayward-like metrics, looking for completely different metrics and ideas. In the framework of the *covariant entanglement entropy production*, one approach is to

reverse the way of reasoning proposed in this Chapter. Instead of computing the canonical map $w(u)$ and the radiation entropy from a given line element, one can choose a particular $w(u)$ (and consequent Page's curve) satisfying all the physical requirements, trying from that to see if it is possible to construct a metric that allow such a map $w(u)$. For instance, one can impose the Page's curve to be symmetric, as in the original Page's argument.

An example of 'completely different metrics and ideas' is the *Black hole fireworks* scenario proposed by Haggard and Rovelli [2014]. As conclusive Section of this thesis, we introduce this unorthodox model, analyzing its plausibility through its Page's curve.

### 6.3.1 Black Hole Fireworks

In the 'black hole fireworks' scenario information is preserved in gravitational collapse by a quantum-gravitational tunneling process, of which Hawking evaporation is only a higher-order 'dissipative" correction.

The corresponding SpaceTime is shown in Fig. 6.12. Start from the Kruskal-Szekeres diagram of an eternal black hole and pick a point $\Delta$ in the exterior region; $\Delta$ has Kruskal-Szekeres coordinates $(U_\Delta = -V_\Delta, V_\Delta)$. Choose then a null surface $V = V_s$ such that $V_\Delta > V_s$ and a point $\mathcal{E}$ on it, with coordinates $(U_\mathcal{E}, V_\mathcal{E} = V_s)$. Finally pick a spacelike surface connecting $\Delta$ to $\mathcal{E}$. Call the resulting patch of Kruskal-Szekeres SpaceTime Region II. This region automatically determines its time-symmetric partner (Region tII) by taking the null surface $U_s = -V_s$ and the point $\overline{\mathcal{E}}$ on it, with coordinates $(V_{\overline{\mathcal{E}}} = -V_s, U_{\overline{\mathcal{E}}} = -U_\mathcal{E})$. See Fig. 6.12-Left. The Carter-Penrose diagram in Fig. 6.12-Right is then obtained by "opening up the wings" of Region II and tII, inserting interpolating III+tIII Regions in between, and gluing two flat Regions (I and tI) respectively along the surface $V = V_s$ and $U = U_s$.

The resulting SpaceTime represents the dynamics of a null in-falling shell that bounces at $r = 0$ and comes out as a null outgoing shell. To allow for this, geodesics must tunnel through a non-classical Region, represented by the unknown quantum Regions III and tIII. The point $\mathcal{E}$ is the point where the ingoing shell reaches Planckian density and quantum effects start to be important, while $\Delta$ is considered as the outmost boundary of the quantum regions. The SpaceTime is event-horizon-free, but displays a trapping and an 'anti-trapping" surface.

The model explicitly disregards Hawking's radiation because of the request of a completely time symmetric non-dissipative process.

Here we are interested in studying the general features of the Page's curve for this model. To do this, let us first observe that Region I and II can be described by the Eddington-Finkelstein coordinates $(v, r)$ and a metric of type (6.39)

$$ds^2 = -F(v,r)\,dv^2 + 2\,dv\,dr + r^2\,d\Omega^2 \tag{6.69}$$

with

$$F(v,r) = \begin{cases} 1 & \text{for } v < v_s\ ; \\ 1 - \dfrac{2m}{r} & \text{for } v \geq v_s \text{ and } (v,r) \in \text{II}. \end{cases} \tag{6.70}$$

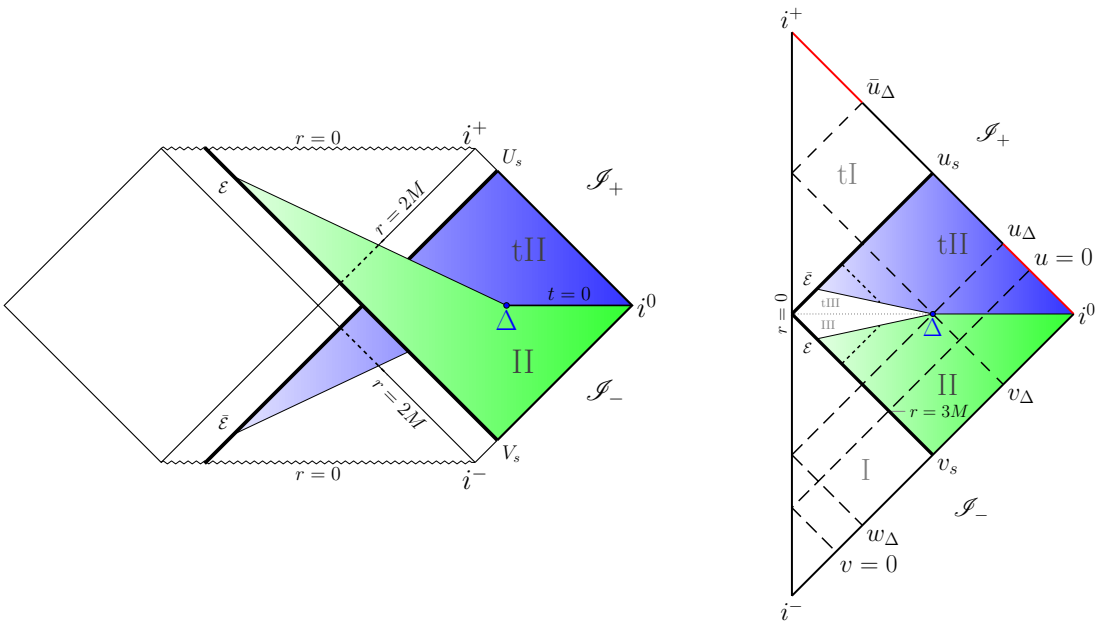


**Figure 6.12.** Geometry of a time-symmetric bouncing shell. Left: Kruskal-Szekeres diagram of the extended Schwarzschild SpaceTime from which the model is constructed. Right: The resulting Carter-Penrose diagram of the Haggard-Rovelli fireworks SpaceTime.

Here $v$ in Region II is related to the Kruskal-Szekeres $V$ by the usual relation $V \propto \exp(v/4m)$. In the same way, Region tI and tII can be described by retarded Eddington-Finkelstein coordinates $(u, r)$, where $U \propto -\exp(-u/4m)$ in Region tII, and a metric of the type

$$ds^2 = -F(u,r)du^2 - 2dudr + r^2\, d\Omega^2 \ . \tag{6.71}$$

with

$$F(u,r) = \begin{cases} 1 & \text{for } u > u_s \ ; \\ 1 - \dfrac{2m}{r} & \text{for } u \leq u_s \text{ and } (u,r) \in \text{II}. \end{cases} \tag{6.72}$$

As before we take the origin $u = 0$ at the retarded time when the in-falling shell crosses $r = 3m$. The two parameters of the model are $r_\Delta > 2m$ and $\Delta v \equiv v_\Delta - v_s > 0$. The retarded time $u_\Delta$ is given by

$$u_\Delta = v_s + \Delta v - 2r_\Delta - 4m \log\left(\frac{2r_\Delta - 4m}{v_s - 4m}\right). \tag{6.73}$$

The canonical map $u \mapsto w(u)$ from $\mathscr{I}_+$ to $\mathscr{I}_-$ giving the entanglement entropy production can be divided in a classical phase, corresponding to the light rays that don't enter in the quantum region when traced back (red thick region on $\mathscr{I}_+$ in Fig. 6.12-Right), and the remaining quantum phase. The relevant advanced times are $u_\Delta$, that by construction gives $u_s - u_\Delta = \Delta v$, and $\overline{u}_\Delta$ defined by $w(\overline{u}_\Delta) = v_\Delta$. The two phases give us different information: the choice of the matching surface connecting $\Delta$ to $\mathcal{E}$ and of the semiclassical metric in the quantum region strongly influence the Page's curve in the domain $u_\Delta < u < \overline{u}_\Delta$, while the result in the

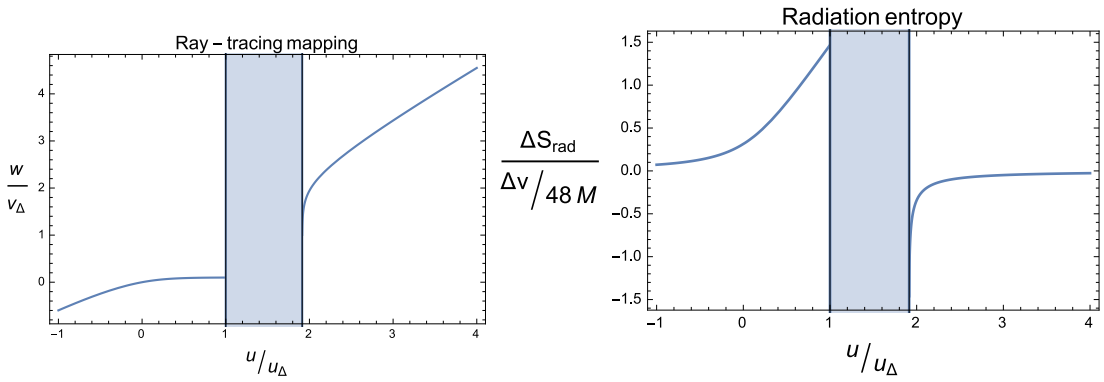


**Figure 6.13.** Ray-tracing mapping $w = w(u)$ (left) and radiation entropy $\Delta S_{\rm rad}(u)$ (right) in the Haggard-Rovelli 'fireworks' model, with $m = 10 m_P$, $r_\Delta = 7m/3$ and $\Delta v = 1.4m$. The shaded region represents the unspecified "quantum tunnelling" phase.

classical regime is completely insensitive to these choices and captures the general features of the model. Since the geometry of the quantum regions III and tIII remains essentially unknown, we will only compute $w(u)$ in the classical phase.

We obtain $w(u)$ for $u \leq u_\Delta$ and $u \geq \overline{u}_\Delta$, finding

$$w(u) = \begin{cases} v_s - 4m \left\{ 1 + W\left[ \dfrac{v_s - 4m}{4m} \exp\left( -\dfrac{u - v_s + 4m}{4m} \right) \right] \right\} & \text{for } u \leq u_\Delta \,, \\ u + 4m \log \dfrac{u - u_s - 4m}{v_s - 4m} & \text{for } u \geq \overline{u}_\Delta \,, \end{cases} \tag{6.74}$$

where $\overline{u}_\Delta$ is given by

$$\overline{u}_\Delta = u_s + 4m \left\{ 1 + W\left[ \frac{r_\Delta - 2m}{2m} \exp\left( \frac{-\Delta v + 2r_\Delta - 4m}{4m} \right) \right] \right\} . \tag{6.75}$$

The ray-tracing map at early times is the identical to the standard Vaidya case, as we expected since in this domain the path of the ray is exactly the same. At late times, on the other hand, it easy to see that $w(u)$ can be obtained from the solution at early times implementing the substitution $u - u_\Delta \leftrightarrow v_\Delta - w$ and solving for $w$.

We can distinguish three phases in the dynamics of the radiation entropy $\Delta S_{\rm rad}(u)$: phase $A$, $B$ and $C$. What we computed in Equation (6.74) is the ray-tracing map for the phases $A$ and $C$, plotted in Fig. 6.13. Exactly as before, phase $A$ is identical to the standard Hawking evaporation in a Vaidya SpaceTime, Eq. (6.36): the entropy grows monotonically and reaches a maximum at

$$S_{\rm max} \equiv \Delta S_{\rm rad}(u_\Delta) = \frac{1}{12} \log \left( \frac{1 + W\left[ \frac{r_\Delta - 2m}{2m} \exp\left( \frac{-\Delta v + 2r_\Delta - 4m}{4m} \right) \right]}{W\left[ \frac{r_\Delta - 2m}{2m} \exp\left( \frac{-\Delta v + 2r_\Delta - 4m}{4m} \right) \right]} \right) . \tag{6.76}$$

In this phase, standard Hawking's radiation is emitted. The requirement of time

symmetry fixes the duration of phase $B$,

$$\Delta u_B \equiv \overline{u}_\Delta - u_\Delta = \Delta v + 4m \left\{ 1 + W\left[ \frac{2r_\Delta - 4m}{4m} \exp\left( \frac{-\Delta v + 2r_\Delta - 4m}{4m} \right) \right] \right\} . \tag{6.77}$$

The radiation entropy in this phase depends on the geometry in the quantum region III, tIII and cannot be computed without a specific model of the effective geometry in this region. In the last in phase $C$, i.e. for $u \geq \overline{u}_\Delta$, $\Delta S_{\rm rad}(u)$ is given by the formula

$$\Delta S_{\rm rad}(u) = -\frac{1}{12} \log \left( 1 + \frac{4m}{u - \overline{u}_\Delta + 4m\, W\left[ \frac{r_\Delta - 2m}{2m} \exp\left( \frac{-\Delta v + 2r_\Delta - 4m}{4m} \right) \right]} \right) . \tag{6.78}$$

The entropy increases monotonically from a minimum negative value to zero, see Fig. 6.13. The minimum value at the beginning of phase $C$ equals the opposite of the maximum value found in Eq. (6.76),

$$S_{\rm min} \equiv \Delta S_{\rm rad}(\overline{u}_\Delta) = -S_{\rm max}. \tag{6.79}$$

At late times the entropy approaches zero from below with the law

$$\Delta S_{\rm rad}(u) \sim -\frac{1}{12} \frac{4m}{u - \overline{u}_\Delta} \tag{6.80}$$

for $u \to +\infty$. As expected, the evolution of the quantum massless field from $\mathscr{I}^-$ to $\mathscr{I}^+$ is unitary and no information is lost.

Let us consider two different scenarios for the scales involved in the model of bouncing black hole. The difference is in the duration of phase $A$, while we assume in both cases that the quantum region III extends outside the horizon up to a macroscopic scale $r_\Delta \gtrsim 2m$.[7]

In the first scenario $\Delta v = \alpha\, m^3$ and phase $A$ lasts a long time $\Delta u_A \sim \tau_H \approx \alpha\, m^3$ that is Hawking-like, i.e. it scales cubically with the mass of the black hole. In this case the entanglement entropy of radiation reaches a maximum $S_{\rm max} \sim m^2$ at the end of phase $A$, and a minimum $S_{\rm min} \sim -m^2$ and the beginning of phase $C$. Moreover, phase $B$ lasts a time $\Delta u_B \sim \alpha\, m^3$ and in phase $C$ the entropy reaches a value of order one, $|\Delta S_{\rm rad}(u_f)| \sim 1$, in a time of order $\Delta u_C = u_f - \overline{u}_\Delta \sim m$. It should be noted that if phase $A$ lasts a time $\tau_H \approx \alpha\, m^3$, most of the mass of the black hole is emitted in Hawking's radiation and 'dissipative' effects in the bounce cannot be neglected.

In the second scenario $\Delta v \sim m^2$ and phase $A$ lasts a time $\Delta u_A \sim m^2$ quadratic in the mass of the black hole. This is the scenario proposed by Haggard and Rovelli [2014] on the basis of an estimate of cumulative quantum effects. In this case the entanglement entropy of radiation reaches a maximum $S_{\rm max} \sim m$ at the end of phase $A$, and a minimum $S_{\rm min} \sim -m$ and the beginning of phase $C$. Phase $B$ lasts a time $\Delta u_B \sim m^2$ and in phase $C$ the entropy becomes of order one, $|\Delta S_{\rm rad}(u_f)| \sim 1$, in a time of order $\Delta u_C = u_f - \overline{u}_\Delta \sim m$. We emphasize that in this scenario the total energy emitted in phase $A$ in the form of Hawking's

[7] For instance $r_\Delta = 7m/3$, as proposed in Haggard and Rovelli [2014].

radiation is small consistently with the assumption that the process is essentially non-dissipative. The purifying phase lasts a time $\Delta u_B + \Delta u_C \sim m^2$.

While the proposal is new and intriguing, more precise conclusions on its validity cannot be given without an explicit choice of the surface $\Delta - \mathcal{E}$ and of the effective geometry in regions III, tIII. The purifying radiation emitted in phases $B$ and $C$, for instance, can carry away a large energy depending on the effective geometry violating again energy conditions.

# Conclusions

In conclusion, we studied non-singular black holes in both static and dynamical metrics. In the former case, the *modified Hayward's metric* proposed in Chapter 4 gives a compelling picture of a non-singular black hole. It improves the metrics so far proposed by including the 1-loop corrections computed in the effective approach to quantum gravity, and a time delay for an observer at the center. The latter has to satisfy a bound in order to preserve the sub-planckianity of the curvature everywhere.

Next, we considered dynamical metrics aimed at modeling the back-reaction due to the evaporation. We used a new covariant definition of entanglement entropy as a tool to interpret black hole entropy, and studied explicitly the process of information loss and recovering, following a scheme proposed by Page. Our results reveal two difficulties with the proposed models of non-singular black holes. The radiated energy in the total evaporation process is much bigger than the initial ADM mass of the SpaceTime. Moreover, a very general lower bound on the purification time is not satisfied.

At the same time, the new definition of entanglement entropy production provides a powerful tool to analyze the physical plausibility of any semi-classical scenario of formation and consequent unitary evaporation of a black hole, as for example the 'black hole firework' one studied in the last Section. Up to now, nevertheless, no one of the proposals we encountered seems to satisfy all the requirements one can impose on it.

The study of Hawking's radiation and evaporating black holes is a very active and fascinating field of research to which this thesis can contribute with original ideas and results.

Appendix A

# Causal Structure and Penrose-Carter Diagrams

## A.1 Causal Structure

In a Lorentzian manifold describing a SpaceTime, the *causal structure* plays a crucial role in the physical interpretation. Indeed, it is interpreted as describing which events in spacetime can influence which other events. In this Appendix we shortly review the main notions defining these structures.

Let us therefore take a SpaceTime $(\mathscr{M}, g_{ab})$. The tangent vectors at each point $x \in \mathscr{M}$, can be classed into three different types. Namely, a tangent vector $X^a$ is

- **timelike** if $g_{ab}X^aX^b < 0$;
- **null** if $g_{ab}X^aX^b = 0$;
- **spacelike** if $g_{ab}X^aX^b > 0$.

Moreover, a **path** in $\mathscr{M}$ is a continuous map $\mu : [a, b] \to M$ where $[a, b] \in \mathbb{R}$ is a non-degenerate interval.

A **curve** in $\mathscr{M}$ is the image of a path or, more properly, an *equivalence class of path-images* related by re-parametrisation, i.e. homeomorphisms or diffeomorphisms of $[a, b]$. A curve is said to be **causal** if the tangent vector is timelike or null at all points in the curve. Similarly we define a timelike curve, a null curve and a spacelike curve.

For any point $x \in \mathscr{M}$ we define

- The **chronological future (resp. past)** of $x$, denoted $\mathcal{I}^+(x)$, as the set of all points $y \in \mathscr{M}$ such that *there exists a future-directed (resp. past-directed) timelike curve* from $x$ to $y$.
- The **causal future (resp. past)** of $x$, denoted $\mathcal{J}^+(x)$, as the set of all points $y \in \mathscr{M}$ such that *there exists a future-directed (resp. past-directed) non-spacelike* curve from $x$ to $y$.

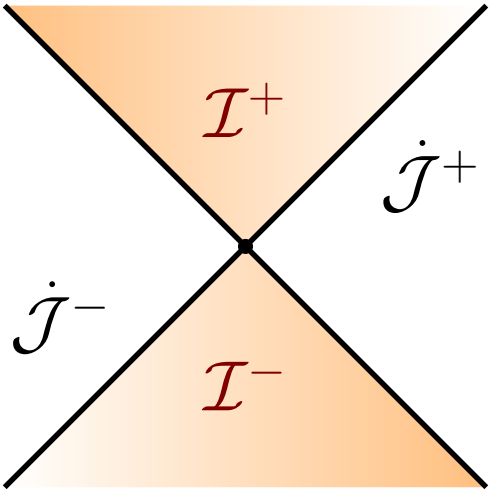


**Figure A.1.** Pictorial representation of chronological future $\mathcal{I}^+$ and past $\mathcal{I}^-$, of a point in $(1+1)$-dimensional Minkowski SpaceTime. In this case the chronological future (resp. past) is a subset of the causal future $\mathcal{J}^+$ (resp. past $\mathcal{J}^-$).

This four objects define the **causal structure** of $(\mathscr{M}, g_{ab})$.

The simplest example is of course the Minkowski SpaceTime, where our intuition of causal structure is rooted. There, the set $\mathcal{I}^+(x)$ is the interior of the future light cone at $x$. The set $\mathcal{J}^+(x)$ is the full future light cone at $x$, including the cone itself. Therefore $\mathcal{I}^\pm \subset \mathcal{J}^\pm$; in a general curved SpaceTime this is not always true. See Fig. A.1. What remain true is that massless objects travel at the speed of light along null curves and physical massive objects along timelike curves.

The generalization of these notions to a set of points $S \subset \mathscr{M}$ is straightforward. We define

$$\mathcal{I}^\pm(S) = \bigcup_{x \in S} \mathcal{I}^\pm(x) \tag{A.1}$$

$$\mathcal{J}^\pm(S) = \bigcup_{x \in S} \mathcal{J}^\pm(x) \tag{A.2}$$

Moreover, we can define other important concepts:

- The future **Cauchy development** of $S$, $\mathcal{D}^+(S)$ is *the set of all points $x$ for which every past-directed inextensible causal curve through $x$ intersects $S$ at least once.* Similarly for the past Cauchy development. The Cauchy development is the union of the future and past Cauchy developments. This concept is really important in the study of determinism. Roughly speaking, indeed, it represents the events in the SpaceTime *completely* determined by the set $S$.

- A subset $S \subset \mathscr{M}$ is **achronal** if there do not exist $q, r \in S$ such that $r \in \mathcal{I}^+(q)$, or equivalently, if $S$ is disjoint from $\mathcal{I}^+(S)$. Roughly speaking, this means that $S$ does not determine itself.

- A **Cauchy surface** $\Sigma \in \mathscr{M}$ is an closed achronal set whose Cauchy development is $M$, i.e. $\mathcal{D}(\Sigma) = \mathscr{M}$.

- A metric is **globally hyperbolic** if it can be foliated by Cauchy surfaces.

The most easy way to understand the causal structure of SpaceTimes is through the diagrammatic technique of *conformal diagrams* due to Penrose and Carter. Strongly following Fabbri and Navarro-Salas [2005, Sec. 2.3], we introduce it in the next Section.

## A.2 Penrose-Carter Diagrams

The main idea is to project the whole spacetime into a finite diagram, called *Penrose* or *Carter-Penrose* diagram, which conserves the causal properties of the original geometry. This is possible by means of a *Weyl (or conformal) transformation*

$$ds^2 \to d\bar{s}^2 = \Omega^2(x^\mu) ds^2, \tag{A.3}$$

where the conformal factor $\Omega^2(x^\mu)$ depends on the space-time point and is in general not vanishing and positive. Since the metric encode distances between points, it is clear that this operation will alter them. In particular, timelike geodesics are not mapped to timelike geodesics, but, and this is important, null geodesics are (see Wald [1984, App. D]). In particular, they are mapped in new null geodesics with a non-affine parameter $\overline{\lambda}$ given by

$$\frac{d\overline{\lambda}}{d\lambda} = c\,\Omega^2 \tag{A.4}$$

where $\lambda$ is the affine parameter in the starting SpaceTime and $c$ is a constant. The way to represent points at infinity within a finite diagram is to use $\Omega^2$ such that

$$\Omega^2 \to 0 \tag{A.5}$$

asymptotically. In such a way, an infinite affine distance in the original metric is transformed into a finite affine distance in the new metric. Therefore points at infinity, which strictly speaking do not belong to the original spacetime, are now represented in this *conformal compactification*.

Let us now see how to built such objects for the two SpaceTimes that play crucial roles in this thesis, namely Minkowski and Schwarzschild spaces.

### A.2.1 Minkowski space

The starting point is to write the Minkowski metric in double null coordinates $v = t + r$, $u = t - r$

$$ds^2 = -dudv + \left(\frac{v-u}{2}\right)^2 d\Omega^2. \tag{A.6}$$

The range of these coordinates is from $-\infty$ to $+\infty$. Only half ($r > 0$) of the two-dimensional $(t - r)$ plane is physically relevant. Let us identify the different asymptotic regions we want to compactify:

| | | | |
|---|---|---|---|
| spacelike infinity | $i^0$ | $r \to +\infty$ at fixed $t$ | $v \to +\infty, u \to -\infty$ |
| future timelike infinity | $i^+$ | $t \to +\infty$ at fixed $r$ | $v \to +\infty$, $u \to +\infty$ |
| past timelike infinity | $i^-$ | $t \to -\infty$ at fixed $r$ | $v \to -\infty$, $u \to -\infty$ |
| future null infinity | $\mathscr{I}_+$ | $t \to +\infty$, $r \to +\infty$ at fixed $t-r$ | $v \to +\infty$ at fixed $u$ |
| past null infinity | $\mathscr{I}_-$ | $t \to -\infty$, $r \to +\infty$ at fixed $t+r$ | $u \to -\infty$ at fixed $v$ |

To motivate the choice of the conformal factor $\Omega$ we shall first perform the following change of coordinates

$$\begin{aligned} v &= \tan \overline{v}, \\ u &= \tan \overline{u}. \end{aligned} \tag{A.7}$$

The range $-\infty < u, v < +\infty$ is now mapped to $-\frac{\pi}{2} < \overline{u}, \overline{v} < +\frac{\pi}{2}$ and the metric can be now written as

$$ds^2 = (2\cos\overline{u}\cos\overline{v})^{-2}\left[-4d\overline{u}d\overline{v} + \sin^2(\overline{v}-\overline{u})d\Omega^2\right]. \tag{A.8}$$

Therefore, we can choose the conformal factor

$$\Omega^2 = (2\cos\overline{u}\cos\overline{v})^2. \tag{A.9}$$

that brings to the line element

$$d\overline{s}^2 = -4\, d\overline{u}\, d\overline{v} + \sin(\overline{v}-\overline{u})^2\, d\Omega^2. \tag{A.10}$$

The conformal compactification of Minkowski spacetime is the obtained by adding to all finite points all the above regions at infinity, which we now identify:

| | | | |
|---|---|---|---|
| spacelike infinity | $i^0$ | $\overline{u} = -\frac{\pi}{2}$ | $\overline{v} = \frac{\pi}{2}$ |
| future timelike infinity | $i^+$ | $\overline{u} = \frac{\pi}{2}$ | $\overline{v} = \frac{\pi}{2}$ |
| past timelike infinity | $i^-$ | $\overline{u} = -\frac{\pi}{2}$ | $\overline{v} = -\frac{\pi}{2}$ |
| future null infinity | $\mathscr{I}_+$ | $\overline{u} \neq \frac{\pi}{2}$ | $\overline{v} = \frac{\pi}{2}$ |
| past null infinity | $\mathscr{I}_-$ | $\overline{u} = -\frac{\pi}{2}$ | $\overline{v} \neq \pm\frac{\pi}{2}$ |

The resulting Penrose-Carter diagram is the triangle depicted in Fig. **??**. Any point has to be thought as a 2-sphere of radius $\sin(\overline{v}-\overline{u})$. The origin $r = 0$ is the vertical line $\overline{u} = \overline{v}$ and the restriction $r \geq 0$ is transformed to $\overline{v} \geq \overline{u}$. The qualitative behavior of geodesics in Minkowski spacetime can be easily understood in the corresponding Penrose diagram. Timelike geodesics (except those that are asympotically null) start at $i^-$ in the past and end at $i^+$ in the future. Null geodesics, starting from $\mathscr{I}_-$, reach the origin, where they 'bounce' and end on $\mathscr{I}_+$. Finally, $i^0$ is the asymptotic point of all spacelike geodesics.

### A.2.2 Schwarzschild SpaceTime

Let us now turn to the Schwarzschild spacetime, starting from the maximal extension of the metric provided by the Kruskal coordinates $(U, V)$ (see Section 1.1.2)

$$ds^2 = -\frac{2Me^{-\frac{r}{2M}}}{r} dU dV + r^2 d\Omega^2. \tag{A.11}$$

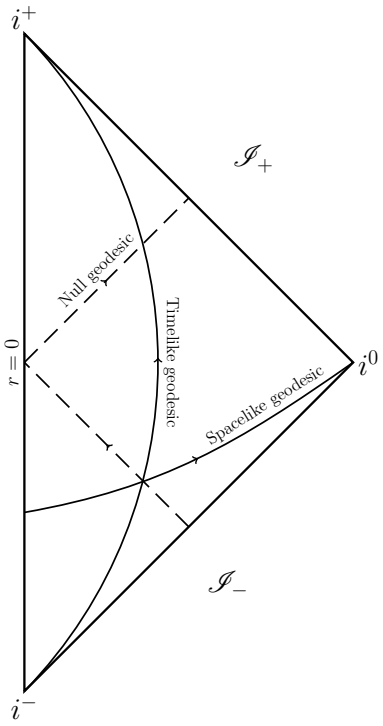


**Figure A.2.** Penrose-Carter diagram of the Minkowski Space-Time.

Performing the same type of change of coordinates (A.7)

$$\begin{aligned} V =& 4m \tan \overline{V}, \\ U =& 4m \tan \overline{U}. \end{aligned} \tag{A.12}$$

we find

$$ds^2 = -\frac{32m^3 e^{-\frac{r}{2m}} d\overline{U} d\overline{V}}{r(\cos \overline{U} \cos \overline{V})^2} + r(\overline{U}, \overline{V})^2 d\Omega^2. \tag{A.13}$$

The conformal factor is chosen to be

$$\Omega^2 = \frac{r e^{\frac{r}{2m}} (\cos \overline{U} \cos \overline{V})^2}{8m^3} \tag{A.14}$$

that transforms the metric into

$$d\overline{s}^2 = -4 d\overline{U} d\overline{V} + \frac{r^3 e^{\frac{r}{2m}} (\cos \overline{U} \cos \overline{V})^2}{8m^3} d\Omega^2. \tag{A.15}$$

The crucial relation we need to construct the Penrose diagram is between the null coordinates $\overline{U}, \overline{V}$ and $r$, namely

$$\left(\frac{r}{2m} - 1\right) e^{\frac{r}{2m}} = -\tan \overline{U} \tan \overline{V}. \tag{A.16}$$

Now the line $r = 0$ is no more a vertical line as in minkowsky, but is made of two disconnected horizontal curves, i.e.

$$\tan \overline{U} \tan \overline{V} = 1, \tag{A.17}$$

that is

$$\overline{U} + \overline{V} = \pm \frac{\pi}{2}. \tag{A.18}$$

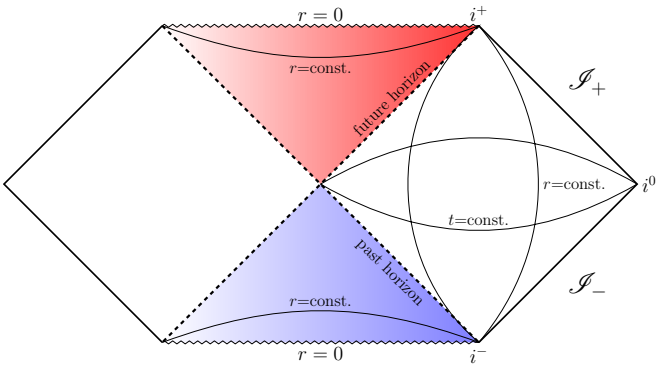


**Figure A.3.** Penrose-Carter diagram of the Kruskal-Szekeres SpaceTime. The black hole region is red-shaded, while the blue-shaded triangle is the white hole region.

The important feature of these curves is that they are spacelike, as opposed to timelike in the previous case. The restriction $r \geq 0$ is now translated to the condition

$$-\frac{\pi}{2} \leq \overline{U} + \overline{V} \leq +\frac{\pi}{2}. \tag{A.19}$$

Therefore the full domain of the coordinates $\overline{U}, \overline{V}$ is

$$\begin{aligned} -\frac{\pi}{2} \leq \overline{U}+\overline{V} \leq +\frac{\pi}{2}, \\ -\frac{\pi}{2} < U < +\frac{\pi}{2} \\ -\frac{\pi}{2} < V < +\frac{\pi}{2}. \end{aligned} \tag{A.20}$$

The resulting Penrose-Carter diagram of the eternal Schwarzschild black hole is given in Fig. **??**. Its complete interpretation is given in Section 1.1.2.

# Appendix B

# Energy Conditions

Einstein Equations read

$$R_{ab} - \frac{1}{2} R\, g_{ab} = 8\pi\, T_{ab} \tag{B.1}$$

and imply the conservation equation

$$\nabla_b\, T^b_a = 0\ . \tag{B.2}$$

If $k^a$ is a tangent vector to a time-like geodesic, an observer sits on it sees a energy-momentum tensor flux given by $-T^a_b\, k^b$ and measures an energy density $T_{ab}\, k^a k^b$.

The components of $T_{ab}$ at each point $p \in \mathcal{M}$ can be expressed, with respect to an orthonormal basis $\{E^{(0)},\, E^{(1)},\, E^{(2)},\, E^{(3)}\}$, in one of the following four canonical forms [Hawking and Ellis 1973, p. 88].

*Type I*

$$T^{\mu\nu} = \begin{pmatrix} \rho & & & \\ & p_1 & & \\ & & p_2 & \\ & & & p_3 \end{pmatrix} \tag{B.3}$$

with $E^{(0)}$ timelike.

*Type II*

$$T^{\mu\nu} = \begin{pmatrix} \nu+\rho & \nu & & \\ \nu & \nu-\rho & & \\ & & p_1 & \\ & & & p_2 \end{pmatrix} \tag{B.4}$$

with $E^{(0)} + E^{(1)}$ null.

*Type III*

$$T^{\mu\nu} = \begin{pmatrix} \nu & & & \\ & -\nu & 1 & 1 \\ & 1 & -\nu & 0 \\ & 1 & 0 & p \end{pmatrix} \tag{B.5}$$

that corresponds to three null eigenvectors.

*Type IV*

$$T^{\mu\nu} = \begin{pmatrix} p_1 & & & \\ & p_2 & & \\ & & -\rho & \nu \\ & & \nu & 0 \end{pmatrix} \tag{B.6}$$

that corresponds to neither timelike nor null eigenvectors.

All known physical non-zero-mass fields have a Type I momentum-energy tensor, while all known zero-mass fields have a Type I or Type II. No observed matter fields satisfy Type III or Type IV.

General Relativity allows in principle all kind of metric that satisfies Einstein Equations with some energy-momentum tensor on the right hand side (or viceversa a random energy-momentum tensor can gives a metric that satisfies EE). On the other hand, some physical requirements called *energy conditions* are usually imposed on $T_{ab}$. The mathematical statements are written in terms of scalar products between tensors and vectors, but it is possible to traslate them in a more useful form in terms of the component of $T_{ab}$ written in one of the above types [Hawking and Ellis 1973; Westmoreland 2013].

**Weak Energy Condition (WEC)** $T_{ab}$ at each $p \in \mathcal{M}$ obeys

$$T_{ab}\, t^a\, t^b \geq 0 \qquad \forall\, t^a \text{ timelike.} \tag{B.7}$$

This relation is automatically satisfied also for null $t^a$.
*Physical meaning:* the energy density, as measured by any observer, is locally non-negative.

*Type I:*

$$\rho \geq 0\,, \quad \rho \geq -p_\alpha \quad (\alpha = 1, 2, 3)\,. \tag{B.8}$$

*Type II:*

$$p_1 \geq 0\,, \quad p_2 \geq 0\,, \quad \rho \geq 0\,, \quad \nu > 0\,. \tag{B.9}$$

**Dominant Energy Condition (DEC)** $T_{ab}$ at each $p \in \mathcal{M}$ obeys

$$T_{ab}\, t^a\, t^b \geq 0 \quad \text{and} \tag{B.10}$$

$$T^{ab} t_b \quad \text{non-spacelike} \quad \forall\, t^a \text{ timelike.} \tag{B.11}$$

*Physical meaning:* the energy density, as measured by any observer, is locally non-negative and the local energy flow cannot travel faster then light.

*Type I:*

$$\rho \geq 0\,, \quad -\rho \leq p_\alpha \leq \rho \quad (\alpha = 1, 2, 3)\,. \tag{B.12}$$

*Type II:*

$$\kappa \geq 0\,, \quad 0 \leq p_\alpha \leq \rho\,, \quad \nu > 0 \quad (\alpha = 1, 2)\,. \tag{B.13}$$

**Strong Energy Condition (SEC)** $T_{ab}$ at each $p \in \mathcal{M}$ obeys

$$R_{ab}\, t^a\, t^b \geq 0 \quad \forall\, t^a \text{ timelike.} \tag{B.14}$$

where $R_{ab}$ is the Ricci tensor. From Einstein Equations this relation can be expressed as

$$T_{ab}\, t^a\, t^b \geq \frac{1}{2}\, T\, t^a\, t_a \tag{B.15}$$

where $T$ is the trace of $T_{ab}$, i.e. $T = g^{ab}T_{ab}$.

*Physical meaning:* gravitational force is attractive.

*Type I:*

$$\rho + p_\alpha \geq 0 \quad (\alpha = 1,2,3) \quad \rho + \sum_{\alpha=1}^{3} p_\alpha \geq 0\,. \tag{B.16}$$

*Type II:*

$$p_1 \geq 0\,, \quad p_2 \geq 0\,, \quad \rho \geq 0\,, \quad \nu > 0\,. \tag{B.17}$$

The WEC is implied by the DEC while the SEC, despite its name, does not imply any of the other two. We need to remark that other energy conditions can be stated, as for example the *null energy condition* (implied by the three mentioned above) or the *trace energy condition* [Visser and Barcelo 1999]. However, they do not play any role in the discussion of this thesis.

## B.1 Generalized Vaidya Solution

This section is based on the paper by Wang and Wu [1998].

Starting from the general dynamical spherically symmetric line element

$$ds^2 = -e^{2\psi(v,r)}F(v,r)dv^2 + 2e^{\psi(v,r)}dvdr + r^2 d\Omega^2\,, \tag{B.18}$$

let us take $\psi(v,r) = 0$ and $F(v,r) = \left(1 - \frac{2\mu(v,r)}{r}\right)$. From EE we can compute the non-vanishing components of $T^a_b$:

$$8\pi T^0_{\ 0} = 8\pi T^1_{\ 1} = -\frac{2\mu_{,r}(v,r)}{r^2} \tag{B.19}$$

$$8\pi T^1_{\ 0} = \frac{2\mu_{,v}(v,r)}{r^2} \tag{B.20}$$

$$8\pi T^2_{\ 2} = 8\pi T^3_{\ 3} = -\frac{\mu_{,rr}(v,r)}{r}\,, \tag{B.21}$$

where "$_{,v}$" (resp. "$_{,r}$") denotes the derivative with respect to the coordinate $v$ (resp. $r$). The $\phi - \theta$ part of the tensor is diagonal with eigenvalue

$$p = -\frac{\mu_{,rr}}{8\pi r} \tag{B.22}$$

while the time-radius $v - r$ part

$$T^\mu_{\ \nu} = \begin{pmatrix} T^0_{\ 0} & T^1_{\ 0} \\ 0 & T^0_{\ 0} \end{pmatrix} \tag{B.23}$$

admits one eigenvalue with $deg = 2$ given by

$$-\rho = T^0_{\ 0} = -\frac{\mu_{,r}(v,r)}{4\pi r^2}\ . \tag{B.24}$$

Definining now

$$\nu = T^1_{\ 0} = \frac{\mu_{,v}(v,r)}{4\pi r^2} \tag{B.25}$$

$$l_\mu = (1,0,0,0) \tag{B.26}$$

$$n_\mu = \frac{1}{2}F(v,r)\delta^{(0)}_\mu - \delta^{(1)}_\mu = \left(\frac{1}{2}F(v,r), -1, 0, 0\right). \tag{B.27}$$

with

$$l_\mu\, l^\mu = n_\mu\, n^\mu = 0\ , \tag{B.28}$$

the stress-energy tensor components can be written as

$$T_{\mu\nu} = \nu\, l_\mu\, l_\nu + (\rho + p) l_{(\mu}\, n_{\nu)} + p\, g_{\mu\nu}\,. \tag{B.29}$$

Now

$$\begin{aligned} g_{\mu\nu} &= -F(v,r)\delta^{(0)}_\mu\,\delta^{(0)}_\nu + \delta^{(0)}_\mu\,\delta^{(1)}_\nu + \delta^{(0)}_\nu\,\delta^{(1)}_\mu + r^2\delta^{(2)}_\mu\delta^{(2)}_\nu + r^2(\sin\theta)^2\,\delta^{(3)}_\mu\,\delta^{(3)}_\nu = \\ &= \left(\delta^{(1)}_\nu - \frac{1}{2}F(v,r)\,\delta^{(0)}_\nu\right)\delta^{(0)}_\mu + \left(\delta^{(1)}_\mu - \frac{1}{2}F(v,r)\,\delta^{(0)}_\mu\right)\delta^{(0)}_\nu + \\ &\qquad + r^2\delta^{(2)}_\mu\delta^{(2)}_\nu + r^2(\sin\theta)^2\,\delta^{(3)}_\mu\,\delta^{(3)}_\nu = \\ &= -l_{(\mu}n_{\nu)} + r^2\delta^{(2)}_\mu\delta^{(2)}_\nu + r^2(\sin\theta)^2\,\delta^{(3)}_\mu\,\delta^{(3)}_\nu \end{aligned} \tag{B.30}$$

and then Eq. (B.29) becomes

$$T_{\mu\nu} = \nu\, l_\mu\, l_\nu + \rho\, l_{(\mu}n_{\nu)} + p\left(r^2\delta^{(2)}_\mu\delta^{(2)}_\nu + r^2(\sin\theta)^2\,\delta^{(3)}_\mu\,\delta^{(3)}_\nu\right)\ . \tag{B.31}$$

The new definitions

$$E^{(0)}_\mu = \frac{l_\mu + n_\nu}{\sqrt{2}} \qquad E^{(1)}_\mu = \frac{l_\mu - n_\nu}{\sqrt{2}} \qquad E^{(2)}_\mu = r\delta^{(2)}_\mu \qquad E^{(3)}_\mu = r\,\sin\theta\,\delta^{(3)}_\mu \tag{B.32}$$

allow to write

$$\begin{aligned} l_\mu\, l_\nu &= \left(\frac{E^{(0)}_\mu + E^{(1)}_\mu}{\sqrt{2}}\right)\left(\frac{E^{(0)}_\nu + E^{(1)}_\nu}{\sqrt{2}}\right) = \\ &= \frac{1}{2}\left(E^{(0)}_\mu\,E^{(0)}_\nu + E^{(0)}_\mu\,E^{(1)}_\nu + E^{(1)}_\mu\,E^{(0)}_\nu + E^{(1)}_\mu\,E^{(1)}_\nu\right) \end{aligned} \tag{B.33}$$

and

$$\begin{aligned} l_{(\mu}n_{\nu)} &= \left(\frac{E^{(0)}_\mu + E^{(1)}_\mu}{\sqrt{2}}\right)\left(\frac{E^{(0)}_\nu - E^{(1)}_\nu}{\sqrt{2}}\right) + \left(\frac{E^{(0)}_\nu + E^{(1)}_\nu}{\sqrt{2}}\right)\left(\frac{E^{(0)}_\mu - E^{(1)}_\mu}{\sqrt{2}}\right) = \\ &= E^{(0)}_\mu\,E^{(0)}_\nu - E^{(1)}_\mu\,E^{(1)}_\nu\ . \end{aligned} \tag{B.34}$$

Finally, combining Eq. (B.31)-(B.32), we can find the following form for the components of the energy-momentum tensor:

$$\begin{aligned} T_{\mu\nu} =& \frac{\nu}{2}\left(E^{(0)}_{\mu}\,E^{(0)}_{\nu} + E^{(0)}_{(\mu}\,E^{(1)}_{\nu)} + E^{(1)}_{\mu}\,E^{(1)}_{\nu}\right) + \\ &+ \rho\left(E^{(0)}_{\mu}\,E^{(0)}_{\nu} - E^{(1)}_{\mu}\,E^{(1)}_{\nu}\right) + p\left(E^{(2)}_{\mu}\,E^{(2)}_{\nu} + E^{(3)}_{\mu}\,E^{(3)}_{\nu}\right) \end{aligned} \tag{B.35}$$

That's it. The energy-momentum tensor for a generalized Vaidya solution is of the *Type II*:

$$T_{\mu\nu} = \begin{pmatrix} \frac{\nu}{2}+\rho & \frac{\nu}{2} & & \\ \frac{\nu}{2} & \frac{\nu}{2}-\rho & & \\ & & p & \\ & & & p \end{pmatrix} . \tag{B.36}$$

**Dynamical Hayward's metric** Let us apply this analysis to the dynamical Hayward metric studied in Chapter 5, for which

$$F(v,r) = 1 - \frac{2\mu(v,r)}{r} = 1 - \frac{2m(v)r^2}{r^3 + 2m(v)L^2} \tag{B.37}$$

that means

$$\mu(v,r) = \frac{m(v)r^3}{r^3 + 2m(v)L^2} . \tag{B.38}$$

Computing the derivative w.r.t. $v$ one finds

$$\mu_{,v}(v,r) = \frac{m'(v)r^6}{(r^3 + 2m(v)L^2)^2} \tag{B.39}$$

and then

$$\begin{aligned} \nu &= \frac{\mu_{,v}(v,r)}{4\pi r^2} = \\ &= \frac{r^4}{4\pi(r^2 + 2m(v)L^2)^2}\, m'(v) = \\ &= \Gamma(v,r)\, m'(v) . \end{aligned} \tag{B.40}$$

Since $\Gamma(v,r)$ is a positive function for all $r$ and $v$ and since all the energy conditions require $\nu > 0$ in order to be satisfied, we can assert that

*All the energy conditions (WEC, SEC, DEC) are violated if* $m'(v) < 0$.

The case with $m'(v) = 0$ is the static Hayward case (Chapter 3) and the energy-momentum tensor becomes of the *Type I*.

Appendix C

# Computations

In this Appendix the explicit computations needed for the results in Chapter 5 are proposed.

## C.1 Hayward's Surface Gravity

Let us consider the generic line element written in advanced Eddington-Finkelstein coordinates

$$ds^2 = -F(r)dv^2 + 2dvdr + r^2 d\Omega^2. \tag{C.1}$$

with

$$F(r) = \left(1 - \frac{2M(r)}{r}\right) . \tag{C.2}$$

The Killing vector field $\chi^a$ relative to translations of $v$ has component

$$\chi^\mu = (1, 0, 0, 0). \tag{C.3}$$

The *surface gravity* $\kappa$ is defined by the equation (see Section 2.3)

$$\nabla^a(\chi^b \chi_b) \stackrel{H}{=} -2\,\kappa\,\chi^a\ . \tag{C.4}$$

or equivalently, using the properties of Killing vector fields, by

$$\chi^b \nabla_b \chi^a \stackrel{H}{=} \kappa\,\chi^a \tag{C.5}$$

where these equations are evaluated at the horizon $r = r_H$. In the case of metric (C.1) it explicitly reads

$$\chi^\nu \nabla_\nu \chi^\mu = \left(\frac{M(r) - rM'(r)}{r^2}, -\frac{\big(r - 2M(r)\big)\big(rM'(r) - M(r)\big)}{r^3}, 0, 0\right). \tag{C.6}$$

When evaluated in $r = r_H$, by definition of horizon $F(r_H) = 0$ the second term is zero as it is proportional to $F(r)$. Thus

$$\kappa = \frac{M(r_H) - r_H M'(r_H)}{r_H^2}. \tag{C.7}$$

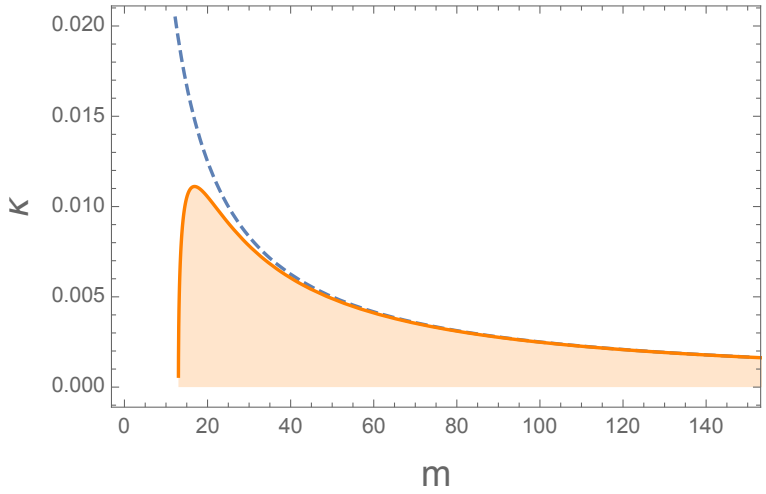


**Figure C.1.** The surface gravity $\kappa$ for the Hayward's metric compared with the classical surface gravity $\frac{1}{4m}$ (dashed line), as a function of the mass $m$. Here $L = 10$ (Planck units).

Taking into account that by definition of horizon $F(r_H) = 0$

$$2M(r_H) = r_H \tag{C.8}$$

we obtain

$$\kappa = \frac{1}{2\,r_H} - \frac{M'(r_H)}{r_H}. \tag{C.9}$$

In the Hayward's metric $M(r) = \frac{m\,r^3}{r^3+2mL^2}$, which implies

$$\kappa = \frac{3}{4m} - \frac{1}{r_H}. \tag{C.10}$$

## C.2 Maximum of $\kappa$

Let us now take the outer horizon $r_H = r_+$ of the Hayward's metric given by Eq. (3.22a)

$$r_+ = \frac{2m}{3}\left(1 + 2\cos\frac{x}{3}\right) \tag{C.11a}$$

$$\cos x = 1 - \frac{27L^2}{8m^2} \qquad \text{with } x \in ]0;\pi]\ . \tag{C.11b}$$

The point $x \to 0$ corresponds to the case $r_+ \to 2m$, while on the contrary the point $x = \pi$ corresponds to the extremal configuration $m_\star = 3\sqrt{3}L/4$. We see that

$$\frac{4m}{3} \leq r_+ < 2m$$

from which $\kappa \geq 0$; the equality sign holding only at the extremal point $x = \pi$. The complete behavior of $\kappa$ as a function of $m$ is plotted in Fig. C.1.

We want now analytically compute the value $m_{\max}$ of the mass for which the maximum arises.

We notice that the function $f = L\kappa$ depends on $m$ and $L$ only through the ratio $m/L$. Since multiplication by $L$ is just a dilatation, it will be the same to find the maximum of $f$ w.r.t. the variable $z = m/L$. So we have

$$f = \frac{3}{4z} - \frac{3}{2z}\frac{1}{\left(1 + 2\cos\frac{x}{3}\right)} \tag{C.12a}$$

$$\cos x = 1 - \frac{27}{8z^2}\ . \tag{C.12b}$$

By differentiation

$$\frac{27}{4z^3} = \frac{d\cos x}{dz} = 3\left(4\cos^2\frac{x}{3} - 1\right)\frac{d\cos\frac{x}{3}}{dz}. \tag{C.13}$$

where we used the *triple cosine formula*:

$$\cos x = \cos\frac{x}{3}\left(4\cos^2\frac{x}{3} - 3\right). \tag{C.14}$$

It follows that

$$\frac{df}{dz} = \frac{3}{2z^2}\left[\frac{9}{2z^2}\frac{1}{\left(1 + 2\cos\frac{x}{3}\right)^2\left(4\cos^2\frac{x}{3} - 1\right)} + \frac{1}{\left(1 + 2\cos\frac{x}{3}\right)} - \frac{1}{2}\right]. \tag{C.15}$$

To find the maximum we solve the equation $\frac{df}{dz} = 0$, namely

$$4\cos^4\frac{x}{3} - 2\cos^2\frac{x}{3} + \left(\frac{1}{2} - \frac{9}{4z^2}\right) = 0\ , \tag{C.16}$$

whose solution is

$$\cos\frac{x}{3} = \frac{1}{2}\sqrt{1 \pm \frac{3}{z}}. \tag{C.17}$$

Substituting into (C.14) we obtain

$$\cos^2 x = 1 - \frac{27}{4z^2} \pm \frac{27}{4z^3}. \tag{C.18}$$

Finally, using (C.12b) it's easy to see that consistency selects the solution with the + sign, that brigs to

$$z = \frac{27}{16}\ . \tag{C.19}$$

Therefore the maximum of $\kappa$ arises for

$$m = m_{\max} = \frac{27}{16}L\ . \tag{C.20}$$

# References


Alesci, Emanuele and Leonardo Modesto (2014). "Particle Creation by Loop Black Holes". In: *Gen.Rel.Grav.* 46, p. 1656. DOI: 10.1007/s10714-013-1656-0. arXiv: 1101.5792 [gr-qc].

Almheiri, Ahmed et al. (2013). "Black Holes: Complementarity or Firewalls?" In: *JHEP* 1302, p. 62. DOI: 10.1007/JHEP02(2013)062. arXiv: 1207.3123 [hep-th].

Ashtekar, Abhay and Martin Bojowald (2006). "Quantum geometry and the Schwarzschild singularity". In: *Class.Quant.Grav.* 23, pp. 391–411. DOI: 10.1088/0264-9381/23/2/008. arXiv: gr-qc/0509075 [gr-qc].

Ashtekar, Abhay and Badri Krishnan (2004). "Isolated and dynamical horizons and their applications". In: *Living Rev.Rel.* 7, p. 10. arXiv: gr-qc/0407042 [gr-qc].

Barcelo, Carlos et al. (2011). "Minimal conditions for the existence of a Hawking-like flux". In: *Phys. Rev.* D83, p. 41501. DOI: 10.1103/PhysRevD.83.041501. arXiv: 1011.5593 [gr-qc].

Bardeen, James M. (1968). "Non-singular general-relativistic gravitational collapse". In: *Proc. Int. Conf. GR5, Tbilisi*, p. 174.

— (2014). "Black hole evaporation without an event horizon". In: arXiv: 1406.4098 [gr-qc].

Bardeen, James M., B. Carter, and Stephen W. Hawking (1973). "The four laws of black hole mechanics". In: *Communications in Mathematical Physics* 31.2, pp. 161–170. URL: http://projecteuclid.org/euclid.cmp/1103858973.

Barrau, Aurelien and Carlo Rovelli (2014). "Planck star phenomenology". In: *arXiv*. arXiv: 1404.5821 [gr-qc].

Bekenstein, Jacob D. (1973). "Black holes and entropy". In: *Phys. Rev.* D7, pp. 2333–2346. DOI: 10.1103/PhysRevD.7.2333.

— (1974). "Generalized second law of thermodynamics in black hole physics". In: *Phys.Rev.* D9, pp. 3292–3300. DOI: 10.1103/PhysRevD.9.3292.

— (1994). "Do we understand black hole entropy?" In: arXiv: gr-qc/9409015 [gr-qc].

Bianchi, Eugenio, Tommaso De Lorenzo, and Matteo Smerlak (2014). "Entanglement entropy production in gravitational collapse: covariant regularization and solvable models". In: arXiv: 1409.0144 [hep-th].

Bianchi, Eugenio and Matteo Smerlak (2014a). "Entanglement entropy and negative energy in two dimensions". In: *Phys.Rev.* D90, p. 041904. DOI: 10.1103/PhysRevD.90.041904. arXiv: 1404.0602 [gr-qc].

— (2014b). "Last gasp of a black hole: unitary evaporation implies non-monotonic mass loss". In: *Gen.Rel.Grav.* 46.10, p. 1809. DOI: 10.1007/s10714-014-1809-9. arXiv: 1405.5235 [gr-qc].

Birkhoff, G. D. and R. E. Langer (1923). *Relativity and Modern Physics*. Harvard University Press. URL: http://books.google.fr/books?id=NEpAAAAAIAAJ.

Birrell, Nicholas D. and Paul C. W. Davies (1984). *Quantum fields in curved space*. 7. Cambridge university press.

Bjerrum-Bohr, N. Emil J., John F. Donoghue, and Barry R. Holstein (2003). "Quantum gravitational corrections to the nonrelativistic scattering potential of two masses". In: *Phys. Rev.* D67, p. 084033. DOI: 10.1103/PhysRevD.71.069903,10.1103/PhysRevD.67.084033. arXiv: hep-th/0211072 [hep-th].

Bombelli, Luca et al. (1986). "Quantum source of entropy for black holes". In: *Phys. Rev. D* 34 (2), pp. 373–383. DOI: 10.1103/PhysRevD.34.373. URL: http://link.aps.org/doi/10.1103/PhysRevD.34.373.

Borde, Arvind (1997). "Regular black holes and topology change". In: *Phys.Rev.* D55, pp. 7615–7617. DOI: 10.1103/PhysRevD.55.7615. arXiv: gr-qc/9612057 [gr-qc].

Calabrese, Pasquale, John Cardy, and Erik Tonni (2009). "Entanglement entropy of two disjoint intervals in conformal field theory". In: *J.Stat.Mech.* 0911, P11001. DOI: 10.1088/1742-5468/2009/11/P11001. arXiv: 0905.2069 [hep-th].

Casini, H. and M. Huerta (2009). "Remarks on the entanglement entropy for disconnected regions". In: *JHEP* 0903, p. 048. DOI: 10.1088/1126-6708/2009/03/048. arXiv: 0812.1773 [hep-th].

Davies, Paul C. W. and S. A. Fulling (1977). "Radiation from Moving Mirrors and from Black Holes". In: *Proc.Roy.Soc.Lond.* A356, pp. 237–257. DOI: 10.1098/rspa.1977.0130.

Davies, Paul C. W., S. A. Fulling, and W. G. Unruh (1976). "Energy-momentum tensor near an evaporating black hole". In: *Phys. Rev. D* 13 (10), pp. 2720–2723. DOI: 10.1103/PhysRevD.13.2720. URL: http://link.aps.org/doi/10.1103/PhysRevD.13.2720.

Dieks, D. (2008). *The Ontology of Spacetime II*. Philosophy and Foundations of Physics. Elsevier Science. ISBN: 9780080569888. URL: http://books.google.fr/books?id=Ov6zaiANlgsC.

Donoghue, John F. (1994). "General relativity as an effective field theory: The leading quantum corrections". In: *Phys.Rev.* D50, pp. 3874–3888. DOI: 10.1103/PhysRevD.50.3874. arXiv: gr-qc/9405057 [gr-qc].

Dymnikova, Irina (1992). "Vacuum nonsingular black hole". In: *Gen. Rel. Grav.* 24, pp. 235–242. DOI: 10.1007/BF00760226.

— (2002). "Cosmological term as a source of mass". In: *Class. Quant. Grav.* 19, pp. 725–740. DOI: 10.1088/0264-9381/19/4/306. arXiv: gr-qc/0112052 [gr-qc].

Eddington, Arthur S (1924). "A Comparison of Whitehead's and Einstein's Formulae". In: *Nature* 113, p. 192.

Einstein, A., B. Podolsky, and N. Rosen (1935). "Can Quantum-Mechanical Description of Physical Reality Be Considered Complete?" In: *Phys. Rev.* 47 (10), pp. 777–780. DOI: 10.1103/PhysRev.47.777. URL: http://link.aps.org/doi/10.1103/PhysRev.47.777.

Fabbri, Alessandro and José Navarro-Salas (2005). *Modeling black hole evaporation*. World Scientific.

Finkelstein, David (1958). "Past-Future Asymmetry of the Gravitational Field of a Point Particle". In: *Phys.Rev.* 110, pp. 965–967. DOI: 10.1103/PhysRev.110.965.

Foong, S. K. and S. Kanno (1994). "Proof of Page's conjecture on the average entropy of a subsystem". In: *Phys. Rev. Lett.* 72 (8), pp. 1148–1151. DOI: 10.1103/PhysRevLett.72.1148. URL: http://link.aps.org/doi/10.1103/PhysRevLett.72.1148.

Ford, L. H. (2010). "Negative Energy Densities in Quantum Field Theory". In: *Int.J.Mod.Phys.* A25, pp. 2355–2363. DOI: 10.1142/S0217751X10049633. arXiv: 0911.3597 [quant-ph].

Ford, L. H. and Thomas A. Roman (1999). "The Quantum interest conjecture". In: *Phys.Rev.* D60, p. 104018. DOI: 10.1103/PhysRevD.60.104018. arXiv: gr-qc/9901074 [gr-qc].

Frolov, Valeri P. (2014). "Information loss problem and a 'black hole' model with a closed apparent horizon". In: *arXiv*. arXiv: 1402.5446 [hep-th].

Frolov, Valeri P. and Andrei Zelnikov (2011). *Introduction to black hole physics*. Oxford University Press.

Goroff, Marc H. and Augusto Sagnotti (1985). "Quantum Gravity at Two Loops". In: *Phys. Lett.* B160, pp. 81–86. DOI: 10.1016/0370-2693(85)91470-4.

Haggard, Hal M and Carlo Rovelli (2014). "Black hole fireworks: quantum-gravity effects outside the horizon spark black to white hole tunneling". In: *arXiv*. arXiv: 1407.0989 [gr-qc].

Hawking, Stephen W. (1974). "Black hole explosions?" In: *Nature* 248, pp. 30–31. DOI: 10.1038/248030a0.

— (1975). "Particle creation by black holes". In: *Communications in Mathematical Physics* 43.3, pp. 199–220. URL: http://projecteuclid.org/euclid.cmp/1103899181.

— (1976). "Breakdown of Predictability in Gravitational Collapse". In: *Phys. Rev.* D14, pp. 2460–2473. DOI: 10.1103/PhysRevD.14.2460.

Hawking, Stephen W. and George F. R. Ellis (1973). *The large scale structure of space-time*. 20th. Vol. 1. Cambridge university press.

Hayward, Sean A. (2006). "Formation and evaporation of regular black holes". In: *Phys. Rev. Lett.* 96, p. 31103. DOI: 10.1103/PhysRevLett.96.031103. arXiv: gr-qc/0506126 [gr-qc].

Hiscock, William A. (1981a). "Models of Evaporating Black Holes". In: *Phys.Rev.* D23, p. 2813. DOI: 10.1103/PhysRevD.23.2813.

— (1981b). "Models of Evaporating Black Holes. II. Effects of the Outgoing Created Radiation". In: *Phys.Rev.* D23, pp. 2823–2827. DOI: 10.1103/PhysRevD.23.2823.

Holzhey, Christoph, Finn Larsen, and Frank Wilczek (1994). "Geometric and renormalized entropy in conformal field theory". In: *Nucl. Phys.* B424, pp. 443–467. DOI: 10.1016/0550-3213(94)90402-2. arXiv: hep-th/9403108 [hep-th].

Hossenfelder, Sabine, Leonardo Modesto, and Isabeau Premont-Schwarz (2010). "A Model for non-singular black hole collapse and evaporation". In: *Phys.Rev.* D81, p. 044036. DOI: 10.1103/PhysRevD.81.044036. arXiv: 0912.1823 [gr-qc].

Isham, Chris J. (2002). *Modern differential geometry for physicists*. Allied Publishers.

Israel, W. (1986). "Third Law of Black-Hole Dynamics: A Formulation and Proof". In: *Phys. Rev. Lett.* 57 (4), pp. 397–399. DOI: 10.1103/PhysRevLett.57.397. URL: http://link.aps.org/doi/10.1103/PhysRevLett.57.397.

Kruskal, M. D. (1960). "Maximal extension of Schwarzschild metric". In: *Phys.Rev.* 119, pp. 1743–1745. DOI: 10.1103/PhysRev.119.1743.

Mazur, Pawel O. and Emil Mottola (2001). "Gravitational condensate stars: An alternative to black holes". In: arXiv: gr-qc/0109035 [gr-qc].

Modesto, Leonardo (2004). "Disappearance of black hole singularity in quantum gravity". In: *Phys. Rev.* D70, p. 124009. DOI: 10.1103/PhysRevD.70.124009. arXiv: gr-qc/0407097 [gr-qc].

— (2006). "Loop quantum black hole". In: *Class.Quant.Grav.* 23, pp. 5587–5602. DOI: 10.1088/0264-9381/23/18/006. arXiv: gr-qc/0509078 [gr-qc].

Nicolini, Piero (2005). "Noncommutative nonsingular black holes". In: *arXiv*, pp. 79–87. arXiv: hep-th/0510203 [hep-th].

Oppenheimer, Julius R and Hartland Snyder (1939). "On Continued Gravitational Contraction". In: *Phys. Rev.* 56 (5), pp. 455–459. DOI: 10.1103/PhysRev.56.455. URL: http://link.aps.org/doi/10.1103/PhysRev.56.455.

Pacilio, Costantino and Roberto Balbinot (2014). "Classical and quantum aspects of black hole dynamics". MA thesis. Università di Bologna. URL: http://amslaurea.unibo.it/7532/.

Page, Don N. (1993a). "Average entropy of a subsystem". In: *Phys. Rev. Lett.* 71 (9), pp. 1291–1294. DOI: 10.1103/PhysRevLett.71.1291. URL: http://link.aps.org/doi/10.1103/PhysRevLett.71.1291.

— (1993b). "Information in black hole radiation". In: *Phys. Rev. Lett.* 71, pp. 3743–3746. DOI: 10.1103/PhysRevLett.71.3743. arXiv: hep-th/9306083 [hep-th].

Penrose, Roger (1973). "Naked Singularities". In: *Annals of the New York Academy of Sciences* 224.1, pp. 125–134. ISSN: 1749-6632. DOI: 10.1111/j.1749-6632.1973.tb41447.x. URL: http://dx.doi.org/10.1111/j.1749-6632.1973.tb41447.x.

— (2014a). "On the Gravitization of Quantum Mechanics 1: Quantum State Reduction". English. In: *Foundations of Physics* 44.5, pp. 557–575. ISSN: 0015-9018. DOI: 10.1007/s10701-013-9770-0. URL: http://dx.doi.org/10.1007/s10701-013-9770-0.

— (2014b). "On the Gravitization of Quantum Mechanics 2: Conformal Cyclic Cosmology". English. In: *Foundations of Physics* 44.8, pp. 873–890. ISSN: 0015-9018. DOI: 10.1007/s10701-013-9763-z. URL: http://dx.doi.org/10.1007/s10701-013-9763-z.

Penrose, Roger and R. M. Floyd (1971). "Extraction of rotational energy from a black hole". In: *Nature* 229.6, pp. 177–179.

Poisson, Eric (2004). *A Relativist's Toolkit*. Cambridge University Press.

Roman, Thomas A. and Peter G. Bergmann (1983). "Stellar collapse without singularities?" In: *Phys.Rev.* D28, pp. 1265–1277. DOI: 10.1103/PhysRevD.28.1265.

Rovelli, Carlo and Francesca Vidotto (2014). "Planck stars". In: *arXiv*. arXiv: 1401.6562 [gr-qc].

Schumacher, Benjamin (1995). "Quantum coding". In: *Phys. Rev. A* 51 (4), pp. 2738–2747. DOI: 10.1103/PhysRevA.51.2738. URL: http://link.aps.org/doi/10.1103/PhysRevA.51.2738.

Solodukhin, Sergey N. (2011). "Entanglement entropy of black holes". In: *Living Rev.Rel.* 14, p. 8. arXiv: 1104.3712 [hep-th].

Sorkin, Rafael D. (1983). "On the entropy of the vacuum outside a horizon". In: *Tenth International Conference on General Relativity and Gravitation (held Padova, 4-9 July, 1983), Contributed Papers*. Vol. 2, pp. 734–736.

Srednicki, Mark (1993). "Entropy and area". In: *Phys. Rev. Lett.* 71 (5), pp. 666–669. DOI: 10.1103/PhysRevLett.71.666. URL: http://link.aps.org/doi/10.1103/PhysRevLett.71.666.

Susskind, Leonard, Larus Thorlacius, and John Uglum (1993). "The Stretched horizon and black hole complementarity". In: *Phys. Rev.* D48, pp. 3743–3761. DOI: 10.1103/PhysRevD.48.3743. arXiv: hep-th/9306069 [hep-th].

Szekeres, G. (1960). "On the singularities of a Riemannian manifold". In: *Publ.Math.Debrecen* 7, pp. 285–301.

Vaidya, P. (1951). "The Gravitational Field of a Radiating Star". In: *Proc.Indian Acad.Sci.* A33, p. 264.

Visser, Matt and Carlos Barcelo (1999). "Energy conditions and their cosmological implications". In: arXiv: gr-qc/0001099 [gr-qc].

Wald, Robert M. (1974). "Gedanken experiments to destroy a black hole". In: *Annals of Physics* 82.2, pp. 548–556. ISSN: 0003-4916. DOI: http://dx.doi.org/10.1016/0003-4916(74)90125-0. URL: http://www.sciencedirect.com/science/article/pii/0003491674901250.

— (1975). "On Particle Creation by Black Holes". In: *Commun.Math.Phys.* 45, pp. 9–34. DOI: 10.1007/BF01609863.

— (1984). "General Relativity". In:

— (2001). "The thermodynamics of black holes". In: *Living Rev.Rel.* 4, p. 6. arXiv: gr-qc/9912119 [gr-qc].

Wang, Anzhong and Yumei Wu (1998). "Generalized Vaidya solutions". In: *Gen. Rel. Grav.* Pp. 107–114. DOI: 10.1023/A:1018819521971. arXiv: gr-qc/9803038 [gr-qc].

Weinberg, Steven (1972). *Gravitation and cosmology: Principle and applications of general theory of relativity*. John Wiley and Sons, Inc., New York.

Westmoreland, Shawn (2013). "Energy Conditions and Scalar Field Cosmology". MA thesis. Kansas State University. URL: https://krex.k-state.edu/dspace/handle/2097/15811.